SAND78-1522
Unlimited Release
UC-83

Laser-Based Analytical Monitoring in Nuclear-Fuel Processing Plants

John P. Hohimer

Sandia Laboratories

SF 2900 Q(7-73)

SAND78-1522
Distribution Category UC-83

LASER-BASED ANALYTICAL MONITORING IN NUCLEAR-FUEL PROCESSING PLANTS

J. P. Hohimer

SANDIA LABORATORIES
LASER APPLICATIONS AND SPECTROSCOPY DIVISION
ALBUQUERQUE, N. M. 87185

PREPARED FOR THE
DEPARTMENT OF ENERGY
FUEL CYCLE PROGRAM OFFICE
UNDER CONTRACT (29-1)-789

Form 189 Number 820.6

CONTENTS

FIGURES

TABLES

FOREWORD

This report assesses the possible areas of application of laser-based analytical measurement methods for accountability, process control, and effluent control in nuclear-fuel processing plants. This study was funded under subtask 820.6 of the Thorium Fuel Cycle Technology Program. This Department of Energy program is administered by the Fuel Cycle Program Office at Savannah River. The technical management for this program is the responsibility of the Savannah River Laboratory, which is operated by E.I. duPont de Nemours and Company for the Department of Energy. This report is submitted in fulfillment of milestone 1 of subtask 820.6.

I would like to acknowledge the support and cooperation of the staffs of the Savannah River Laboratory and Savannah River Plant in compiling this report. In particular, I would like to thank Dr. R. S. Swingle, II who was instrumental in initiating this program and for providing the technical management for it. I would also like to acknowledge helpful discussions with Drs. M. C. Thompson, J. C. Eargle, Jr., D. A. Orth, and G. H. Sykes concerning the operation and monitoring requirements of a fuel processing plant.

ABSTRACT

The use of laser-based analytical methods in nuclear-fuel processing plants is considered. The species and locations for accountability, process control, and effluent control measurements in the Coprocessing, Thorex, and reference Purex fuel processing operations are identified and the conventional analytical methods used for these measurements are summarized. The laser analytical methods based upon Raman, absorption, fluorescence, and nonlinear spectroscopy are reviewed and evaluated for their use in fuel processing plants. After a comparison of the capabilities of the laser-based and conventional analytical methods, the promising areas of application of the laser-based methods in fuel processing plants are identified.

INTRODUCTION AND SUMMARY

This report considers the potential use of laser-based analytical methods for accountability, process control, and effluent control in a nuclear-fuel processing plant. A wide range of laser-based methods are available, some of which can be used for on-line real-time measurements of atomic and molecular species while other methods are best suited to off-line measurements using very small sample sizes. The laser spectroscopic methods have a very high sensitivity for low-level detection, and are expected to require little or no sample preparation. Finally, laser-based methods are available which permit the measurement of specific isotopes or molecular forms of a given elemental species.

In the first chapter of this report, the important species and their measurement locations for accountability, process control, and effluent control in a fuel processing plant are identified. The conventional analytical methods presently used in fuel processing plants as well as additional methods which are under development for future application in these plants are summarized in Chapter 2.

In Chapter 3, the analytical use of a number of laser spectroscopic methods is reviewed; and the potential use of these methods in fuel processing plants is evaluated. The laser-based methods which are considered in this report can be grouped into four general categories:

I. Raman scattering
   1. Spontaneous Raman scattering
   2. Coherent anti-Stokes Raman scattering
   3. Stimulated Raman scattering

II. Absorption spectroscopy
   1. External absorption spectroscopy
   2. Optoacoustic spectroscopy
   3. Intracavity absorption spectroscopy

III. Fluorescence spectroscopy
    1. Atomic fluorescence spectroscopy
    2. Molecular fluorescence spectroscopy

IV. Nonlinear spectroscopy
    1. Saturated absorption spectroscopy
    2. Two-photon spectroscopy

In the final chapter of this report, the laser-based analytical methods are compared with the conventional methods to determine the promising areas for the development of laser-based analytical instruments for use in nuclear-fuel processing plants.

A number of highly accurate analytical methods have been developed for use at primary accountability points, and on-line non-destructive assay (NDA) methods are being developed for use in process streams. For these reasons, the laser-based methods are probably best suited for use at secondary accountability points such as first cycle process streams and liquid waste streams where the SNM concentration is low. At these points the high sensitivity and rapid response of the at-line or on-line laser-based methods will help to close the material balance for accountability. When "spiked" or Civex fuel cycles are considered, the laser-based methods should successfully compete with the conventional NDA methods for accountability measurements in second and third cycle process streams.

The process control applications of the laser-based methods include: the measurement of the loss of uranium and plutonium to the aqueous waste streams; the measurement of plutonium in its various oxidation states as well as the measurement of the concentrations of oxidizing or reducing agents used for plutonium valence adjustment; the measurement of solvent degradation products in first cycle process and acid wash streams; and the measurement of actinide element impurities in product solutions. In the area of effluent control, the high sensitivity of the laser-based methods

will permit on-line real-time measurements of HTO, $^{129}I_2$, and $^{14}CO_2$ and possibly ^{85}Kr at various points in the off-gas control system in a fuel processing plant. Additionally, measurements of specific fission product and actinide elements present in the high and low activity waste streams may be made using the laser spectroscopic methods.

The high sensitivity, selectivity, and speed of the laser-based analytical methods have been demonstrated in numerous applications outside of the nuclear fuel cycle. The application of these methods to measurements in nuclear-fuel processing plants will greatly improve the response times for critical process and effluent control measurements, will improve dynamic accountability measurements at secondary process and waste streams, and will improve the measurement sensitivity for low-level species in gaseous and liquid effluent streams. The use of active stabilization and/or parallel data acquisition techniques should permit these measurements to be made with a precision and accuracy comparable to that of the conventional analytical methods. Thus the laser-based analytical methods offer exciting possibilities for an improved measurement capability in nuclear-fuel processing plants and elsewhere in the nuclear fuel cycle.

1. Summary of Important Species and Locations for their Measurement in a Nuclear-Fuel Processing Plant

1.1 Introduction

Since the specific flowsheets for the Thorex and Coprocessing solvent extraction processes for irradiated light water reactor (LWR) fuel are still in the definition stage, this discussion of the monitoring requirements (species and locations) in a nuclear-fuel processing plant will deal primarily with operating experience at the duPont Savannah River Plant (SRP). Additional monitoring species and locations which may be necessary or desirable for processing of the higher-burn-up LWR fuels will also be considered. As the technical data summaries for the specific processes become available, the specific monitoring requirements will become better defined.

1.2 Species and Measurement Locations for SNM Accountability

Presently two general approaches are used for the accountability of special nuclear material (SNM) in a fuel processing plant [1.1]. The first is based on the measurement of the total weight or volume of material and a laboratory assay of a representative sample to determine the SNM concentration. This sample assay can be performed by a variety of techniques which include alpha counting, absorption edge densitometry, coulometry, gamma ray counting, gravimetry, isotope dilution mass spectrometry, neutron activation analysis, and x-ray fluorescence [1.2, 1.3]. Presently the standard low-precision method for the analysis of plutonium is alpha counting, and the standard method for the isotopic determination of uranium and plutonium is mass spectrometry. The total measured quantity of SNM (fissionable uranium and plutonium) is then determined by multiplying the weight or volume of

material by its SNM concentration. This measurement approach is generally applied to homogeneous materials which are well characterized and which can be accurately sampled.

The second measurement approach is that of counting the nuclear radiation (induced or spontaneous neutrons or gamma rays) emitted from the total quantity of material. This approach is especially useful for the measurement of SNM in materials which are either inhomogeneous or inaccessable (e.g. solid scrap and waste and the residual hold-up in processing equipment after run-out or clean-out).

In a fuel processing plant, primary and secondary accountability points have been designated [1.4]. The primary accountability points are located in areas of major material flow and in areas where SNM exists in a relatively pure chemical form (e.g. the input dissolver solution and the output product solution). The waste streams, minor side streams and solid wastes where SNM does not exist in a pure form or where the SNM concentration is low have been designated secondary accountability points. The primary accountability points will utilize on-line measurement methods for timeliness and for backup while off-line measurement methods will be used for their high accuracy. The eventual goal for an accountability system is to use automated non-destructive assay (NDA) measurements at all accountability points when high accuracy NDA methods have been developed and demonstrated.

The measurements for SNM accountability in a fuel processing plant are listed in Table 1.1. The measurements for a thorium fuel processing plant will be similar to those listed in Table 1.1 with additional measurements of protactinium-233 required in the input and waste streams to account for the uranium-233 which will be generated by decay.

Table 1.1. SNM accountability measurements in a fuel processing plant[a]

Input Analysis (Primary)	
U	determination in dissolver solution (total solution weight or volume and % U)
Pu	determination in dissolver solution (total solution weight or volume and % Pu)
U	isotopic determination in dissolver solution
Pu	isotopic determination in dissolver solution
U	determination in return scrap solutions
Pu	determination in return scrap solutions
Output Analysis (Primary)	
U	determination in output $UO_2(NO_3)_2$ (total solution weight and % U)
Pu	determination in output $Pu(NO_3)_4$ (total solution weight and % Pu)
U	isotopic determination in output solution
Pu	isotopic determination in output solution
Waste Stream Analysis (Secondary)	
U	determination in liquid wastes
Pu	determination in liquid wastes
U	determination in insoluble solid wastes
Pu	determination in insoluble solid wastes
Analysis of Wash Acid (Secondary, used for annual or semiannual plant cleanup)	
U	determination (total acid weight, % U, and isotopic)
Pu	determination (Total acid weight, % Pu, and isotopic)

[a]Reference 1.5

Mass spectrometry is the principal method used for measuring the isotopic abundances of plutonium and uranium. This isotope measurement is required in all material-balance accounting systems in order to balance both the element and the fissile-isotope inventory [1.1]. A measurement of isotopic abundance is also required in order to compare the results of measurement methods which are isotope selective (e.g. alpha or gamma counting) with those of elemental measurement methods (e.g. wet chemistry and x-ray fluorescence).

The chemical-analytical techniques which are presently used or applicable for use in fuel processing plants have been reviewed [1.2, 1.3, 1.5-1.8] and will be summarized in Chapter 2 of this report. The majority of these analytical methods involve manual operations which are complex and require a trained technician or chemist. For these reasons, any falsification of analytical measurement results would be difficult to detect. Therefore the thrust for future accountability measurements is towards automated on-line analyses for which the falsification of results will be much more difficult and the potential for human error reduced. However, these on-line measurement methods will most likely still be calibrated using standards which have been characterized by the more accurate and reliable off-line methods [1.9].

1.3 Species and Measurement Locations for Process Control

1.3.1 Head-End Operations

A generalized flowsheet for the head-end operations in a Coprocessing fuel processing plant is shown in Figure 1.1. The Coprocessing head-end operations are similar to those of a conventional Purex plant. The head-end operations for the Thorex process, on the other hand, will be different in several important respects:

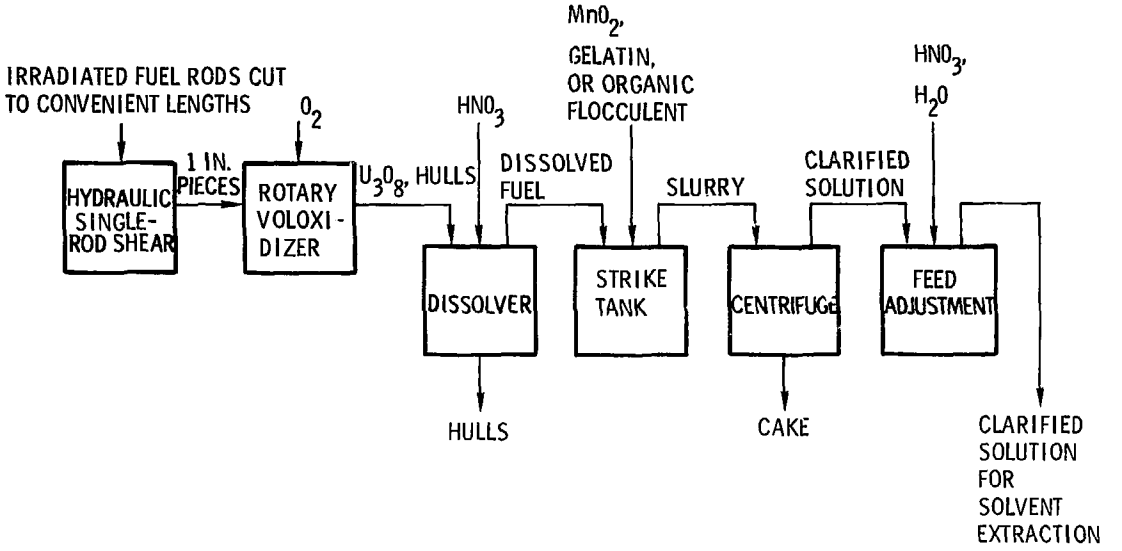

Figure 1.1. Head-end operations for nuclear-fuel processing [1.10].

1. The planned voloxidation of uranium fuels to release tritium as tritiated water relies on a change in crystalline structure in the oxidation of UO_2 to U_3O_8 which occurs at a relatively low temperature ($\sim$ 400°C) [1.11]. A similar voloxidation process does not occur with ThO_2, and it may be necessary to heat the ThO_2 fuel to a very high temperature to release tritium by diffusion. Studies on these differences are currently underway at the duPont Savannah River Laboratory (SRL).

2. In past experience with thorium fuels at SRP the addition of a fluoride ion catalyst (HF) to the dissolver solution was required to obtain an acceptable dissolution rate [1.12]. To improve dissolution, the addition of MgO to the fuel in the manufacture of fuel pellets has been planned in the preliminary Reference Thorium Fuel Cycle [1.13]. However, the use of a fluoride catalyst in the dissolver tank may still be required for fuel dissolution. Studies of the dissolution of thorium fuels are also planned at SRL.

The measurements in the head-end operations (dissolver solution and adjusted feed) which should be considered for process control in a fuel processing plant are listed in Table 1.2. The off-gases released in the head-end operations will be discussed in the section on off-gas monitoring (Section 1.4.1). The concentration of fissionable isotopes in the dissolver tank are measured and when necessary are balanced by the addition of a neutron poison (gadolinium) as a nuclear safety control [1.14]. A measurement of the % Pu(IV) and valence adjustment to Pu(IV) is necessary in the first cycle feed (1AF) to ensure efficient extraction into the solvent thereby minimizing the loss of plutonium to the aqueous waste stream (1AW). A measurement of the neptunium-237 concentration is required so that proper

Table 1.2. Measurements in the head-end operation for process control.

Species	Measurement	Coprocessing Process	Thorex Process
U	concentration	x	x
U	isotopic composition	x	x
Pu	concentration	x	x
Pu	isotopic composition	x	x
Pu	% Pu(IV)	x	x
Th	concentration		x
Gd	concentration	x	x
Np-237	concentration	x	x
Pa-231, 233	concentration		x
---	γ activity	x	x
---	solution density	x	x
HNO_3	concentration	x	x
HF	concentration		x
---	solution temperature	x	x
---	solution flow rate	x	x

steps can be taken to isolate it from the second and third uranium cycles. This is necessary to insure that the uranium product solution will meet the alpha decontamination standards (the proposed specification is < 25-50 alpha disintegrations per minute per gram of uranium [1.15]). A measurement of the protactinium concentration in the Thorex process may be required for this same reason. Additionally, a determination of the protactinium-233 concentration in the Thorex process will be required for future recovery of its decay product uranium-233.

The data in Table 1.3 give an indication of the concentration and isotopic composition of the Coprocessing dissolver solution when irradiated LWR fuel is processed. The typical expected composition of irradiated fuel in the Reference Thorium Fuel Cycle is shown for comparison in Table 1.4.

If voloxidation or a similar process is used, the concentration of tritium in the dissolver solution is expected to be very small. Measurements of voloxidized spent fuel on a laboratory scale have indicated that voloxidation reduces the tritium concentration in the dissolver solution by a factor of 10^4 or more over that measured for dissolved UO_2 fuel [1.17]. If tritium water recycle is used as an alternative to voloxidation, measurements of the tritium concentration in solution will be required to limit the maximum tritium concentration to ~ 2 Ci-ℓ^{-1}($\sim 10^{-4}$M) for safety reasons and effluent control [1.18]. The measured tritium concentration in a LWR fuel dissolver solution in the laboratory was 0.075 Ci-ℓ^{-1}(3.6×10^{-6}M) [1.19].

1.3.2 Solvent Extraction

A generalized solvent extraction flowsheet is shown in Figure 1.2; and a possible flowsheet for Coprocessing is shown in Figure 1.3. This Coprocessing

Table 1.3. Composition of dissolver olution for H. B. Robinson fuel (Purex).[a,b]

Species		Total Concentration
Ura		g-ℓ$^{-1}$
Isotopic composition (atom %)		
^{233}U	0.03	
^{234}U	0.02	
^{235}U	0.67	
^{236}U	0.34	
^{238}U	98.94	
Plutonium		2.56 g-ℓ$^{-1}$
Isotopic composition (atom %)		
^{238}Pu	1.5	
^{239}Pu	56.5	
^{240}Pu	24.6	
^{241}Pu	12.1	
^{242}Pu	5.3	
^{237}Np		0.127 g-ℓ$^{-1}$
^{241}Am		0.055 g-ℓ$^{-1}$
^{242}Cm		0.00013 g-ℓ$^{-1}$
^{244}Cm		0.0067 g-ℓ$^{-1}$

[a] 2.55% U-235 enrichment, 28,000 MWD/MTHM average burnu

[b] Reference 1.16.

Table 1.4. Typical irradiated fuel composition for the reference thorium fuel cycle[a]

Species	Composition of Irradiated Thorium Fuel[b]
Total Thorium	79.16% (by wt.)
^{233}U	1.08
^{235}U	1.79
^{238}U	17.69
Total Fissile Plutonium	0.28

[a]Reference 1.13, p. 12.

[b]Irradiated to 29,000 MWD/MTHM.

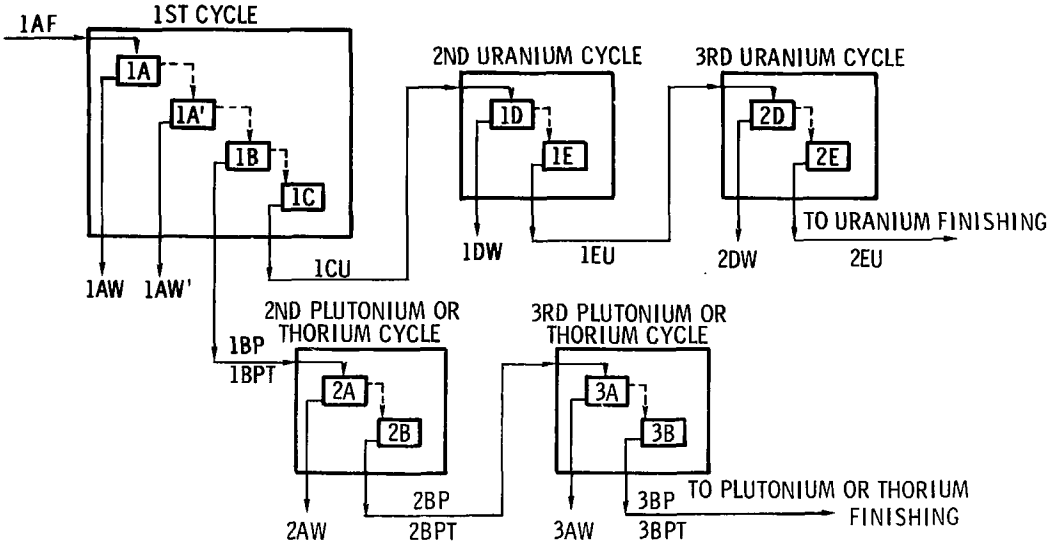

Figure 1.2. Generalized solvent extraction flowsheet [1.20].

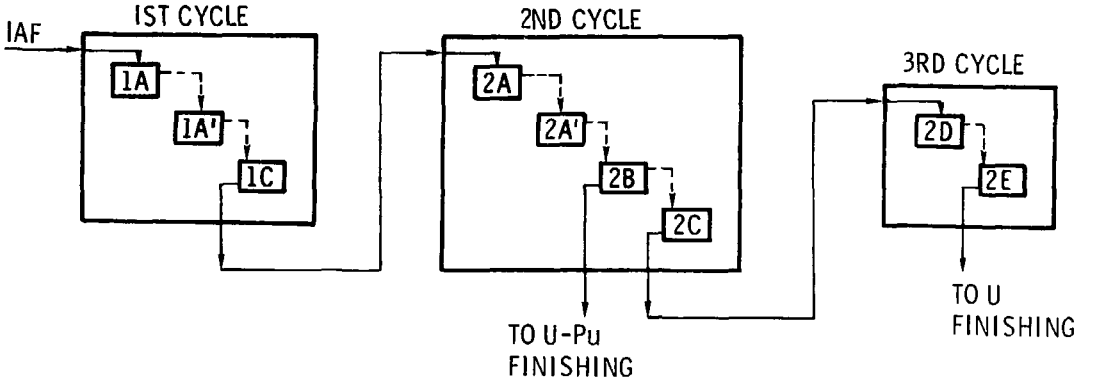

Figure 1.3. Possible coprocessing flowsheet "1.21".

scheme is simpler than either the Purex or Thorex processes in that no further processing of the uranium-plutonium stream is required after partitioning in the 2B bank [1.21].

The possible measurements for the solvent extraction process are listed in Table 1.5. Measurements of the uranium and plutonium concentrations in process streams are required for proper process operation and also for nuclear safety. Measurements of the concentrations of uranium and especially plutonium in the aqueous waste streams will give the first indication of improper operation of the solvent extraction banks. Measurements of the uranium concentration in the 1BP plutonium and 1BPT thorium streams and plutonium or thorium in the 1BU uranium stream are required for optimum partitioning in the 1B bank as well as assurance that the product will meet specifications and thereby minimize recycle.

Proper valence adjustment of plutonium is required to maintain its loss to the aqueous waste streams at or below the design guidelines (< 0.05% loss to any waste stream) and to permit it to be stripped from the solvent at the specified points (1B, 2B, and 3B banks in Figure 1.2). These valence adjustments are accomplished by the addition of reducing agents (e.g. hydroxylamine nitrate (HAN), ferrous sulfamate (FS), or U(IV)) or oxidizing agents (e.g. NO_2^-) to the process solution. A slight excess ($\sim$ 0.01 M) of nitrite is required, for example, to assure a complete conversion to Pu(IV), while a large or variable excess can be detrimental. A large excess of nitrite could consume a portion of the reductant in the 2B contactor and could lead to plutonium reflux [1.22].

For Coprocessing the plutonium/uranium ratio must be closely controlled to simultaneously meet the requirements for mixed oxide (MOX) fuel rod fabrication and safeguards considerations. These requirements require the

Table 1.5. Measurements for solvent extraction process control.

Species	Measurement	Coprocessing	Thorex Process
U	concentration	x	x
Pu	concentration	x	x
Pu	valence	x	x
Pu, U	Pu/U ratio	x	
Th	concentration		x
Np-237	concentration	x	x
Np-237	valence	x	x
Pa-231, 233	concentration		x
Gd	concentration	x	x
HNO_3	concentration	x	x
Reducing agent[a]	concentration	x	x
Oxidizing agent[b]	concentration	x	x
$(HNO_3)_{aq}$	concentration in solvent streams	x	x
TBP[c]	concentration in aqueous streams	x	x
TBP	concentration in solvent streams	x	x
solvent degradation products[d]	concentration	x	x
---	α, γ activity	x	x
---	solution density	x	x
---	solution temperature	x	x
---	solution flow rate	x	x

[a] Hydroxylamine Nitrate, Ferrous Sulfamate, or U(IV).

[b] NO_2^-

[c] Tributyl Phosphate

[d] Dibutyl Phosphate, Monobutyl Phosphate, and PO_4^{-3}.

plutonium/uranium ratio to be in the range of ~ 5-11.7% [1.15]. A higher ratio may possibly be used in process streams with dilution by uranium in the final product solution.

A measurement of the neptunium concentration and valence in the first cycle is required since Np(IV) and (VI) are co-extractable with uranium and, if present in large amounts, can give the uranium product solution an unacceptably high alpha activity thereby necessitating uranium recycle. The current conceptual design for LWR fuel processing assumes that neptunium will be rejected to the 1AW waste stream after valence adjustment to Np(V) with nitrous acid [1.23]. Similarly, special measures such as the addition of phosphate ion (PO_4^{-3}) to the scrub may be required to provide decontamination from protactinium-231 and -233 in the thorium fuel cycle.

A close control of the concentrations of nitric acid in the aqueous streams and tributyl phosphate (TBP) in the solvent streams as well as minimizing cross contamination of the aqueous and solvent streams is required for optimum performance of the solvent extraction process. In addition, the presence of flammable solvents in the high level liquid waste (HLLW) streams should be minimized since it poses a potential fire hazard.

Solvent degradation products (e.g. dibutyl phosphate, monobutyl phosphate, PO_4^{-3} and n-butanol) are present in the first cycle solvent streams and the acid wash streams due to radiolytic decomposition of TBP and should be monitored due to their effect on the solvent extraction process. For example, the presence of dibutyl phosphate (DBP) in the first cycle solvent streams has been shown to decrease the decontamination for Zr-Nb [1.24].

1.4 Species and Measurement Locations for Effluent Control

1.4.1 Off-Gases

The atmospheric releases of radionuclides from fuel reprocessing plants are greatly reduced by the use of effluent control systems and will be even further reduced as improved effluent control systems become available. The present or proposed systems for off-gases include voloxidation and trapping for tritium (HTO) removal, fluorocarbon absorption of ^{85}Kr and ^{14}C (as CO_2), volatilization of iodine (as $^{129}I_2$) from the dissolver solution followed by sorption in a scrubber system, and improved filtration for particulate removal [1.25].

The off-gases (voloxidizer, dissolver, vessel, and waste solidification) in a nuclear-fuel processing plant contain quantities of NO_x (principally as NO_2), HTO, $^{14}CO_2$, ^{85}Kr, $^{129}I_2$, and particulates containing fission products and transuranics. In order to determine the monitoring requirements in off-gas effluent control systems, order-of-magnitude estimates have been made for the temperature and off-gas composition at various stages of the off-gas system of a prototype fuel processing and waste solidification facility [1.26]. These estimates are reproduced in Tables 1.6, 1.7, and 1.8.

Although not listed in Table 1.7, low concentrations of TBP vapors are expected to be present in the vessel off-gases and air cleaning processes are being developed to remove these vapors [1.27]. In addition, fluorine will probably be present in the dissolver and HLLW solidification off-gases in a Thorex plant.

The estimated concentrations of NO_x, ^{85}Kr, ^{3}H, ^{129}I, and ^{106}Ru in the main stack gas are listed in Table 1.9. According to regulatory guidelines and recent

Table 1.6. Estimated dissolver off-gas composition[a,b]

Measurement	Measurement Location					
	After Dissolver	After NO_x Absorber	After Condenser-Demister	After Heater & Filter	After Iodine Adsorber	After Rare Gas Recovery
Temperature (°C)	50	50	25	100	80	25
N_2 (vol. %)	82	86	96	96	96	99
H_2O (vol. %)	12	12	3	3	3	---
NO_x (vol. %)	2	0.5	0.3	0.3	0.3	---
^{85}Kr ($\mu Ci\text{-}cm^{-3}$)	2×10^{1}	2×10^{1}	2×10^{1}	2×10^{1}	2×10^{1}	1
($atoms\text{-}cm^{-3}$)	5×10^{14}	5×10^{14}	5×10^{14}	5×10^{14}	5×10^{14}	3×10^{13}
HTO, HT ($\mu CI\text{-}cm^{-3}$)	6×10^{-2}	6×10^{-3}	6×10^{-4}	6×10^{-4}	6×10^{-4}	---
($mol.\text{-}cm^{-3}$)	2×10^{12}	2×10^{11}	2×10^{10}	2×10^{10}	2×10^{10}	---
$^{14}CO_2$ ($\mu Ci\text{-}cm^{-3}$)	1×10^{-3}	1×10^{-3}	1×10^{-3}	1×10^{-3}	1×10^{-3}	---
($mol.\text{-}cm^{-3}$)	1×10^{13}	1×10^{13}	1×10^{13}	1×10^{13}	1×10^{13}	---
$^{129}I_2$ ($\mu Ci\text{-}cm^{-3}$)	6×10^{-5}	6×10^{-5}	6×10^{-5}	6×10^{-5}	6×10^{-8}	---
($mol.\text{-}cm^{-3}$)	1×10^{15}	1×10^{15}	1×10^{15}	1×10^{15}	1×10^{12}	---
Particulates ($\mu Ci\text{-}cm^{-3}$)	1×10^{-3}	1×10^{-4}	1×10^{-6}	1×10^{-7}	1×10^{-7}	---
($\mu g\text{-}cm^{-3}$)	1×10^{-3}	1×10^{-4}	1×10^{-6}	1×10^{-7}	1×10^{-7}	---

a. Reference 1.26, p. 8.

b. Estimated flow rate 170 $Nm^3\text{-}hr^{-1}$ or 100 scfm.

Table 1.7. Estimated vessel off-gas composition.[a,b]

Measurement	Measurement Location					
	Combined Streams to NO_x Absorber	After NO_x Absorber	After Condenser-Demister	After Heater-Filter	After Iodine Adsorber	After NO_x Reactor
Temperature (°C)	50	50	25	100	80	250
N_2 (vol. %)	66	66	75	75	75	75
O_2 (vol. %)	19	19	20	20	20	20
H_2O (vol. %)	12	12	3	3	3	4
NO_x (vol. %)	1	0.5	0.3	0.3	0.3	5×10^{-3}
HTO ($\mu Ci\text{-}cm^{-3}$)	2×10^{-4}	2×10^{-5}	2×10^{-6}	2×10^{-6}	2×10^{-6}	2×10^{-6}
($mol.\text{-}cm^{-3}$)	6×10^{9}	6×10^{8}	6×10^{7}	6×10^{7}	6×10^{7}	6×10^{7}
I-129[c] ($\mu Ci\text{-}cm^{-3}$)	1×10^{-8}	1×10^{-8}	1×10^{-8}	1×10^{-8}	1×10^{-11}	1×10^{-11}
($mol\text{-}cm^{-3}$)	1×10^{11}	1×10^{11}	1×10^{11}	1×10^{11}	1×10^{8}	1×10^{8}
Particulates ($\mu Ci\text{-}cm^{-3}$)	1×10^{-3}	1×10^{-4}	1×10^{-6}	1×10^{-7}	1×10^{-7}	1×10^{-7}
($\mu g\text{-}cm^{-3}$)	1×10^{-3}	1×10^{-4}	1×10^{-6}	1×10^{-7}	1×10^{-7}	1×10^{-7}

a. Reference 1.26, p. 9,

b. Estimated flow rate 8500 $Nm^3\text{-}hr^{-1}$ or 5000 scfm.

c. 50% as I_2, 50% as organic iodides.

Table 1.8. Estimated HLLW solidification off-gas composition.[a,b]

Measurement	Measurement Location					
	After Calciner Filters	After Scrubber K.O. Pot	After Condenser	After NO_x Removal	After Ru Adsorber and Filter	After Iodine Adsorber and Filter
Temperature (°C)	350	70	25	25	35	35
N_2 (vol. %)	50	52	74	74	74	74
O_2 (vol. %)	15	16	22	22	22	22
H_2O (vol. %)	35	31	3	3	3	3
NO_x (vol. %)	0.1	5×10^{-2}	3×10^{-2}	2×10^{-2}	2×10^{-2}	2×10^{-2}
^{106}Ru[c] ($\mu Ci\text{-}cm^{-3}$)	5	5×10^{-1}	5×10^{-3}	5×10^{-4}	5×10^{-8}	5×10^{-8}
($mol.\text{-}cm^{-3}$)	1×10^{13}	1×10^{12}	1×10^{10}	1×10^{9}	1×10^{5}	1×10^{5}
HTO[c] ($\mu Ci\text{-}cm^{-3}$)	1×10^{-1}	1×10^{-1}	1×10^{-2}	1×10^{-2}	1×10^{-2}	1×10^{-2}
($mol.\text{-}cm^{-3}$)	3×10^{12}	3×10^{12}	3×10^{11}	3×10^{11}	3×10^{11}	3×10^{11}
$^{129}I_2$[c] ($\mu Ci\text{-}cm^{-3}$)	6×10^{-8}	6×10^{-8}	6×10^{-8}	6×10^{-8}	6×10^{-8}	6×10^{-11}
($mol.\text{-}cm^{-3}$)	1×10^{12}	1×10^{12}	1×10^{12}	1×10^{12}	1×10^{12}	1×10^{9}
Particulates ($\mu Ci\text{-}cm^{-3}$)	7×10^{-1}	7×10^{-4}	7×10^{-6}	7×10^{-7}	7×10^{-9}	7×10^{-10}
($\mu g\text{-}cm^{-3}$)	7×10^{-2}	7×10^{-5}	7×10^{-7}	7×10^{-8}	7×10^{-10}	7×10^{-11}

a. Reference 1.26, p. 10.

b. Estimated flow rate 170 $Nm^3\text{-}hr^{-1}$ or 100 scfm.

c. Assuming voloxidation is not used.

Table 1.9. Estimated main stack gas composition.

Species	Concentration			Reference
	$\mu Ci/cm^3$	atoms-or $mol\text{-}cm^{-3}$	ppm	
NO_x	---	1×10^{14}	5	a
^{85}Kr	2×10^{-3}	5×10^{10}	2×10^{-3}	a
	8×10^{-3}	2×10^{11}	8×10^{-3}	b
HTO, HT	2×10^{-5}	6×10^{8}	2×10^{-5}	a
	3×10^{-4}	1×10^{10}	4×10^{-4}	b
$^{129}I_2$	1×10^{-12}	2×10^{7}	7×10^{-7}	a
	3×10^{-11}	6×10^{8}	2×10^{-5}	b
^{106}Ru	$1 \times 10\text{-}10$	2×10^{2}	---	a
	1×10^{-9}	2×10^{3}	---	b

[a]Reference 1.26, p. 11

[b]Reference 1.28, p. 11

EPA standards, the release of particulates, tritium, I-129/131, Kr-85, and alpha transuranics should be monitored on at least a periodic basis [1.26]. Additional measurements at each stage of the plant's effluent control system are required for proper control of the various stages.

1.4.2 Liquid Effluents

The high-level liquid wastes (HLLW) from the fuel processing plant may be concentrated and stored at the plant site for a year or more to permit the short-lived fission products to decay before further processing [1.25]. Alternatively, the HLLW may be solidified immediately after generation [1.29]. Present federal regulations require these HLLW wastes to be solidified within five years after their generation. The expected composition of the HLLW stream at the Allied-General Nuclear Services (AGNS) Barnwell plant is shown in Table 1.10. Monitoring of the waste streams and stored wastes is essential for proper process control, for minimizing environmental release, and also for insuring the integrity of the waste storage tanks.

Table 1.10 Expected composition of the AGNS Barnwell HLLW stream.[a]

Origin	Constituent	Total Abundance grams per MT [b]	Concentration M[c]
Dissolution Acid	HNO_3	---	~ 1
Fission Products	Se	14.4	0.0003
	Br	13.7	0.0003
	Rb	347	0.0071
	Sr	828	0.0166
	Y	416	0.0082
	Zr	3,710	0.072
	Mo	3,560	0.065
	Tc	822	0.016
	Ru	2,330	0.041
	Rh	505	0.0086
	Pd	1,520	0.025
	Ag	82	0.0013
	Cd	136	0.0021
	In	1.2	0.00002
	Sn	25.7	0.00038
	Sb	10.8	0.00016
	Te	535	0.0074
	Cs	2,600	0.034
	Ba	1,750	0.022
	La	1,320	0.0167
	Ce	2,540	0.032
	Pr	1,280	0.016
	Nd	4,180	0.051
	Pm	35.6	0.0004
	Sm	1,010	0.0118
	Eu	174	0.002
	Gd	122	0.0014
	Tb	1.8	0.00002
			0.46
Actinides	U	10,000	0.074
	Np	482	0.0036
	Pu	100	0.0007
	Am	525	0.0038
	Cm	24	0.0002
			0.0823
Impurities and Corrosion	Na	100	0.0077
	Fe	2,000	0.063
	Cr	200	0.0068
	Ni	80	0.0024
			0.080
Soluble Nuclear Poison	Gd	9,000	0.1007
TBP Decomposition	PO_4^{-3}	2,000	0.037
		54,376	

a. Reference 1.30
b. Based on one metric ton of 35,000 MWD/MTHM fuel processed after 150 day cooling period.
c. Waste contained in 150 gal (568ℓ).

2. Summary of Conventional Analytical Methods in Use or Proposed for Use in Nuclear-Fuel Processing Plants

The intent of this chapter is to briefly summarize the principal analytical methods which are presently in use in nuclear-fuel processing plants and those which are being developed for future use in such plants. In Chapter 4 these conventional analytical methods will be compared with the laser-based methods which show promise for use in fuel processing plants. A more detailed explanation of the conventional methods and analytical techniques can be found in one or more of the many reviews and catalogues of the various methods [2.1-2.12].

2.1 Methods for the Determination of Uranium and Plutonium

The analytical methods used for the determination of uranium and plutonium for accountability and process control in a fuel processing plant can be classified as either off-line chemical methods which require separations and manipulations of the sample, or on-line non-destructive assay (NDA) methods. The off-line chemical methods are proven and reliable and are generally very precise as far as the chemistry goes, but are subject to sampling errors and are time consuming [2.5]. The on-line NDA methods, on the other hand, are not as widely applicable as the chemical methods and must be calibrated with standards characterized by the more reliable chemical methods.

2.1.1 Mass Spectrometry

Mass spectrometry is the most important method for the determination of the isotopic concentration of uranium and plutonium in irradiated fuel [2.6].

The use of thermal-ionization mass spectrometry permits a measurement of the isotopic abundances of uranium and plutonium for accountability in a fuel processing plant. From these measurements, the effective atomic weights of uranium and plutonium are also calculated for use in later calculations involving the results of the various element specific methods [2.7]. The use of isotope-dilution mass spectrometry, in which the sample is spiked with an accurately known amount of a selected isotope (e.g. ^{233}U, ^{234}U, ^{242}Pu, ^{244}Pu) prior to the chemical separation stage, permits a quantitative determination of both the isotopic abundance and total concentration of uranium and plutonium.

The chemical separation of uranium and plutonium from each other and from other actinides in the sample is necessary since interferences in mass spectrometry occur from ions having the same m/e ratio (e.g. ^{238}U and ^{238}Pu, ^{241}Am and ^{241}Pu). The chemical separation of the analyte species from fission products prevents contamination of the mass spectrometer and eliminates interferences from the alkali elements (especially K_6 polymers). This separation is performed by solvent extraction and/or ion exchange methods and is time consuming.

Very accurate and precise mass spectrometric measurements can be made with nanogram to microgram quantities of uranium and plutonium. The precision for mass spectrometry can be as high as 0.01 to 0.02% relative standard deviation (RSD) for the major isotopes of uranium and plutonium in well characterized standard solutions but decreases with isotopic abundance to ~ 1% RSD for a relative isotopic abundance of 1% [2.7]. The use of alpha counting provides a more accurate measurement for ^{238}Pu when this isotope is present at a relative abundance of less than 0.7% [2.7]. However, for high-burnup LWR

fuels the isotopic abundance of ^{239}Pu is expected to be in the range of 1-2% [2.13], thus making mass spectrometry the preferred method for the measurement of this isotope at primary accountability points for LWR fuel processing.

The high cost and complexity of the mass spectrometer as well as the long measurement time have generally limited its use in fuel processing plants to primary accountability points (input dissolver solution and output product solution). The isotopic composition and concentration of uranium and plutonium in dissolver solutions are generally determined by thermal-ionization and/or isotope-dilution mass spectrometry [2.6]. Mass spectrometry is also used to determine the isotopic composition of these elements in product solutions. In this case the concentration of uranium and plutonium in these product solutions is generally determined by titrimetry or gravimetry.

2.1.2 Alpha Counting

Alpha counting (pulse-height analysis) is an isotope selective method which is based upon a measurement of the energy spectrum of alpha particles emitted by a sample. This method is generally used for the determination of ^{238}Pu when it is present at an isotopic abundance in the range 0.01-0.7% [2.2]. Due to the short range of alpha particles in solution quantitative alpha analysis is generally performed by depositing a thin film of a purified sample solution on a counting disk. Interference from overlapping alpha peaks from ^{241}Am is minimized by chemically separating the analyte species from the sample solution prior to the measurement. Quantitative ^{238}Pu measurements are made by comparing the integrated count rate of ^{238}Pu with those from ^{239}Pu and

^{240}Pu which have been independently determined by mass spectrometry [2.2]. Measurement precisions of 2% or better have been reported for a counting time of 10 minutes [2.2].

On-line alpha particle detectors have also been used to monitor plutonium in process and waste streams at concentration levels of 10^{-5} to 1 $g\text{-}\ell^{-1}$ [2.5, 2.7, 2.14]. For these measurements, the alpha detector is placed in direct contact with the radioactive solution. Interferences occur from self-absorption and the presence of other alpha emitters in the stream thus requiring the empirical calibration of these monitors using independent methods. With suitable calibration, plutonium can be measured in waste streams with an accuracy of 5-10% [2.14].

2.1.3 Titrimetric Methods

The use of the off-line titrimetric methods based upon oxidation-reduction reactions provides a very precise and accurate method for the determination of uranium and plutonium when the isotopic composition of the sample is accurately known. The titrimetric methods are generally classified as visual-indicator, amperometric, potentiometric, or coulometric methods depending upon the way in which the titration end point is determined. In the visual-indicator method, an exact determination of the end point is difficult and is subject to the personal bias of the analyst [2.5]. This measurement bias is eliminated by the use of the other titrimetric methods which employ electrometric determination of the end point.

The precision of the titrimetric methods can be very high (< 0.1% RSD) when weight burets are used [2.3, 2.5] and thus these methods are used for the measurement of product-type materials in fuel processing plants [2.8].

All titrimetric methods, however, are subject to chemical interferences caused by ions that are electronegative at the oxidation-reduction potentials used or by species that prevent complete oxidation or reduction of the uranium and plutonium [2.2]. For accurate measurements, these interfering species must be removed by chemical separation methods or else their presence must be ascertained and corrected for [2.5].

The titrimetric methods are generally time consuming requiring up to several hours for a measurement. Recently, however, a modified Davies-Gray method has been automated for the determination of uranium [2.8, 2.15, 2.16]. This has reduced the analysis time to less than 15 minutes (1 hour elapsed time if an evaporation or separation is required). With this automated instrument, solutions containing 12-180 mg of uranium have been analyzed with a precision varying from 0.25 to 0.01%; and an accuracy of ~ 0.1% has been measured for solutions containing 80-100 mg of uranium [2.8].

2.1.4 Gamma-Ray Counting

Gamma-ray counting is an isotope specific NDA method for the measurement of uranium and plutonium. Passive gamma-ray measurements permit the accurate determination of all plutonium isotopes except ^{242}Pu which is not a gamma-emitter [2.8, 2.17]. In the quantitative use of gamma-ray counting the emission spectrum of gamma-rays from the sample is measured and the complex spectrum with many overlapping lines is unraveled with the use of a computer and sophisticated algorithms [2.8, 2.13, 2.17-2.19].

The precision of gamma-ray spectrometry depends upon the plutonium concentration and the counting time. For a total sample disintegration rate of about 10^{10} disintegrations per second and a 10 minute counting time a

measurement precision of < 1% has been measured for the least abundant plutonium isotope (^{238}Pu), and the precision increased to 0.05% for the most abundant isotope (^{239}Pu) [2.8]. Similar measurements have been made with total plutonium concentrations between 0.5 and 2.0 $g\text{-}\ell^{-1}$ for which a precision in the range of 0.05-0% was obtained after counting for 1 hour [2.19]. In order to calibrate gamma-ray counting a well-characterized standard solution is used and the detector efficiency must be known. Passive gamma-ray counting can be used as either an at-line [2.19] or an in-line [2.8] measurement method for non-destructive assay in process streams in a fuel processing plant.

Gamma-ray counting has also been used to measure ^{235}U in the concentration range 1-50 $g\text{-}\ell^{-1}$ [2.19]. In this instance, transmission measurements with a ^{169}Yb source were used to correct the measurement results for self-absorption in the sample. Gamma-ray counting can also be used to measure ^{241}Am.

2.1.5 Absorption Edge Densitometry

In contrast to gamma-ray counting which is isotope specific, the total concentration of uranium and plutonium in solution can be determined by measuring the transmission of a collimated external gamma-ray beam through the sample (differential absorptimetry or absorption-edge densitometry) [2.8, 2.14, 2.19-2.21]. Measurements are made with photon sources emitting gamma-rays with energies directly above and below either the K or L-III absorption edges in uranium or plutonium. The photon source can be in the form of an x-ray generator or a natural radioactive source (e.g. $^{75}Se/^{57}Co$ for plutonium measurements and $^{169}Yb/^{57}Co$ for uranium measurements) [2.8, 2.19, 2.20].

Using this method with a $^{75}Se/^{57}Co$ source, plutonium concentrations in the range of 130-360 $g\text{-}\ell^{-1}$ have been made with an accuracy of 0.3 ± 0.2% for

a 20 minute counting time [2.8]. Absorption edge densitometric measurements using the K edges of uranium and plutonium are limited to concentrations on the order of 10 $g\text{-}\ell^{-1}$ or larger [2.20]. The use of the L-III edges permits more sensitive measurements. Concentrations of uranium in the range of 5-35 $g\text{-}\ell^{-1}$ were measured with an accuracy better than 1% (1σ confidence level) for a measurement time of 30 minutes using an x-ray generator at the L-III edge [2.19]. Plutonium measurements were also made in the range of 10-25 $g\text{-}\ell^{-1}$ with a precision of about 0.6% RSD using the L-III edge.

Absorption-edge densitometry shows promise as an in-line or at-line NDA method for measurements of the concentration of uranium and plutonium in process streams after the first cycle of solvent extraction. The method is also applicable for measurements of the thorium concentration in the Thorex process.

2.1.6 X-Ray Fluorescence

X-ray fluorescence spectrometry is an NDA method for the measurement of uranium and plutonium in solid or liquid samples. The method is based upon the detection of the fluorescent x-rays emitted from a sample after excitation by an x-ray generator or a gamma-ray source. Both energy- and wavelength-dispersive detection systems have been used for x-ray fluorescence measurements. Wavelength-dispersive systems offer the best resolution for x-ray energies of $\leq$ 20 keV (L x-rays) while energy-dispersive detection systems offer the best resolution and efficiency at higher energies (K x-rays) [2.19].

X-ray fluorescence solution measurements are generally made off-line with the only sample preparation being the addition of an internal standard to the sample and evaporating the sample solution on a counting disk. This thin film

method increases the measurement sensitivity by reducing the scattered background as compared to the analyte signal [2.19]. The principal source of interference in x-ray fluorescence spectrometry arises from K lines of other elements which overlap the L lines of uranium and plutonium [2.6]. Internal standards are generally used to correct for these matrix effects.

Using x-ray fluorescence spectrometry, plutonium and thorium have been measured in a 50 $g\text{-}\ell^{-1}$ uranium solution at concentrations in the range of 0.1-1 $g\text{-}\ell^{-1}$ with a precision of less than 1% when a counting time of 10-100 minutes was used [2.8]. The possibility of making x-ray fluorescence measurements in a highly radioactive solution (up to 1-2 $Ci\text{-}\ell^{-1}$) has led to its consideration as an alternative to isotope-dilution mass spectrometry for the measurement of uranium and plutonium in dissolver and accountability solutions [2.19].

2.1.7 Neutron Counting

Passive neutron counting can be used as an NDA method for the determination of uranium and plutonium if their isotopic abundances are known. Neutron coincidence counting of ^{238}U and ^{240}Pu spontaneous fissions forms the basis of this method. The spontaneous fission rate is about 460 fissions per second per gram of ^{240}Pu and about 7×10^{-3} fissions per second per gram of ^{238}U. This method has been used primarily for the measurement of solid process line scrap or waste materials and also as a fissionable material hold-up monitor in process lines [2.22].

The active neutron assay method consists of irradiating a sample with neutrons and observing the resulting fission neutrons and gamma rays. The use of active neutron assay has been applied to the measurement of heterogeneous solid scrap and waste materials and also to process streams [2.22].

2.1.8 Gravimetry

Gravimetry is an important and precise method for the measurement of the total uranium concentration in a variety of uranium-bearing materials (uranium in uranium metal, uranyl nitrate solutions, UO_2, UO_3, U_3O_8, UF_4, and UF_6) [2.6]. A gravimetric analysis of these materials is performed by igniting the sample to U_3O_8 and weighing it. For accurate measurements, the presence of any non-volatile metallic impurities is determined spectroscopically and the final measured weight of U_3O_8 is corrected accordingly [2.5]. Measurements are generally made using 1-15 grams of uranium-bearing material and the measurement precision is in the range of 0.02 to 0.08% [2.6]. Gravimetry is rarely used for plutonium due to the difficulty of producing a stoichiometric end product and also because of the problems associated with handling plutonium-containing powders [2.3].

2.1.9 Spectrophotometry

The spectrophotometric measurement of uranium and plutonium in solution is based upon the formation of absorbing complexes of these elements. Spectrophotometric measurements of uranium and plutonium can be made at concentrations of a few $g\text{-}\ell^{-1}$ or less after complexation with one of the colometric agents such as Arsenazo III, basic peroxide, or dibenzoylmethane [2.5]. For the highest measurement precision (0.05% at 12-18 $g\text{-}\ell^{-1}$ of plutonium) a differential spectrophotometric technique is used in which the sample absorbance is compared to that of a reference standard [2.7].

Spectrophotometry has been used to measure uranium and plutonium in fuel processing plants for process control and for the analysis of waste streams and

scrap material [2.7, 2.23]. Measurements of uranyl-nitrate solutions have been made for process control using this method [2.7]. The method has also been used to measure the molar concentration of the various plutonium oxidation states in pure plutonium nitrate solutions [2.24] and can be used for the measurement of the concentration of plutonium-nitrate product solutions with a precision equivalent to that obtained by the best titrimetric methods [2.7]. Spectrophotometric measurements of uranium in waste streams have been made over the concentration range of 0.5 to 5 mg-ℓ^{-1} with a precision varying from 2 to 20%, and thus this method offers an alternative to isotope-dilution mass spectrometry and fluorimetry for the measurement of uranium in waste streams [2.25].

Interferences in spectrophotometry can arise from fission products and actinides which also react with the complexing agents to form colored complexes. These sources of interferences are eliminated by chemically separating the uranium and plutonium in the sample from each other and from other interfering species in the sample. These chemical separations are time consuming but in one instance have been automated to reduce the measurement time to about 5 minutes per sample [2.23]. With this automated instrument, uranium and plutonium were measurable in solution at concentrations in the range of 2-28 g-ℓ^{-1}.

2.1.10 Fluorimetry

The fluorimetric method for the determination of low concentrations of uranium is based on the fluorescence of the uranyl ion [$(UO_2)^{+2}$] when excited by ultraviolet light. This method is applicable to the determination of uranium in waste streams when the uranium concentration is less than 50 mg-ℓ^{-1} [2.5], and can be used to detect uranium in quantities as low as 10^{-10}g [2.26].

Interferences in this method can arise from solution species (esp. transition elements) which quench the uranium fluorescence [2.7]. However, these interferences can be minimized by chemically separating the uranium from the sample or by diluting the sample.

In a fluorimetric measurement, the sample is normally evaporated and fused with a fusion mixture (NaF, Na_2CO_3, or K_2CO_3); and the uranium fluorescence in the fused mixture is excited by a high-intensity mercury lamp at 365 nm. The uranium fluorescence at 535 nm is measured and the concentration in the sample is determined from a calibration curve by interpolation. The reported precision of the method is 13% for measurements of uranium in simulated processing plant waste streams [2.7]. More recently, uranium measurements have been made with a linear range of 0.02 to 10 mg-ℓ^{-1} and a precision of about 9% for a 2 mg-ℓ^{-1} concentration [2.27].

2.2 Methods for the Determination of Fission Product and Actinide Elements

The analytical methods for the determination of the fission product and actinide elements in a nuclear-fuel processing plant are in most cases based upon the detection of the decay radiation (alpha, beta, and gamma) from the analyte species or from one or more of its daughter products. Many of the actinide elements (e.g. ^{237}Np, ^{241}Am, ^{244}Cm) are alpha emitters and thus, after they are chemically separated from other interferring species, they can be detected by alpha spectrometry. Beta decay, which is characteristic of most of the fission products, can be detected by a number of different counting methods such as scintillation detectors, ionization chambers, gas proportional counters, solid state detectors, and Geiger-Mueller (G-M) tubes [2.9]. Prior to using these counting methods, the chemical separation of the

analyte species is generally required to minimize interferences from other beta emitters in the sample. Gamma-ray counting can also be used to monitor a number of fission products (e.g. ^{95}Zr-Nb, ^{106}Ru-Rh, and ^{131}I) and actinides (^{228}Th, ^{233}Pa, and ^{237}Np) in a fuel processing plant. The measurement of specific species will be discussed in more detail in the following sections.

2.2.1 Tritium

Measurements of tritium are difficult due to the very low energy of the beta particles emitted (E_{max} = 18.6 keV and E_{ave} = 5.7 keV). For solution measurements, tritium is chemically separated from any interfering species and is generally determined by liquid scintillation counting [2.9]. In liquid scintillation counting, the analyte species is mixed with a liquid scintillator. When excited by beta particles, the scintillator molecules emit fluorescence which is detected by a sensitive photomultiplier tube (PMT). This method can be extremely sensitive (< 1 pCi-cm^{-3} or ~ 3 x 10^{7} molecules-cm^{-3} of tritium can be detected), and suffers from few interferences (after the chemical separation of the sample). Its primary disadvantage is that it is time-consuming when a chemical separation is required.

The on-line measurement of gaseous HT and HTO can be performed by flowing the gas sample through an ionization chamber or a gas proportional counter after filtering it to remove any radioactive particulates which could interfere with the measurement. Ionization chambers are the most commonly used method for monitoring tritium in air, and can be made sensitive enough to detect as little as 2pCi-cm^{-3} (~ 6 x 10^{7} mol-cm^{-3}) of tritium in air [2.9]. The primary difficulty with using ionization chambers arises from the presence

of ^{85}Kr which has a much higher energy beta (E_{max} = 672 keV) and therefore can produce many times the ionization of a tritium disintegration. Thus the use of an ionization chamber is not recommended unless tritium is known to be the only significant radionuclide present [2.9].

The use of a gas proportional counter for tritium measurements offers an advantage over ionization chambers in that energy discrimination is possible using pulse height detection techniques. The disadvantage of proportional counters for on-line measurements is that the expensive counting gas must be continually mixed with the sample gas and flowed through the counter. Using a gas proportional counter it has been possible to detect as low as 0.1 pCi-cm^{-3} of tritium with a response time of a few minutes [2.9].

Liquid scintillation counting provides a sensitive means for the off-line detection of tritiated water vapor. The HTO is removed from the air over a period of time using a bubbler, dessicant material, or a molecular seive. HT gas can also be measured with this technique by first converting it to HTO. The use of silica gel to trap HTO permits the attainment of sensitivities well below 0.01 pCi-cm^{-3} [2.9]. The sensitivity when using a bubbler is on the order of 0.1 pCi-cm^{-3} [2.9]. The primary disadvantage of these trapping techniques for liquid scintillation counting is that many hours are required to make a measurement.

2.2.2 Krypton-85

Krypton-85 can be measured by detecting its beta decay (E_{max} = 672 keV) or by counting its 0.4% yield gamma-ray emission (514 keV). The most sensitive measurement methods for ^{85}Kr are made by pre-concentrating the krypton prior

to counting. The off-line methods employing liquid or plastic scintillation detectors are extremely sensitive, permitting the detection of the natural ^{85}Kr background levels in the atmosphere ($\sim$ 10 pCi-m^{-3} or $\sim$ 250 atoms-cm^{-3}) with an accuracy ranging from 4-10% [2.9]. Flow-through ionization counters can be used for on-line measurements with a minimum detectable concentration in the range of 40,000 to 130,000 pCi-m^{-3} [2.9]. The interference from tritium in a ^{85}Kr measurement is usually insignificant.

On-line measurements of ^{85}Kr can also be made by detecting its gamma-ray emission using a NaI gamma detector. This method has been installed at the AGNS Barnwell fuel processing plant to monitor the level of ^{85}Kr in the main gas stack [2.12].

2.2.3 Carbon-14

Carbon-14 is a pure beta emitter (E_{max} = 155 keV) with a very long half life (>730 years). The techniques for measuring carbon-14 are similar to those used for tritium and so are the interferences. As a gas, $^{14}CO_2$ can be measured with a gas proportional counter by introducing the $^{14}CO_2$ sample into the counter with the counting gas mixture. Alternatively, $^{14}CO_2$ can be trapped in an organic solvent and detected using liquid scintillation counting. This is the most common carbon-14 measurement method in use today; and activities as low as 0.2 pCi-cm^{-3} (2.7 x 10^{9} mol-cm^{-3}) of organic solvent can be measured [2.9]. This method, however, requires the trapping of carbon 14 over a period of time and also a chemical separation from other interfering radionuclides.

2.2.4 Iodine-129

Iodine-129 has a 17 million year half-life and in decaying emits a low energy beta (E_{max} = 150 keV) followed by a low energy gamma-ray (40 keV), both of which are difficult to detect. The primary methods used for the detection of iodine-129 are liquid scintillation counting and neutron activation analysis; both of which are time-consuming and require that the radioiodine be chemically separated from the sample prior to a measurement.

In the liquid scintillation counting method, the isolated iodine sample is dissolved in the scintillator solution and then irradiated under a fluorescent lamp for two hours to decolor the iodine before counting [2.9]. This is necessary since the iodine would otherwise greatly reduce the counting efficiency by absorbing the fluorescence emitted by the scintillation molecules.

The neutron activation method is based on the transformation of iodine-129 to iodine-130 by a neutron capture reaction. The iodine-130 produced has a very short half-life (12.4 hours) and emits high energy gamma-rays (538 and 669 keV). In the vapor phase, $^{129}I_2$ is trapped on a silver-zeolite material and then transferred to lead-zeolite for neutron activation analysis [2.23]. In measurements of dissolver solutions, the iodine-129 is chemically extracted prior to activation. The sensitivity for a neutron activation measurement is ultimately limited by the presence of iodine-127 and cesium-133 in the sample which can be converted to iodine-130 by multiple activation and n,α reactions respectively [2.9].

2.2.5 Ruthenium-106

Ruthenium-106 is a pure beta emitter which has a very short lived (30 s) daughter, ^{106}Rh, which decays emitting a very energetic beta (E_{max} = 3.53 MeV)

and several gamma-rays (~ 0.5 MeV). In nuclear-fuel reprocessing solutions, ^{106}Ru is a major contributor to the gamma-ray spectrum and is generally counted directly without prior separation. Low concentrations of ^{106}Ru are measured by adsorption on polyethylene beads with subsequent laboratory analysis by counting the decay from its ^{106}Rh daughter [2.1].

2.3 Analytical Methods for Process Control

The measurement of a number of stable species is required for process and effluent control in a fuel processing plant. These species include nitrogen oxides and tributyl phosphate which are present in the off-gases, solvent degradation products such as dibutyl phosphate and monobutyl phosphate which are present in first cycle solvent extraction streams, and nitrite which is added prior to the second plutonium cycle for adjustment to Pu(IV).

2.3.1 Nitrogen Oxides

A number of methods have been developed to measure nitrogen oxides (NO, NO_2) for air analysis. Commercially available automated NO_x analyzers are based upon chemiluminescence, colorimetry, absorption spectrometry (dispersive and non-dispersive), ion-selective electrodes, electrochemical cells, amperometry, and bioluminescence [2.29].

Chemiluminescence analyzers are perhaps the most sensitive and interference-free type of NO_x analyzers. These analyzers are based upon the chemiluminescent reaction between nitric oxide (NO) and ozone with a sensitive PMT used to detect the chemiluminescence. Chemiluminescence analyzers permit the detection of NO in the range from 0.001 to 10,000 ppm [2.29]. They can also be used to measure NO_2 by first catalitically reducing it to NO. These analyzers are free from interferences from other pollutants normally present in the atmosphere and permit real time measurements.

2.3.2 Tributyl Phosphate Vapors

Three methods are presently being investigated for the detection of tributyl phosphate (TBP) vapors in the off-gases in a fuel processing plant. These methods are gas chromatography, x-ray fluorescence, and flame photometry [2.28]. For analysis by gas chromatography, the TBP vapor is collected with an impinger system using ethylene glycol, extracted into hexane, and finally concentrated prior to injection into the gas chromatograph. With x-ray fluorescence, the TBP vapors are trapped by charcoal filters which are analyzed for phosphorous. The detection limit is ~ 0.1 mg of phosphorous per filter [2.28].

Real-time commercially available photometric phosphorous gas analyzers can also be used for the measurement of TBP vapors [2.30]. These analyzers can detect phosphorous in air over the range 0.001 to 10.0 ppm with a response time of less than 10 seconds [2.31].

2.3.3 Solvent Degradation Products

Gas chromatography can be used to determine the concentrations of the solvent degradation products dibutyl phosphate (DBP) and monobutyl phosphate (MBP in irradiated solvent samples [2.32, 2.33]. These species are chemically pretreated to convert them into volatile methyl derivatives prior to injection into the gas chromatograph [2.32].

2.3.4 Nitrite

The nitrite ion concentration in the 2AF feed makeup tank in a fuel processing plant can be monitored on-line by determining the nitrogen dioxide concentration in air which is sparged through the nitric-nitrous acid mixture

[2.34, 2.35]. The NO_2 concentration in the air is determined by measuring its absorbance at 395 nm using a commercial photometric analyzer and is related to the nitrite ion concentration in solution. This method is sensitive to nitrite ion concentrations of 0.01 M or lower [2.34] and will be used at the AGNS Barnwell fuel processing plant for on-line monitoring of nitrite [2.35].

3. Review of Laser-Based Analytical Methods and their Potential for Use in Nuclear-Fuel Processing Plants

3.1 Introduction

With the development of tunable lasers during the past decade, a revival in the field of optical spectroscopy has taken place and a number of new spectroscopic techniques have emerged, some of which were not previously possible using conventional light sources [3.1-3.8]. The usefulness of tunable lasers for spectroscopic applications arises from the unique properties of these spectral sources which include a very high spectral irradiance, a high degree of spatial and temporal coherence, a widely tunable wavelength, and the possibility of operating in either a continuous (cw) or pulsed mode. The properties of lasers which are important for spectroscopic applications are summarized below.

The spectral irradiance of a light source is defined as the amount of power delivered per unit area and frequency interval [$W\text{-}cm^{-2}\text{-}nm^{-1}$]. In the case of lasers this can be some ten or more orders of magnitude greater than that of conventional (incoherent) light sources. Thus the response of a system being probed by a laser is greatly enhanced thereby increasing the sensitivity of the measurement. In addition, the high spectral irradiance of lasers makes possible the observation of a number of nonlinear effects in atomic and molecular systems.

The light emerging from a laser is emitted as a highly collimated beam with a very small angular divergence (typically 10^{-4} - 10^{-7} sr) in contrast to conventional sources which emit light into a large solid angle (typically 4π sr). The highly collimated output from a laser can be transmitted over long distances for remote spectroscopic analysis using LIDAR techniques or can be focused onto very small surface areas ($\leq 10^{-6}$ cm^2) for local

spectroscopic analysis using microprobe techniques. The tunability of laser sources also allows the use of very small sample sizes (< 10^{-12} l) or provides a high degree of spatial resolution (up to 10^{-3} cm) for spectroscopic measurements.

The temporal coherence of a spectral source is reflected in the transform limit by its emission linewidth. In the case of conventional sources the emission linewidth is determined by the combination of Doppler and collisional broadening and is typically ~ 1 GHz. The linewidth of a laser, however, is determined by the interaction of the fluorescence line profile of the corresponding transition in the laser medium and the eigenfrequencies of the laser cavity modes [3.1]. By ensuring that the threshold condition for sustained laser action is fulfilled for only one cavity mode it is possible to obtain laser linewidths on the order of 1 MHz or less. The narrow linewidth of the laser permits the use of coherent detection techniques in a manner similar to radio frequency and microwave spectroscopy thereby further increasing their sensitivity for spectroscopic applications.

The wavelength range over which a laser can be tuned depends upon the particular type of laser under consideration. Organic-dye lasers can be tuned over the range of 360-1200 nm and can be frequency doubled to obtain wavelengths from 197-360 nm. Semiconductor diode lasers are available to cover the range of 0.62-34 μm. Figure 3.1 summarizes the tuning characteristics of these and other tunable lasers.

For many classes of tunable lasers, the user has the choice of cw or pulsed operation. With pulsed operation, laser pulses of ~ 10^{-8} s time duration can be achieved by using either a short time duration pumping pulse or Q-switching the laser. Some types of lasers (e.g. dye lasers)

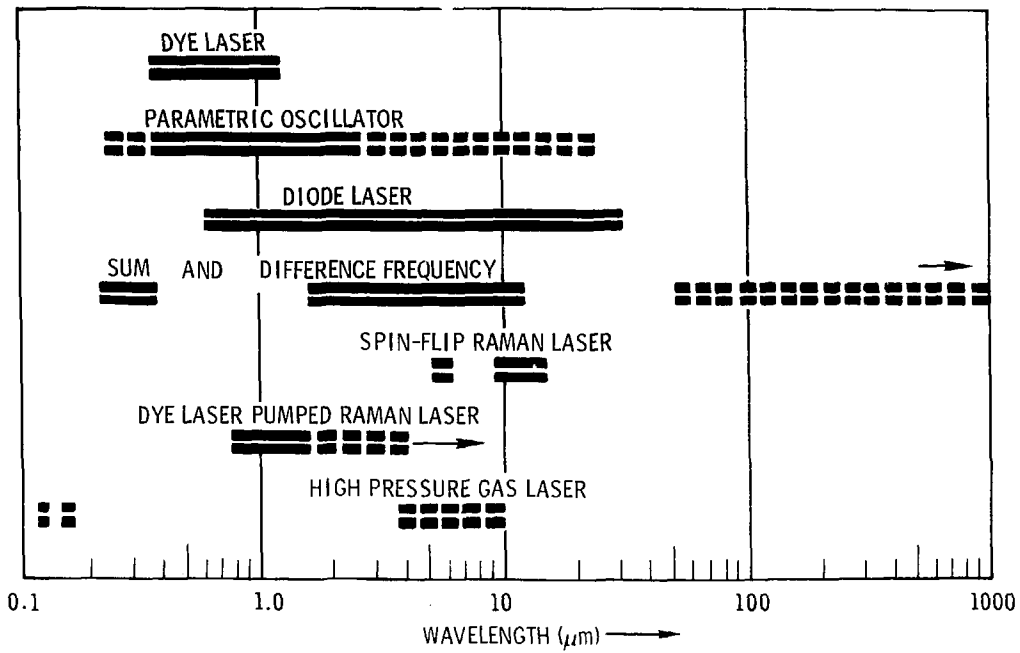

Figure 3.1. Summary of the tuning characteristics of known broadly tunable coherent light sources (solid lines: tuning intervals for which reliable sources are available; dashed lines: possible extensions of tuning intervals which have been demonstrated in laboratory experiments and which are under development). Reproduced from [3.1] with permission.

can be mode-locked for an even shorter pulse time duration ($< 10^{-12}$ s). The use of pulsed-laser operation provides high-peak-power levels which are useful for nonlinear spectroscopy, permit time gating for background noise suppression, and permit range gating. This latter mode of operation is especially important for remote spectroscopic measurements using LIDAR techniques.

The laser-based analytical methods which will be reviewed in this chapter and evaluated for use in nuclear-fuel processing plants are grouped into the four general categories which are listed below:

A. Raman scattering
   1. Spontaneous Raman scattering
   2. Coherent anti-Stokes Raman scattering
   3. Stimulated Raman scattering

B. Absorption spectroscopy
   1. External absorption spectroscopy
   2. Optoacoustic spectroscopy
   3. Intracavity absorption spectroscopy

C. Fluorescence spectroscopy
   1. Atomic fluorescence spectroscopy
   2. Molecular fluorescence spectroscopy

D. Nonlinear spectroscopy
   1. Saturated absorption spectroscopy
   2. Two-photon spectroscopy

The potential of each laser-based method as an analytical tool will be examined in detail in this chapter. In Chapter 4 an evaluation of the laser-based methods will be made comparing them to the conventional analytical techniques.

3.2 Raman Scattering

Raman scattering arises from a change in the polarizability of a molecule which is undergoing a vibration or rotation. The Raman scattered light is shifted from the incident laser frequency by certain characteristic frequencies of the substance [3.10]. Since the Raman effect is extremely

weak, the use of the intense beams from lasers was necessary to promote its use as an analytical method. Presently, spontaneous Raman spectroscopy is the most widely used laser-based analytical method.

Recently, a number of nonlinear Raman effects have been discovered which show promise for use as analytical techniques. The most promising of these nonlinear Raman techniques are coherent anti-Stokes Raman spectroscopy (CARS) and stimulated Raman spectroscopy (SRS).

3.2.1 Spontaneous Raman Scattering

Spontaneous Raman scattering and infrared spectroscopy are complimentary techniques for the study of molecules. Raman scattering arises from a change in the polarizability with coordinate, whereas infrared absorption arises from a change in the dipole moment with coordinate [3.11]. Thus Raman scattering provides insight into molecular structure and dynamics that compliments the information derived from infrared absorption measurements. Raman scattering occurs in gases, liquids, and solids and is useful for chemical analysis of molecular species in all three phases. Because of its widespread use, a number of reviews of Raman scattering have appeared in recent years [3.5, 3.8, 3.10 - 3.16], and it has become the subject of a number of textbooks [3.17 - 3.21].

3.2.1.1 Explanation of Method

Consider a medium placed in an alternating electric field given by,

$$\bar{E} = \bar{E}_o \cos \omega t \ . \tag{3.1}$$

This field induces a polarization which can be written as

$$\bar{P} = \alpha \bar{E} \tag{3.2}$$

where α is the polarizability consisting of two components: a constant term, α_o, which represents the static polarizability, and a second component which is a sum of terms each of which has the periodic dependence of an internal motion or normal frequency of the molecules making up the medium. Thus the polarizability can be written as

$$\alpha = \alpha_o + \sum_n \alpha_n \cos \nu_n t \tag{3.3}$$

where ν_n are the characteristic vibrational or rotational frequencies of the molecule.

Substituting Eqns. 3.1 and 3.3 into Eqn. 3.2 the result is:

$$\begin{aligned} \bar{P} &= \alpha \bar{E}_o \cos \omega t + \bar{E}_o \sum_n \alpha_n \cos \omega t \cos \nu_n t \\ &= \bar{E}_o \cos \omega t + \tfrac{1}{2} \bar{E}_o \sum_n \alpha_n [\cos(\omega - \nu_n)t + \cos(\omega + \nu_n)t] \end{aligned} \tag{3.4}$$

The first term in Eqn. 3.4 gives rise to scattered radiation at the frequency of the incident light and accounts for Rayleigh scattering. The second term results in scattered radiation at the frequencies $\omega \pm \nu_n$. This inelastically scattered light is termed Raman scattering. The components of the scattered light at $\omega - \nu_n$ and $\omega + \nu_n$ are known as the Stokes and anti-Stokes components respectively. The intensity of these components depends on the number of excitations

$$n = [\exp(h\nu_n/kT) - 1]^{-1}$$

present in thermal equilibrium, being proportional to $n + 1$ for the Stokes components and to n for the anti-Stokes components.

In a Raman scattering experiment, the scattered power reaching the detector is given by [3.22]:

$$P_s = P_o\, NL \left[\int \left(\frac{d\sigma}{d\Omega}\right) d\Omega \right]$$

$$\approx P_o\, NL \left(\frac{d\sigma}{d\Omega}\right) \Omega_c \quad \text{(for 90° detection)} \qquad (3.5)$$

where P_o is the incident light power,

N is the concentration of the scattering species,

L is the interaction length viewed by the collection optics,

$\frac{d\sigma}{d\Omega}$ is the differential Raman scattering cross section,

and Ω_c is the light collection solid angle. Eqn. 3.5 shows the spontaneous Raman signal to be linear in the exciting power, concentration of scattering species, and the Raman scattering cross section.

3.2.1.2 Experimental Techniques for Spontaneous Raman Scattering

Figure 3.2 shows a schematic diagram of the experimental apparatus typically used for Spontaneous Raman measurements. An argon ion laser operating at 488.0 nm provides a continuous source of exciting radiation (up to several watts of light power). The laser beam is focused into a volume containing the sample to be studied. The scattered light is collected at right angles to the incident light and, with the aid of lenses and a dove prism, is imaged onto the entrance slit of a spectrometer. As the transmission wavelength of the spectrometer is scanned the Raman lines are detected with a cooled photomultiplier tube (PMT) and the signal is electronically processed and recorded. Photon counting electronics are often used to increase the signal-to-noise ratio of the measurement.

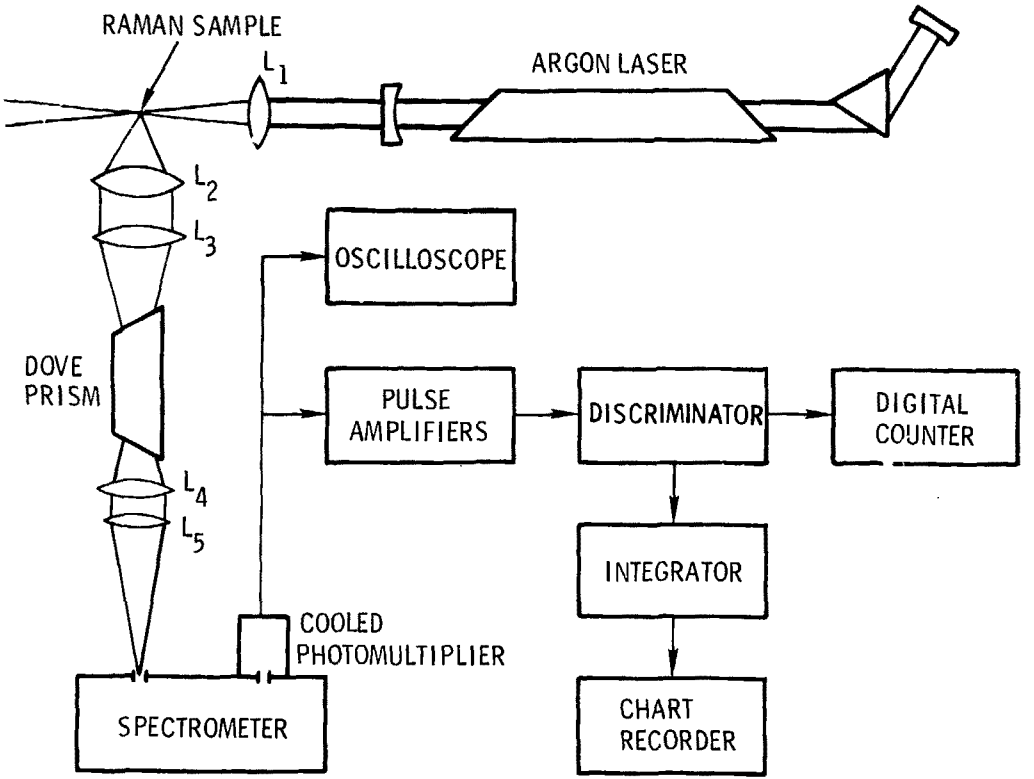

Figure 3.2. Experimental apparatus for spontaneous Raman scattering measurements.

In certain instances, the spectrometer in Fig. 3.2 can be replaced by a narrowband interference filter with a fixed center frequency. In this case, the Raman spectrum is recorded by scanning the laser wavelength using a tunable dye laser as the excitation source [3.23]. In other cases such as for process control where it is desirable to monitor the relative concentration of a particular species with time, the scanning capability of a monochromator is not required. In this case, it may be possible to use a fixed-frequency laser and a narrowband interference filter centered at the Raman line of interest [3.24].

Laser Raman scattering in liquids may be performed on very small sample volumes (as small as 8 nℓ) contained in sealed capillary tubes (typically 0.1 - 1.0 mm i.d.) [3.25]. This greatly simplifies the handling of radioactive solutions for analysis by Raman scattering [3.26, 3.27].

Multiple-pass light trapping cells may be used to increase the Raman signal level and are especially useful for the study of gases. An experimental signal level gain of 93 has been realized with the use of a carefully designed ellipsoidal multiple-pass cell [3.28].

3.2.1.3 Use of Spontaneous Raman Scattering for Quantitative Analysis

Relatively little work has been published on the quantitative analytical applications of laser Raman spectroscopy. The primary reason for this is that the Raman effect is by nature weak, limiting analyses to concentrations on the order of 10^{-4} - 10^{-3} M for most species in solution. The experimentally obtained detection limits for a number of anions in aqueous solution are listed in Table 3.1 and are compared with the calculated limits of detection under ideal conditions. The minimum detectable concentrations of organic substances are similar. For example, benzene has been measured in distilled water at

Table 3.1. Spontaneous Raman scattering detection limits for anions in aqueous solution.

Anion	Lowest Reported Limit of Detection	Calculated Limit of Detection Under Ideal Circumstances
NO_2^-	---	3×10^{-2} M[a]
NO_3^-	3.2×10^{-4} M[b]	7.1×10^{-5} M[c]
SO_4^{2-}	8.9×10^{-5} M[b]	7.6×10^{-5} M[e]
CO_3^{2-}	1.3×10^{-3} M[d]	1.9×10^{-4} M[c]
PO_4^{3-}	5.3×10^{-4} M[d]	2×10^{-2} M[a]
CrO_4^{2-}	1.4×10^{-3} M[e]	3×10^{-4} M[a]
$Al(OH)_4^-$	---	2×10^{-2} M[a]
HPO_4^{2-}	---	1.6×10^{-4} M[c]
$H_2PO_4^-$	---	2.5×10^{-4} M[c]
HCO_3^-	---	1.6×10^{-1} M[c]

a. Reference 3.27
b. Reference 3.29
c. Reference 3.30
d. Reference 3.31
e. Reference 3.26

concentrations down to 6.4×10^{-4} M [3.29]. The ultimate detection limit of benzene in water has been calculated to be $\sim 10^{-5}$ M [3.29]. The generally accepted limit of detection for gaseous species in air at atmospheric pressure using spontaneous Raman scattering is about 100 ppm (parts-per-million) or $\sim 3 \times 10^{18}$ molecules-cm^{-3} [3.22, 3.32, 3.33].

There are several factors which can interfere with a spontaneous Raman measurement: sample fluorescence, Rayleigh and Mie (particulate) scattering, and a background signal from adjacent Raman lines in the sample due to the solvent or other species in a multicomponent mixture. Any sample fluorescence is Stokes-shifted from the excitation frequency and can easily overlap the Raman spectrum. Since fluorescence is a much stronger effect than Raman scattering, any trace amount of a fluorescing impurity in the sample can completely mask out a weak Raman signal. The background from Rayleigh and Mie scattering of the laser light can extend as far as 1000 cm^{-1} from the exciting laser frequency when a large amplification factor is used in an attempt to make Raman measurements at very low analyte concentrations [3.31]. Fluctuations of this background signal due to momentary scattering from dust or suspended solids in the sample can show up as spurious "lines" in the Raman spectrum.

Several techniques are available for minimizing the effects of these interferences on the Raman spectrum. The interference due to sample fluorescence can be either lessened or eliminated through the use of one of the following techniques: irradiating the sample with laser light for a period of time to quench the fluorescence; shifting the laser frequency to a non-fluorescing region of the spectrum; adding a fluorescence quenching agent (e.g. nitrobenzene) to the sample; and chemically purifying the sample or selectively filtering the sample to remove fluorescing impurities [3.21]. The instrumental techniques which have been used to minimize fluorescence interference include: using a

high power laser to saturate the fluorescence but not the Raman signal [3.34]; modulating the wavelength of the laser and phase sensitive detecting the Raman signal while rejecting the essentially constant fluorescence signal [3.35, 3.36]; and using a very short time-duration laser pulse (< 1 ns) and a time-gated detector [3.37]. The presence of Mie scattering in a liquid sample can generally be minimized by pre-filtering the sample solution. Interferences in a spontaneous Raman measurement due to Raman lines of the solvent or other solution species can generally be minimized by the use of an alternate Raman line of the analyte species.

Resonance Raman scattering (which involves the interaction of vibrational and electronic transitions in a molecule) can be used to increase the Raman signal thereby lowering the limit of detection for a given species [3.38]. For gas phase species the increase in Raman signal from resonance enhancement is often offset by an equally large increase in fluorescence. However, in liquids the fluorescence is very often quenched allowing the resonant Raman spectrum to be observed. Resonance enhancement can provide up to a factor of 10^6 increase in Raman signal [3.21].

The use of resonance enhancement should permit the detection of molecular species in solution at concentrations on the order of 10^{-6} M or lower. However, the experimental apparatus for resonant Raman scattering is somewhat more complicated due to the requirement of a tunable laser in the visible or ultraviolet region of the spectrum. In addition, it is more difficult to make highly accurate measurements with resonant Raman scattering due to the sharp variation in Raman scattering cross-section with wavelength near the absorption bands of a substance and due to possible attenuation of the Raman lines by the highly absorbing sample. A Raman difference technique with a rotating cell has been used to eliminate the latter problem of correcting for absorption of the

scattered signal by the sample [3.39]. Rotation of the sample cell will also solve the problem of local heating in the highly absorbing sample.

Resonance Raman spectroscopy has not been used to date for quantitative analysis and further research is needed to develop the technique more fully.

3.2.2 Coherent Anti-Stokes Raman Scattering

Coherent anti-Stokes Raman scattering (CARS) is a nonlinear Raman technique which utilizes two lasers to force the oscillation of a particular normal mode of a Raman-active medium. This in turn generates an oscillating dielectric constant which interacts with the field of one of the lasers to produce a coherent output beam at the anti-Stokes frequency. The generation of a coherent Raman beam greatly increases the ability to collect the scattered light and permits discrimination against unwanted radiation by means of spectral and/or spatial filtering of the CARS signal. A number of reviews and critiques of the CARS technique have been published [3.5, 3.22, 3.32, 3.33, 3.39-3.44].

3.2.2.1 Explanation of Method

The nonlinear nature of the CARS process can be seen from Figure 3.3. In this process, photons from a "pump" laser (ω_p) and a "Stokes" laser (ω_s) interact by means of the third order nonlinear susceptibility, $\chi^{(3)}(-\omega_{as}, \omega_p, \omega_p, -\omega_s)$, in a Raman-active medium to generate photons at the anti-Stokes frequency

$$\omega_{as} = 2\omega_p - \omega_s .$$

The conservation of wave momentum requires that

$$\Delta\bar{k} = 2\bar{k}_p - \bar{k}_s - \bar{k}_{as} = 0$$

where $|\bar{k}| = \frac{\omega n}{c}$. This phase-matching condition is fulfilled by adjusting the angle θ between the two laser beams as shown in Figure 3.4. Using colinear

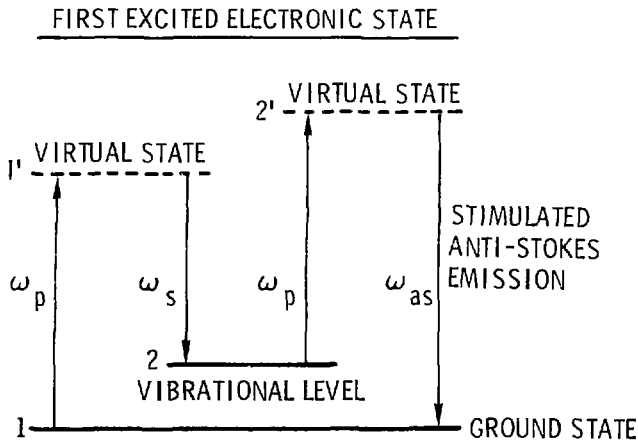

Figure 3.3. Energy level diagram for CARS.

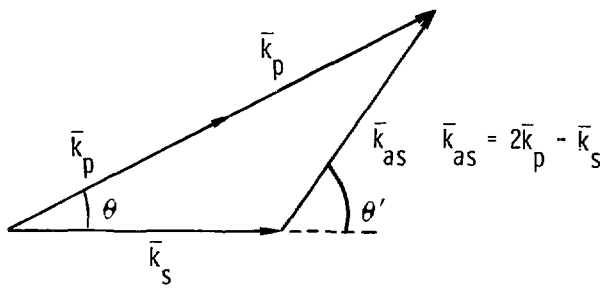

Figure 3.4. Phase-matching conditions for CARS.

laser beams, the phase-matching condition is identically satisfied in gases over reasonable path lengths, while for liquids it can be achieved at a relatively small angle $\theta \leq 1°$ [3.39].

In a CARS experiment the scattered power at the anti-Stokes frequency is given by [3.40]

$$P_{as} \propto \frac{\omega_{as}^2}{n^4} |\chi^{(3)}|^2 L_{coh}^2 \left(\frac{P_p}{A}\right)^2 P_s \qquad (3.6)$$

where n is the refractive index of the medium,

$\chi^{(3)}$ is the bulk susceptibility of the medium,

L_{coh} is the coherence length in the medium,

P_p is the power from the pump laser,

A is the cross-sectional area of the overlap of the laser beams,

and P_s is the power from the Stokes laser.

If the laser beams are tightly focused in the medium the scattering efficiency increases and Eqn. 3.6 reduces to [3.40]

$$P_{as} \propto \frac{\omega_{as}}{n^2} |\chi^{(3)}|^2 P_p^2 P_s \qquad (3.7)$$

Eqns. 3.6 and 3.7 show that the CARS signal varies as the square of the magnitudes of the third order bulk susceptibility (which is proportional to species concentration and to differential Raman scattering cross section), as the square of the pump laser power, and linearly with the Stokes laser power.

The anti-Stokes conversion efficiency, ϵ, given by

$$\epsilon = \frac{P_{as}}{P_s}$$

has been calculated to be 2×10^{-3} for the 992 cm^{-1} Raman line of benzene when a 1 kW pump laser is used [3.39]. For comparison, this same incident power

level would give a spontaneous Raman signal some five orders of magnitude smaller. In addition, the CARS signal is emitted into a 10^{-4} sr diffraction limited beam as compared to 4π sr for spontaneous Raman scattering. These factors together with the fact that the CARS signal is on the anti-Stokes side of the pump laser wavelength are responsible for the excellent background fluorescence discrimination available with the CARS technique (approximately nine orders of magnitude greater than that of spontaneous Raman scattering [3.39]).

Assuming all frequencies are far removed from the electronic levels, the third order nonlinear susceptibility can be written in the form [3.22, 3.39]

$$\chi^{(3)} = N_r \chi_r \frac{\Delta_j \Gamma_R}{(\Delta\nu + i\Gamma_R)} + N_{nr}\chi_{nr} \tag{3.8}$$

where N_r, N_{nr} are the concentrations of the analyte species and solvent respectively,

$\chi_r = \chi_r' + i\chi_r''$ is the complex resonant part of the susceptibility contributed by the closest vibrational-rotational transition,

χ_{nr} is a slowly varying nonresonant susceptibility contributed by the electronic transitions and remote resonances,

Δ_j is the fractional population difference between the upper and lower vibrational-rotational levels,

Γ_R is the half width at half-maximum of the Raman mode,

and $\Delta\nu = \nu_p - \nu_s - \nu_R$ is a detuning frequency. Eqn. 3.8 can be rewritten in the form

$$\chi^{(3)} = \left(N_r \chi_r' \frac{\Delta_j \Gamma_R}{(\Delta\nu + i\Gamma_R)} + N_{nr}\chi_{nr} \right) + iN_r\chi_r'' \frac{\Delta_j \Gamma_R}{(\Delta\nu + i\Gamma_R)}$$

to separate the real and imaginary contributions to the nonlinear susceptibility. The CARS signal is proportional to the square of the absolute value of $\chi^{(3)}$:

$$|\chi^{(3)}|^2 \propto |N_r\chi_r' + N_{nr}\chi_{nr}|^2 + |N_r\chi_r''|^2$$

$$= N_r^2\left(|\chi_r'|^2 + |\chi_r''|^2\right) + N_{nr}|\chi_{nr}|^2 + 2N_rN_{nr}|\chi_r'||\chi_{nr}| \qquad (3.9)$$

For small analyte concentrations, N_r, the resonant susceptibility is small; and since the nonresonant susceptibility is relatively independent of frequency, the contribution of $\chi^{(3)}$ to the CARS spectrum is in the form of the last term in Eqn. 3.9:

$$|\chi^{(3)}|^2 \propto 2N_rN_{nr}|\chi_r'||\chi_{nr}|.$$

Thus the CARS lineshape will reflect the asymmetry of the real part of the susceptibility χ_r' and the CARS signal will be linear with the concentration of the analyte species. As the relative contribution of the resonant susceptibility changes with increasing analyte concentration, the lineshape and concentration dependence of the CARS signal will change.

The lowest concentration level which can be detected using CARS will in general be determined by the nonresonant background signal from the solvent. Recently, four-wave mixing techniques have been demonstrated which promise to reduce this background signal contribution [3.43, 3.45]. The sensitivity of CARS can be further increased by using resonant enhancement which occurs when either the pump or Stokes laser frequency is tuned to coincide with an electronic transition of the analyte species.

3.2.2.2 Experimental Techniques for CARS

Figure 3.5 shows the experimental apparatus for CARS. Pulsed and/or cw lasers can be used for CARS although pulsed lasers have generally been used due to the nonlinear dependence of the scattering efficiency on the pump laser power. Often, a high power pump laser is also used to excite a tunable dye laser which serves as the Stokes laser. The two laser beams are focused in the sample at the required phase-matching angle, θ, and the CARS signal emerges from the sample with an angular displacement, θ'. The CARS signal is generally spatially and spectrally filtered to prevent sample fluorescence and/or resonantly scattered laser light from reaching the detector which is usually a photodiode. As the frequency of the Stokes laser is scanned the CARS spectrum is generated and recorded.

In the case of CARS in gases, phase-matching is identically satisfied and the two laser beams can be colinear. Dispersive elements such as prisms or gratings are then used to separate the CARS signal from the laser beams.

3.2.2.3 Use of CARS for Quantitative Analysis

The CARS detection limits for some liquid and gaseous species are listed in Table 3.2. The sensitivity for measurements in liquid solutions is in general limited by the nonresonant background signal from the solvent to concentrations on the order of 0.05 M [3.48]. The nonresonant background signals from a number of solvents have been measured relative to that of water and are shown in Table 3.3. In compiling Table 3.3, competition from stimulated Raman emission prevented accurate measurements of the nonresonant background levels from benzene, toluene, m-xylene, and benzyl chloride [3.49].

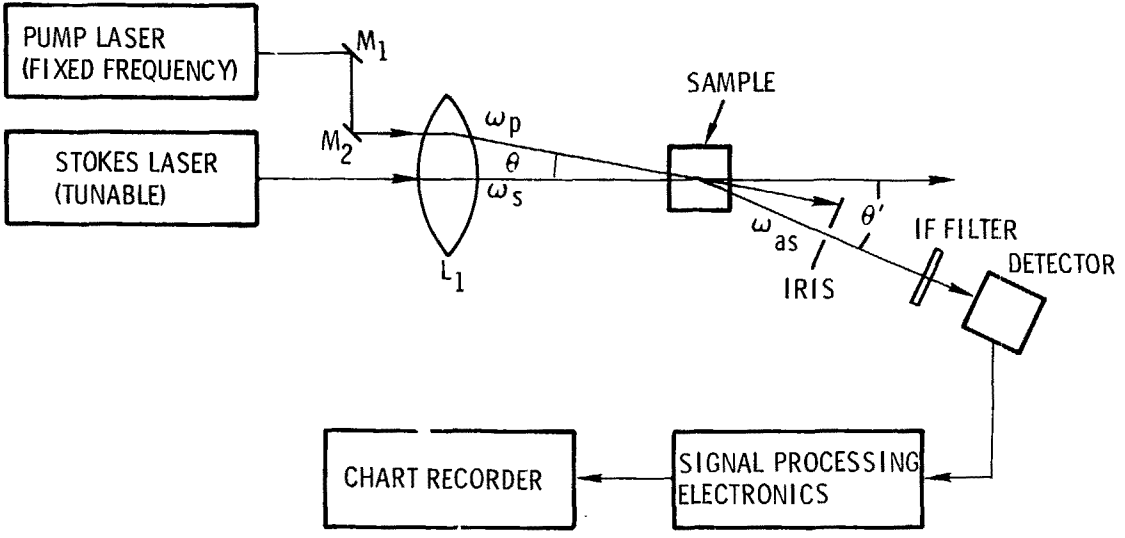

Figure 3.5. Experimental apparatus for CARS measurements.

Table 3.2. CARS detection limits for liquids and gases.

Analyte Species	Solvent	Minimum Detectable Concentration	Reference
Sodium Benzoate	Water	0.08 M	3.40
Benzene	Toluene	< 0.005 M	3.46
Benzene	$(\text{Sodium Benzoate})_{aq.}$	< 0.5 M	3.46
H_2	N_2	~ 100 ppm	3.47
H_2	Air	4 ppm[a]	
N_2	Air	160 ppm[a]	
O_2	Air	160 ppm[a]	3.33
CO	Air	160 ppm[a]	

a. Calculated for S/N = 1.

Table 3.3. Nonresonant background signal levels in CARS.[a]

Solvent	Background Level Relative to water = 1.0
D_2O	1.0
Methanol	1.0
Ethanol	1.8
Tetrahydrofuran	2.3
Carbon tetrachloride	2.6
Chloroform	2.6
Methylene Chloride	2.6

a. Reference 3.49.

The measurement of trace gas constituents at atmospheric pressure is generally limited to concentrations $\geq$ 100 ppm due to the nonresonant background signal levels of the major gas constituents. In the case of measurements of H_2 in N_2, the background contribution from N_2 gives a constant signal level below $\sim$ 100 ppm of H_2 [3.47].

The minimum detectable concentration in either gas or liquid phase measurements can be lowered by some 1-3 orders of magnitude through the use of pre-resonance or resonance enhancement of CARS. Pre-resonance enhancement occurs when either ω_p or ω_{as} approaches an electronic resonance in the material, and resonance enhancement occurs at an electronic resonance. Table 3.4 lists the minimum detectable concentrations of some species measured using resonant CARS. The diffraction limited CARS signal can be filtered to provide excellent discrimination against any fluorescence which may be generated in gases as the pump laser is tuned to an electronic resonance. In a spontaneous Raman experiment, on the other hand, the presence of fluorescence in gases generally prevents full utilization of resonance enhancement.

The CARS technique is also capable of measuring minor constituents in flowing sample cells [3.48, 3.52]. The use of a flowing sample cell permits the possibility of on-line measurements and also minimizes sample heating and the resultant formation of thermal gradients. CARS measurements have been made at flow rates of 0-900 $cm\text{-}s^{-1}$ with no observed variation in the signal-to-noise ratio [3.48].

In making quantitative CARS measurements, special consideration must be given to the factors which affect the amplitude and lineshape of the scattered signal. Since the CARS signal varies as $P_p^2 P_s$, any amplitude fluctuations in the laser intensities will be reflected in the scattered signal. For example,

Table 3.4. Detection limits for resonance CARS.

Analyte Species	Solvent	Minimum Detectable Concentration	Reference
Cyanocobalamin	H_2O	$\sim 10^{-3}$ M	3.49
Ferrocytochrome c	H_2O	$< 10^{-3}$ M	3.49
Diphenyloctatraene	Benzene	$\sim 5 \times 10^{-5}$ M	3.50
β-carotene	Benzene	$\sim 10^{-7}$ M	3.48
I_2	Air	$< 10^{3}$ ppm	3.51

an amplitude variation of 5% in both lasers will give rise to an 11% variation in the CARS signal. This effect, however, can be minimized by normalizing the CARS signal to the nonresonant background signal from a suitable gas or solvent contained in a reference cell.

From Eqns. 3.7 and 3.9 it can be seen that the CARS signal varies as the square of species concentration at high concentrations and linearly with species concentration at relatively low concentrations. The nonlinear susceptibility $\chi^{(3)}$ also varies as the fractional population difference between the upper and lower vibrational-rotational levels (Eqn. 3.8). Thus, in the case of gases a very high pump laser power can alter this population difference thereby producing a change in the scattered signal level which would be interpreted as a change in species concentration [3.53]. This problem can be avoided by operating at a lower laser power level and using a sensitive PMT to detect the CARS signal.

The relative contributions of the resonant and nonresonant parts of the total susceptibility will also affect the lineshape of the CARS spectrum. This variation in lineshape with analyte concentration may make it very difficult to interpret the CARS data in a quantitative manner. The CARS lineshape can vary with concentration from a positive-shaped Lorentzian to a dispersion-shaped curve, and then to a negative-shaped Lorentzian. If resonance enhancement of CARS is used this change in lineshape can be a very sensitive function of the analyte concentration. In the case of resonance CARS measurements of β-carotene, the lineshape was observed to vary from a positive to a negative Lorentzian as the analyte concentration was decreased by a factor of 5 ($\sim 2.5 \times 10^{-4}$ to $\sim 5 \times 10^{-5}$M) [3.53].

Much work still needs to be performed to develop coherent anti-Stokes Raman scattering into a reliable technique for quantitative analysis. The sensitivity of the technique is slightly lower than that of spontaneous Raman scattering, but it has a distinct advantage in areas where background fluorescence is a problem or where time resolved measurements must be made. In addition, the CARS technique offers the possibility of resonance enhancement in both liquids and gases, and in this respect has an advantage over spontaneous Raman scattering for which resonance enhancement of gases is often completely masked by fluorescence. However, great care must be exercised in interpreting the CARS spectrum to obtain reliable quantitative information.

3.2.3 Stimulated Raman Scattering

Stimulated Raman scattering (SRS) is similar to CARS in that two lasers are used to force a particular normal mode of a Raman-active medium. However, in the case of SRS the measured signal is in the form of an induced loss (gain) of the laser at the anti-Stokes (Stokes) frequency. The SRS signal is imposed upon a collimated laser beam thereby permitting discrimination against sample fluorescence in a manner similar to that used for CARS. However the SRS technique has certain advantages over CARS in that phase-matching is not required, there is no nonresonant background susceptibility term in the scattered signal, and the generated gain (loss) in the small-signal approximation is linear in the species concentration, the third order susceptibility and the power from each laser so that the spectra obtained are similar to the spontaneous Raman spectra.

Stimulated Raman scattering has also been termed "Raman amplification" or "inverse Raman scattering" depending on whether a gain or loss is generated

by the Raman-active medium. SRS was first observed in 1964 [3.54] but, as in the case of CARS, it is only recently that the technique has been considered for analytical use. However, it is included in this study since it retains most of the advantages of the better-known CARS technique with few of the disadvantages; and thus shows great promise as a nonlinear Raman scattering technique.

3.2.3.1 Explanation of Method

The SRS process occurs when a pump laser beam of intensity I_p and a colinear Stokes or anti-Stokes probe beam (I_s, I_{as}) interact with a Raman-active medium. The intensity of the probe beam is increased or decreased as it traverses the Raman-active medium when one of the following conditions are satisfied:

$$\omega_p - \omega_s = \omega_R \quad (gain)$$

$$\omega_{as} - \omega_p = \omega_R \quad (loss) ,$$

where ω_R is the frequency of Raman normal mode. The intensity of a Stokes probe beam exiting a sample in a SRS experiment is given by [3.55]:

$$I_s(L) = I_s(0) \exp\left(gN \int_0^L I_p(z)\, dz\right)$$

where L is the path length in the sample,

g is the Raman gain coefficient for a single molecule,

N is the molecular species concentration,

and $\int_0^L I_p(z)\, dz$ accounts for the attenuation of the pump laser beam due to absorption and scattering.

The Raman gain coefficient in a wavelength region free from electronic or vibrational resonances is given by

$$g = \frac{8\pi c^4}{\hbar \omega_p n^2 \Delta\nu_R} \frac{\partial\sigma}{\partial\Omega}$$

where $\Delta\nu_R$ is the Raman linewidth.

The change in intensity of the Stokes probe beam upon traversing the sample is

$$\Delta I_s = I_s(L) - I_s(0)$$

$$= I_s(0) \left[\exp\left(gN \int_0^L I_p(z)\, dz\right) - 1 \right] . \qquad (3.10)$$

In the small-signal approximation for which the Raman gain is low and absorption of the pump beam is negligible, Eqn. 3.10 can be written as

$$\Delta I_s \approx gNLI_s I_p . \qquad (3.11)$$

Similarly, the loss in intensity of a probe beam at the anti-Stokes frequency is

$$\Delta I_{as} \approx -gNLI_{as} I_p . \qquad (3.12)$$

From Eqns. 3.11 and 3.12 the SRS signals are seen to be linear in species concentration, differential Raman scattering cross-section, sample path length, and laser intensities.

An alternative theoretical description of the SRS process in terms of the nonlinear polarization and third order susceptibility [3.22] shows the

Raman gain (loss) to be proportional to $\mathrm{Im}\chi^{(3)}$ and therefore directly reflects the Raman spectra. In addition, a refractive index change, in proportional to $\mathrm{Re}\chi^{(3)}$ is induced in the medium at the frequency of the probe beam. The electronic background contribution $\chi_{nr}^{(3)}$ is identical to that in a CARS experiment but affects the SRS measurement only indirectly through the refractive index variation which may lead to a slight distortion of the probe beam at very high pump powers.

3.2.3.2 Experimental Techniques for SRS

The experimental apparatus used for a SRS measurement is similar to that shown in Figure 3.5. In the case of SRS, the pump and probe beams can also be made colinear since phase-matching is not required. If this is done, dispersive elements are used to separate the probe beam from the pump beam after exiting the sample. If the pump laser is pulsed or amplitude modulated, the periodic SRS signal impressed on the Stokes laser beam can be detected using gated or synchronous detection techniques.

SRS measurements have been demonstrated using both cw and pulsed lasers. The use of a narrowband cw probe beam permits the attainment of a resolution limited only by the laser linewidth [3.56, 3.57]. Alternatively, a broadband probe laser can be used in conjunction with a spectrometer and a linear array detector to record an entire SRS spectrum in a single laser pulse (as short as 10 ns). The sensitivity of these measurement techniques may also be increased by placing the sample within the cavity of the probe laser [3.55, 3.58-3.60].

3.3.3.3 Use of SRS for Quantitative Analysis

The little reported work on the quantitative use of SRS indicates the minimum detectable concentration of individual components in mixtures lies in the range of 10^{-3} - 10^{-1}M [3.58, 3.60]. Thus the sensitivity of SRS is intermediate between that of CARS and spontaneous Raman scattering. Resonance SRS measurements are also possible, and intracavity measurements of organic dyes in ethanol have been demonstrated at concentrations as low as 10^{-6}M using inverse Raman scattering and 2 x [illegible] using Raman amplification [3.59].

Estimates of the detection capabilities of SRS for gases at atmospheric pressure indicate that H_2 could be detected at a concentration of ~ 1 ppm using a 1 MW frequency-doubled Nd:YAG pump laser (10 ns pulse time duration and operated at 20 pps), a 1 W cw dye probe laser, and a 3 s integration time [3.61]. Lower hydrogen concentrations could be measured by increasing the integration time and/or the pump laser power. However, the maximum pump power which can be used will be limited by saturation or the threshold for stimulated Raman scattering in the solvent.

Since phase-matching is not required for SRS, multi-pass light trapping cells may be used to further increase the sensitivity of SRS measurements. Such multiple-pass cells are capable of providing an estimated 50-100 fold increase in sensitivity [3.61]. The use of hollow-core optical fibers has also been suggested as a means of increasing the interaction path length for solution measurements and thereby lowering the detection limit [3.41].

3.2.4 Evaluation of Raman Scattering Methods for Use in Nuclear-Fuel Processing Plants

3.2.4.1 Previous Use in the Nuclear Fuel Cycle

Spontaneous Raman spectroscopy has been used in the nuclear fuel cycle to measure oxyanions in nuclear waste materials. Measurements have been made on waste liquors from the Savannah River Plant [3.26] and on waste liquors, salt cake, and sludge (composed of insoluble salts and hydroxides) from the Hanford Plant [3.27]. The measurement of the ionic composition of these radioactive waste materials is essential for monitoring the integrity of the liquid nuclear waste storage tanks, developing nuclear waste solidification methods, and reducing waste liquors to salt cake using previously developed procedures [3.27].

In making these spontaneous Raman measurements the radioactive waste samples were first clarified by filtration or centrifugation and then sealed in glass capillaries for control of radioactivity. The 488.0 or 514.5 nm lines from an argon ion laser were used to excite the sample, and the Raman spectra were recorded using commercial Raman spectrometers. The oxyanions measured included NO_2^-, NO_3^-, SO_4^{2-}, CO_3^{2-}, PO_4^{3-}, CrO_4^{2-}, $A\ell(OH)_4^-$, and $C\ell O_4^-$. No difficulties were experienced with sample fluorescence although the radioactive waste samples were observed to be distinctly yellow or yellow-green in color due to high nitrite and chromate ion concentrations [3.26].

In measuring the Savannah River Plant waste solution, the 1050 cm^{-1} line of NO_3^-, which is present at a high concentration in the waste, was used as an internal standard [3.26]. The NO_3^- concentration was then independently measured relative to the 935 cm^{-1} line of $C\ell O_4^-$ after the addition of a known quantity of 2M $NaC\ell O_4$ to a radioactive waste sample. Peak height measurements were made with the reproducibility of a single peak height measurement being ± 4.6% at the 95% confidence level.

The measurement of $CO_3^{=}$ at 1087 cm^{-1} in the waste solution was not possible without prior separation due to a strong nitrate peak at 1049 cm^{-1} (Ref. 11). With the exception of $CO_3^{=}$, the total measurement time for analysis of the anions in the Hanford waste by spontaneous Raman scattering was 1.6 hours. When compared to the estimated 2.2-3.6 hours which would be required to measure these same anions using a number of different conventional analytical methods, the advantage of the simultaneous analysis capability of spontaneous Raman spectroscopy is evident.

3.2.4.2 Possible Measurement Species

The measurement of gaseous species in a nuclear-fuel processing plant by the Raman scattering methods will not be considered here since, with the exception of NO_x, the concentrations of interest for the off-gases are all at or below the detection limit for the Raman methods (~ 100 ppm). A number of species in solution could possibly be measured at concentrations above 10^{-4} - $10^{}$ using the various Raman scattering methods. The area of greatest applicability for these methods would probably be for process control although measurements could also be made for accountability and effluent control.

In the head-end operations for the coprocessing process, Raman scattering could be used to measure the concentrations of uranium, plutonium and possibly neptunium in the form of nitrates in the dissolver tank and adjusted first cycle feed (1AF in Figure 1.2) at or below the concentration levels listed in Table 1.3. In the Thorex process, Raman measurements of thorium and possibly protactinium concentrations in the head-end operation could be made. The concentration of HTO in the dissolver solution will probably not be measurable with these methods unless resonance enhancement is used to increase the sensitivity of the Raman methods or tritium recycle

is used to increase the HF concentration. Additionally, the Raman methods could possibly be used as a valence monitor of plutonium in the feed adjustment tank prior to the first cycle of solvent extraction.

In the solvent extraction process, the Raman measurements which could be made include the determination of the concentrations of uranium, plutonium, thorium, and the reducing and oxidizing agents; the relative abundances of TBP and n-paraffin in the solvent and aqueous streams; the relative abundance of HNO_2 in the solvent streams. The Raman methods may also permit a measurement of solvent degradation products, particularly in the first cycle where the concentrations are greatest. Additionally, the Raman methods could be used to monitor the valence of plutonium throughout the solvent extraction process and could possibly serve as a Pu(IV) monitor for coprocessed streams. The presence of suspended solids which have been observed in the clarified feed and process streams when high-burnup LWR fuels are processed [3.62] will most likely require that the sample solution be filtered prior to any Raman measurement.

From the design guidelines for the loss of uranium and plutonium to the aqueous waste streams ($\leq$ 0.01% for uranium, $\leq$ 0.05% for plutonium [3.63]) and the expected concentration ranges in the various process streams resonance enhancement of Raman scattering will likely be required for the measurement of uranium and certainly for plutonium in the aqueous waste streams. Resonance enhancement of Raman scattering should be possible using tunable dye laser sources since both $UO_2(NO_3)_2$ and $Pu(NO_3)_3$ have strong absorption bands in the visible region of the spectrum.

The Raman methods could be used for accountability measurements in homogeneous solutions containing SNM. These methods could measure the total concentration of uranium and plutonium but are not expected to be

is not specific. In addition, the low precision of these methods [illegible] expected for spontaneous Raman scattering would likely eliminate their use [illegible] secondary assay and/or safeguards methods rather than as primary assay and/or safeguards methods.

Spontaneous Raman spectroscopy already has a demonstrated capability for the measurement of oxyanions in radioactive waste solutions [3.66, 3.67]. The Raman method could be applied to the simultaneous measurement of these and a number of other molecular species in the HLLW stream at or below the concentration levels listed in Table 1.1[illegible].

The selection of the Raman method to be used for a particular measurement will depend upon a number of factors: the expected concentration ranges and species to be measured; the matrix in which the measurement is to be made; the required measurement precision and accuracy; the availability of suitable standardization procedures, and requirements for rapid measurements, on-line capability, and automated operation. These factors will be discussed at greater length in the following sections and the principal advantages and disadvantages of the Raman scattering methods will be summarized.

3.2.4.3 Isotope and Molecule Specificity

The Raman methods are isotope specific for the light elements due to the large isotope shifts in the vibrational spectra of molecules containing these elements [3.64]. However, in the case of the heavy elements such as the actinides, the isotope shifts are not expected to be resolvable in Raman scattering.

Each Raman line arises from a normal mode in a molecular species and thus the total Raman spectrum provides a unique signature of that species. However, a specific Raman line arising from a particular bond pair will not in general be molecule specific since this line will occur in any molecule containing this

same bond pair with perhaps a slight shift in the Raman frequency. Therefore, when molecule specificity is desired in Raman scattering either the entire Raman spectrum should be measured or else one or more lines should be selected which are unique to the molecule of interest in the sample. On the other hand if an entire class of molecular species are to be measured, one or more Raman lines can be chosen which occur in every species in that class. For example, to monitor the relative concentration of solvents in the aqueous waste and process streams the CH, CH_2, and CH_3 stretching vibrations in the region between 2850 and 2970 cm^{-1} can be used [3.65].

The isotope and molecule specificity of coherent anti-Stokes Raman scattering will be slightly better than that of spontaneous Raman scattering or stimulated Raman scattering due to the smaller linewidth of the CARS bands. This slight decrease in linewidth of the CARS bands arises from the interaction between the real parts of the susceptibility of the solute (χ_r) and the solvent (χ_{nr}) which combine in such a way as to lower the total susceptibility between the Raman lines [3.32].

The selection rules for CARS are also slightly different from those of spontaneous Raman scattering since CARS is a four-photon process and the polarization of each laser beam can be oriented independently [3.40]. The selection rules for CARS indicate that all Raman-active modes will be CARS-active and, in addition, certain modes will be CARS-active which are neither Raman- or infrared-active [3.66]. These additional CARS-active modes may prove useful in increasing the molecule specificity of this method in instances where spectral interferences may prevent the use of the Raman-active modes.

[illegible] Sensitivity & Matrix Variations

The measurement of small concentrations of a given species in solution may not be possible under certain conditions using the Raman method due to the interference of nearby Raman lines from other species which are present in much larger concentrations. In the case of the solvent extraction streams in a fuel reprocessing plant potential sources of interference are the many Raman lines of the tributyl phosphate (TBP) solvent (~ 30% by volume concentration) and the n-paraffin diluent (~ 70% by volume concentration). The Raman lines from NO_3^- and water may also interfere with measurements on the aqueous process and waste streams. A careful choice of the Raman lines used for each measurement species and the use of an independently measured internal standard will help to minimize these and other matrix effects.

In the case of CARS, matrix effects will be more pronounced since the CARS signal varies as the square of the bulk susceptibility and therefore reflects the properties of both the analyte species and the solvent. Consequently, any variation in the solvent concentration will appear as an apparent change in the analyte concentration. At low analyte concentrations, this effect can be minimized by normalizing the CARS signal to the average nonresonant background signal some 10-15 cm^{-1} on each side of the analyte peak [3,67].

Fluorescence interference, which is often a problem in spontaneous Raman scattering, can be eliminated by using either of the nonlinear Raman methods (CARS or SRS). However, when using these nonlinear methods the presence of absorption and Mie scattering will have a more pronounced effect on the scattered signal due to its nonlinear dependence on the overall laser power. In the case of resonant CARS it has been shown that absorption of the incident and generated

beams leads to an optimum set of experimental parameters (temp and P for laser frequencies, laser beam crossing location in the sample cell, and analyte concentration) for maximum CARS signal generation [3.68].

3.3.4.2 Measurement Precision and Accuracy

The precision and accuracy of Raman scattering measurements will depend on the factors which affect the scattered signal and the availability of suitable standardization procedures. In spontaneous Raman scattering, the factors determining the measurement precision include shot noise in the weak signal, dark current in the detector, and stray light (e.g. fluorescence, Rayleigh and Mie scattering) reaching the detector. Under ideal circumstances using photon counting the detected signal is shot noise limited, and the signal-to-noise ratio, S/N, is given by [3.69]

$$S/N = N_s T^{1/2} (N_s + N_d)^{-1/2} \qquad (3.13)$$

where N_s is the signal count rate,

N_d is the dark current count rate,

and T is the counting time.

In general, maximizing the signal-to-noise ratio will result in the best precision and lowest detection limits.

The use of photon counting techniques permits the detection of weak spontaneous Raman signals with a satisfactory signal-to-noise ratio. From Eqn. 3.13, the measurement precision using photon counting can be increased by increasing either the counting rate or the counting time. However, in practice there are two distinct error contributions which affect the precision of photon

counting measurements. One source of error arises from the finite counting time (Eqn. 3.13) and the other from fluctuations in the experimental conditions (e.g. source intensity fluctuations) [3.69]. For moderate count rates and times, the error in the experimental conditions will generally be much larger than the standard deviation based on counting statistics and will be the limiting factor in the precision of the measurement. The relative standard deviation (RSD) for spontaneous Raman measurements is expected to be in the range of 5-20% [3.70] although lower standard deviations have been reported [3.26].

The predominant source of noise in the nonlinear Raman methods is expected to be due to amplitude fluctuations in the lasers since the generated Raman signals vary nonlinearly with laser power. The power fluctuations of pulsed lasers are typically 5% which would result in an 11% fluctuation in the generated CARS signal [3.33] and a 7% fluctuation in a SRS signal. CW lasers have better amplitude stability and beam quality than pulses lasers but are probably not powerful enough to be of practical use for low level detection using the nonlinear Raman methods [3.32].

With presently available pulsed lasers, the precision of the nonlinear Raman methods is expected to be in the range of 10-25%. The accuracy of these measurements will depend upon the development of suitable standards to which the Raman signals can be referenced, and the independent measurement of the concentrations of these standards.

Multichannel data acquisition techniques in which a number of Raman lines are simultaneously measured have also been used. These techniques have an advantag over serial data acquisition by wavelength scanning in that the effect of any source fluctuations is minimized. This should increase the measurement precision while simultaneously reducing the measurement time [3.71].

A number of possible sources of interferences can exist, and if present will affect the precision and accuracy of a Raman measurement. Interferences from fluorescence, nearby Raman lines from other species in solution, and the wings of the Rayleigh and Mie scattering profile far from the source frequency are additive in nature and pose a particular problem for DIAL. These sources of additive interference have the effect of increasing the measured signal level and will show up as a change in the intercept of a plot of Raman signal vs analyte concentration [3.70]. The techniques for minimizing the effect of these sources of additive interference have been previously discussed (see Sec. 3.2.1.3).

The absorption of the incident laser radiation or the Raman signal in the sample solution results in a multiplicative interference. The effect of this interference is to change the slope of the analytical curve [3.70]. Absorption in the sample can be minimized by the proper choice of the excitation frequencies, and if present must be corrected for in the measurement.

3.2.4.6 Standardization Procedures

The use of an internal standard provides the greatest measurement accuracy for Raman scattering since it undergoes the same irradiation conditions and has the same light collection efficiency as the analyte species. This internal standard can be a Raman line from either the solvent or another species in solution which can be accurately measured independently, or else a substance which is added to the sample in a known concentration. For the greatest measurement accuracy, the concentration of the standard should be chosen so that the intensity of the standard line is in the range of that expected for the analyte. Some commonly used internal standards are NO_3^- and ClO_4^- for

aqueous samples and CCl_4 for organic samples. The use of the nonresonant background signal from the solvent in a CARS measurement has also been suggested as a possible internal standard [3.53, 3.67].

For on-line measurements in a fuel processing plant, the addition of a foreign substance as a standard to the process solution could possibly alter the chemical system and adversely affect the separation process. Therefore the first choice for internal standards should be those substances already present in the process solutions and which can be accurately measured independently. For off-line Raman measurements the addition of a known concentration of a standard substance should be considered.

The use of an internal standard also reduces the time required for a measurement since only a single sample need be measured. In contrast, when an external standard is used the accepted procedure is to run spectra in the order standard-sample-standard and then compare the integrated line intensity of the sample to the average of the two standard measurements [3.12].

4.7 Measurement Time and On-Line Capability

The measurement time for the various Raman techniques is a function of the intensity of the scattered signal. The measurement time for the nonlinear Raman methods is five or more orders of magnitude shorter than that required for SRS. Multichannel data acquisition techniques have been used to significantly reduce the time required for a measurement thereby permitting on-line measurement in real time.

In a spontaneous Raman measurement of a dilute analyte species the time required to scan the entire Raman spectrum (0-3000 cm^{-1}) will probably be in the range of 0.5-1.5 hours or longer. On the other hand, using a multichannel

detection system spontaneous Raman measurements have been made over a range of several hundred cm^{-1} in 20 ms for specie concentrations in the range of 0.15-0.50% [3.71]. A laser Raman spectrometer capable of real time on-line monitoring of gaseous species at pressures as low as 0.8 torr has also been reported [3.24].

Due to the high conversion efficiencies of the nonlinear Raman processes the time required for a measurement can be extremely short. For example, the entire Q-branch CARS spectrum from H_2 or HF can be recorded in 20 ns by using a Q-switched ruby laser, a broadband dye laser, and a multichannel detection system [3.72]. The measurement time for liquid solutions using CARS will depend upon the spectral range to be covered due to the requirement for phase-matching. In general, measurements can be made over ~ 150-300 cm^{-1} before readjustment of the phase-matching angle is required [3.67]. Phase-matching is not necessary with SRS and single pulse measurements have been made over a range of more than 700 cm^{-1} with a time resolution of 30 ns [3.55].

The on-line capabilities of CARS have been demonstrated by making measurements in flowing capillary cells at flow rates from 0-900 $cm\text{-}s^{-1}$ with no observed reduction in the signal to noise ratio [3.48]. The only restrictions for on-line CARS measurements are that the sample solution should be filtered to remove suspended solids which would cause Mie scattering and that absorption losses in the solution should be kept to a minimum. The existence of absorption in the sample will affect the CARS signal level but not the signal-to-noise ratio of the measurement [3.68]. The on-line capabilities of SRS have yet to be demonstrated but should be similar to those of the CARS method.

3.2.4.8 Capability for Automated Operation

Programmable calculators and multi-channel analyzers have been used in automating spontaneous Raman measurements [3.73, 3.74]. These automated Raman systems utilized photon counting electronics to obtain the Raman signal in a digital form. The use of digital data collection and analysis has several advantages for use in Raman scattering measurements: the signal-to-noise ratio of weak Raman lines can be improved by either collecting data over long counting times or alternatively through multiscan averaging; the data can be smoothed by numerical convolution; the peak positions can be accurately determined by numerically calculating the first and second derivatives of the spectrum; the Raman lines can be numerically integrated and referenced to lines of the standard, and other operations can be performed on the data automatically as desired [3.73].

Digital data acquisition is particularly important if a multichannel detection system is used to simultaneously measure the Raman spectrum over a wide spectral range. Computerized processing of CARS spectra may also be required to unravel the changes in lineshape with analyte concentration to obtain meaningful results.

Microprocessor- and calculator-controlled dye lasers have recently come into the marketplace [3.75] and offer completely automated wavelength scanning. In the case of the nonlinear Raman methods (especially CARS) automated laser operation is desirable for continuous scanning capability. As the frequency interval $\omega_p - \omega_s$ in a CARS experiment is varied a number of parameters must be adjusted: (1) the wavelength of the Stokes laser; (2) the phase-matching angle of the Stokes and pump laser beams; (3) the mechanical stage containing the detector, monochromator or interference filter, and the spatial filter; and

(4) the bandpass of the monochromator (if used) [3.67]. All of these parameters can be computer controlled although the completely automated operation of a CARS experiment has yet to be reported.

3.2.4.9 Summary of the Principal Advantages and Disadvantages of the Raman Scattering Methods

The principal advantages and disadvantages of the Raman methods for quantitative analysis are summarized in Tables 3.5-3.7.

Table 3.5. Summary of spontaneous Raman scattering.

Advantages:

1. Spontaneous Raman scattering is simple in concept and straightforward in operation; complete packaged instruments are commercially available. It uses a technology which is well understood and developed and therefore is the most widely used laser-based analytical method.

2. The scattered light contains the entire Raman spectrum of each molecular species in a sample, and the method is molecule specific so that a number of species including internal standards can be simultaneously measured. Its multichannel detection capability can permit rapid measurements and minimize source instabilities. Spontaneous Raman scattering is also isotope specific for molecules containing light atoms.

3. Spontaneous Raman scattering can be used for on-line non-destructive assay (NDA) or off-line measurements using small samples (≤ 1 uℓ) sealed in melting point capillary tubes.

4. The Raman signal scales linearly with sample concentration so that interpretation of the data is straightforward.

Disadvantages:

1. The Raman signal is extremely weak and incoherent. The minimum detectable concentrations are $\sim 10^{-4}$ - 10^{-2}M in solution and $\sim$ 100 ppm for gases at atmospheric pressure. Resonance enhancement can be used to detect lower concentrations at the expense of greater experimental complexity, loss of simultaneous measurement capability, and more difficult data interpretation and standardization.

2. Possible sources of interferences such as Rayleigh and Mie scattering, fluorescence, and Raman lines from the solvent or major sample constituents may partially or completely mask the Raman signal.

Table 3.6. Summary of coherent anti-Stokes Raman scattering (CARS).

Advantages:

1. The CARS signal is in the form of a coherent diffraction-limited beam at the anti-Stokes frequency. This provides a very high signal collection efficiency (~ 100%), permits excellent rejection of background fluorescence (~ 10^9 better than spontaneous Raman scattering), and allows the signal to be transmitted over long path lengths for remote measurements.

2. The CARS process has a very high light scattering efficiency (up to 1% or > 10^5 better than spontaneous Raman scattering) which provides a real-time measurement capability (≤ 20 ns time resolution).

3. The spectral resolution is dependent on the bandwidth of the Stokes laser. This permits the use of a narrowband Stokes laser for high spectral resolution (e.g. for gases) or a broadband Stokes laser for simultaneous measurement capability of many species.

4. There is a possibility of detecting vibrational modes which are neither Raman-or infrared-active since CARS is a four-photon process.

Disadvantages:

1. The sensitivity of CARS is limited by the generation of a nonresonant background signal due to $\chi_{nr}^{(3)}$. This generally limits the detection limit to ~ 0.05M for liquid solutions and ~ 100 ppm for gases at atmospheric pressure. Resonance enhancement or four-wave mixing techniques are required for lower detection levels.

2. The CARS signal is nonlinear in N, $\chi^{(3)}$, and P_p:

   a. The CARS signal scales as N^2 at high concentrations and as N at low concentrations (due to the cross term in $|\chi^{(3)}|^2$).

   b. Interactions with neighboring Raman lines, the nonresonant background, and electronic transitions can cause strong perturbations of the CARS spectrum. At present a computer fit to the CARS spectrum is considered necessary for its interpretation.

   c. Amplitude fluctuations of the lasers will be the major source of noise in CARS and limit its precision to ~ 10-25%.

3. Clearly defined standardization procedures must be developed for CARS to become a reliable quantitative analytical method.

Table 3.7. Summary of stimulated Raman scattering (SRS).

Advantages:

1. The SRS signal is in the form of a coherent diffraction-limited beam at the Stokes or anti-Stokes frequency. This provides a very high signal collection efficiency (~ 100%), permits excellent rejection of background fluorescence, and allows the signal to be transmitted over long path lengths for remote measurements.

2. The SRS process has a high light scattering efficiency which permits real-time measurements to be made with a time resolution $\leq$ 20 ns.

3. The spectral resolution is dependent on the bandwidth of the probe laser. A narrowband probe laser provides high spectral resolution ($\leq$ 0.01 cm^{-1}) while a broadband probe laser provides a simultaneous measurement capability over several hundred cm^{-1}.

4. The scattered signal scales linearly with N, $Im\chi^{(3)}$, P_p, $P_{s,as}$. The SRS spectrum resembles that for spontaneous Raman scattering so that data interpretation is simplified.

Disadvantages:

1. The sensitivity of SRS is limited by the background "bias" level of the probe beam. The minimum detectable concentration is ~ 10^{-3} - 10^{-1}M in solution and ~ 100 ppm for gases at atmospheric pressure. Resonance enhancement can be used to lower these detection limits.

2. The maximum pump power which can be used is limited by the onset of stimulated Raman or Brillouin scattering in the solvent.

3.3 Absorption Spectroscopy

Absorption spectroscopy with conventional light sources has been developed into a reliable analytical method for the measurement of atomic and molecular species. The use of tunable laser sources in absorption spectroscopy has greatly increased the measurement sensitivity and resolution while simultaneously decreasing the measurement time. The impact of lasers in absorption spectroscopy has been most dramatic for gaseous measurements permitting the measurement of a number of species at concentrations below 1 ppb (part-per-billion). Species in liquid solutions can also be measured by laser absorption spectroscopy at concentrations $\geq 10^{-4}$M.

The laser absorption methods which will be considered in this study are external absorption spectroscopy, optoacoustic spectroscopy, and intracavity absorption spectroscopy. Conventional light sources (e.g. hollow cathode and electrodeless discharge lamps) have proven to be very sensitive in atomic absorption spectroscopy, and have inherently better stability than laser sources. For these reasons, the use of lasers for atomic absorption spectroscopy will not be considered in this report.

In external absorption spectroscopy the sample is placed outside the laser cavity, and the laser power transmitted through the sample is measured to determine the absorption by the analyte species. An alternative to this method is optoacoustic spectroscopy in which the energy absorbed by the analyte species is measured directly by detecting the pressure or temperature rise in the sample. A third method for laser absorption spectroscopy places the sample inside the cavity of a homogeneously broadened laser and observes the effect of the analyte absorption on the spectral output of the laser. This technique, termed intracavity absorption spectroscopy, can enhance the measurement sensi-

tivity by some two to five orders of magnitude over that which would be obtained for the same sample by external absorption spectroscopy. A number of reviews of these and other laser absorption methods have appeared in the literature [3.1, 3.2, 3.4-3.6, 3.8, 3.76].

3.3.1 External Absorption Spectroscopy

The simplest spectroscopic method that can be used to measure the concentration of a substance is direct absorption based upon Beer's law. The high spectral power density and narrow emission linewidth of tunable laser sources provides increased sensitivity and resolution in absorption measurements. In addition, the highly collimated output beam from a laser permits very-long-path absorption measurements of localized species (using multiple-pass cells) or of remote species (using LIDAR techniques). In the case of gases it has been possible to measure absolute absorption coefficients as small as 10^{-9} cm^{-1} using external absorption spectroscopy [3.77].

3.3.1.1 Explanation of Method

When a light beam of intensity I_o traverses an absorbing medium, the intensity of the emerging beam can be expressed by Beer's law:

$$I(L) = I_o e^{-N\sigma L} \tag{3.14}$$

where N is the concentration of the absorbing species,

σ is the absorption cross-section,

and L is the path length traversed through the absorbing medium.

The absorbance, A, of the medium is given by

$$A = -\log_{10}\left(\frac{\bar{I}(L)}{I_o}\right).$$

This is the quantity which is generally measured by conventional absorption spectrophotometers.

For multi-component mixtures, the absorbance is additive as long as there are no interactions between the absorbing species. On the other hand, the absorbance is influenced by chemical factors (e.g. the shifting of chemical equilibria, changes in temperature, solvent effects, and scattering of the light beam) as well as instrumental factors (e.g. variations in source intensity, nonlinear detector response, and the presence of stray light reaching the detector) [3.70, 3.78].

Quantitative absorption spectroscopy is performed by comparing the absorption of light at a selected wavelength by a sample with that of a series of standards. In the absence of matrix effects a series of neutral density filters, each being a specified optical density, can be used to null the signal in a differential absorption measurement. If matrix effects are present the composition of the standards should closely resemble that of the sample for greatest measurement accuracy.

3.3.1.2 Experimental Techniques for External Absorption Spectroscopy

The experimental apparatus for external absorption spectroscopy in its simplest form consists of a tunable laser, a sample cell, and an optical radiation detector. As the output from the laser is passed through the absorbing sample, the transmitted power is measured by the detector. If the laser wavelength is scanned the absorption spectrum of the sample can be measured. Alternatively, if the concentration of a particular analyte species is to be

monitored as a function of time, the laser wavelength may be locked to an absorption line of the analyte species.

In the visible region of the spectrum tunable dye lasers are generally used as the spectral source for absorption measurements. These lasers may also be frequency-doubled for measurements in the ultraviolet. In the case of absorption measurements in the infrared, a number of spectral sources are available: semiconductor diode lasers, high pressure gas lasers, parametric oscillators, frequency mixing techniques, F-center lasers, and spin-flip Raman lasers. The choice of a specific laser type will depend upon the particular measurement species and circumstances.

3.3.1.3 Use of External Absorption Spectroscopy for Quantitative Analysis

The largest body of work on the quantitative use of the external absorption method has been in the area of air analysis. In localized absorption measurements the use of tunable lasers has made possible the detection of gaseous species at relative concentrations of 10^{-9} in a volume of 1 cm^3 when the total gas pressure is several tens of torr [3.5]. The development of laser absorption techniques for solution measurements has received little attention until recently due to the strong absorption of water and other solvents in the infrared. However, with a CO_2 laser ($\sim$ 1 W cw) and a short pathlength absorption cell ($\sim$ 100 μm) it has been possible to measure a number of species in aqueous solution at concentrations of $\leq 10^{-4}$M [3.79].

A large number of gaseous molecular species have been measured with tunable infrared lasers and these measurements are summarized in Table 3.8. In the case of the paramagnetic molecules NO and NO_2, absorption measurements could be made by Zeeman-shifting the molecules into resonance with a fixed frequency CO laser. With tunable diode lasers, gaseous species have been

Table 3.8. Localized measurements of gaseous species by external absorption spectroscopy.

Analyte Species	Total Gas Pressure (torr)	Laser Type	Excitation Frequency(cm^{-1})	Absorption Pathlength(cm)	Minimum Detectable Concentration (ppb)	Reference
NO	30	CO	1884.3	90	250	3.80
NO_2	27	CO	1616	18	1500	3.81
NO	10	Diode	1880	3×10^4	0.03[a]	3.77
NO_2			1600		0.02	
N_2O			1150		2	
CO			2120		0.01	
CO_2			1075		300	
CO_2			2350		0.001	
H_2O			1435		50	
SO_2			1140		3	
SO_2			1370		.3	
O_3			1050		0.5	
NH_3			1050		0.05	
CH_4			1300		0.03	
CO	760	--	--	10^3	0.8[b]	3.33
$^{14}CO_2$	2.7	Diode	2226	300	8.5×10^{10} mol-cm^{-3} [c]	3.82
$^{14}CO_2$	10	Diode	2226	--	$\sim 10^9$ mol-cm^{-3} [c]	3.83

a. These minimum detectable concentrations estimated assuming a sensitivity of 10^{-9} cm^{-1}.

b. Estimated for S/N = 1

c. Estimated

measured with absorption coefficients as low as 10^{-9} cm^{-1} [3.77]. And with a long path (~ 300 m) White cell it has been estimated that gas concentrations of ~ 1 ppb could be measured for weakly absorbing molecules such as SO_2 and several ppt (parts-per-trillion) for strongly absorbing molecules such as CO.

Absorption measurements in aqueous solutions are difficult in the infrared due to the strong background absorption of water which requires the use of very thin sample cells. The small analyte absorption over such short path-lengths generally restricts measurements to analyte concentrations of typically several $g\text{-}l^{-1}$ when conventional infrared spectrophotometers are used [3.79]. However, with a CO_2 laser source the detection sensitivity for a number of anions in aqueous solution has been improved by over two orders of magnitude. This improved sensitivity was attributed to the much higher spectral irradiance of the laser source. The details of these measurements are summarized in Table 3.9.

In these measurements only about 10^{-4} of the incident power from the 1W cw CO_2 laser was transmitted through the ~ 100 μm thick sample cell; and continuous flowing of the sample solution was required to minimize localized heating effects. Later measurements showed that an equal detection sensitivity for $SO_4^{=}$ could be achieved using a Q-switched CO_2 laser which operated at a much lower average power level (~ 20 mW) and therefore minimized sample heating. Since high average power cw lasers are available only for restricted wavelength ranges in the infrared, the possibility of using pulsed lasers should greatly increase the wavelength range over which absorption measurements can be made in liquid solutions.

The use of tunable lasers for absorption spectroscopy in the visible has received little attention although a number of techniques have been developed for the rapid electronic wavelength scanning of cw dye lasers [3.84-3.87]. An

Table 3.9. External absorption measurements of anions in aqueous solution using a CO_2 laser.[a]

Anion	CO_2 Laser Wavelength		Minimum Detectable Concentration	
	μm	Lasing Line	$mg\text{-}\ell^{-1}$	M
SO_4^{2-}	9.28	R18	10	5.7×10^{-5}
HPO_4^-	9.26	R22	8	5.6×10^{-5}
$H_2PO_4^-$	9.26	R22	15	1.3×10^{-4}
ClO_3^-	10.25	R20	30	2.5×10^{-4}
ClO_4^-	9.20	R34	27	2.0×10^{-4}
$Cr_2O_7^{2-}$	10.59	P20	35	1.4×10^{-4}

a. Reference 3.79.

electrooptically scanned cw dye laser has been used to repetitively measure the absorption of a crystalline Nd:YAG sample over a wavelength range of 12.5 nm with a scanning time of 10 μs [3.87]. This permitted the absorption spectrum to be displayed in real time on an oscilloscope. Although this technique has not yet been used for quantitative analysis, it nevertheless shows the potential use of electronically scanned dye lasers for visible absorption measurements.

3.3.2 Optoacoustic Spectroscopy

External absorption spectroscopy measures the small change in the transmitted laser power due to sample absorption, whereas optoacoustic spectroscopy measures directly the power absorbed in the sample. The absorption of energy by a substance produces a localized rise in pressure and temperature within that substance due to nonradiative relaxation processes. The periodic pressure variation in a substance produced by the absorption of energy from a source which is modulated at an acoustic frequency can be detected if the substance is placed in a cell containing a sensitive microphone. Although the discussion below will be confined to the use of laser sources, the optoacoustic effect has also been observed at microwave frequencies [3.88].

3.3.2.1 Explanation of Technique

When the wavelength of a laser coincides with that of a vibrational-rotational transition in a molecular species, the energy absorbed by the molecular species, ΔE, is:

$$\Delta E = E_o(1 - e^{-N\sigma L}) \approx E_o N\sigma L \quad \text{for } N\sigma L \ll 1 \tag{3.15}$$

where E_c is the incident laser energy lying within the absorption linewidth

N is the concentration of the molecular species

σ is the absorption cross-section

and L is the absorption pathlength.

This absorption of energy transfers the molecules to a higher lying vibrational-rotational state(s) with subsequent relaxation to the ground state by either radiative or nonradiative (collisional) processes. The nonradiative relaxation of molecules to the ground state releases energy producing a pressure and temperature rise in the sample cell. And, if the exciting laser radiation is periodic in nature, a periodic variation in pressure will be produced which can be detected with the aid of a sensitive microphone placed in the cell. In the small signal approximation of Eqn. 3.15, the detected signal will scale linearly with the laser intensity and species concentration for a sample cell of fixed dimensions.

The sensitivity of a capacitor microphone is sufficient to detect absorbed powers in the range of 10^{-9} - 10^{-8}W for an absorption pathlength of 10 cm when the detection system has a bandpass of 1 Hz [3.5]. Theoretically, the minimum detectable power is set by Brownian noise in the microphone membrane. However, in practice it is much higher due to absorption of laser light by the windows and walls in the sample cell resulting in the generation of a synchronous background optoacoustic signal.

To date, the optoacoustic method has been used to detect a number of gaseous species in the 1-10 ppb range and solution species at concentrations as low as 9×10^{10} mol-cm^{-3} (0.08 μg - ℓ^{-1}) [3.89]. And although the method is generally applied to vibrational transitions in the infrared due the requirement that the absorbed energy be converted into heat, it can also be used in

the visible or ultraviolet for electronic transitions having a low radiative quantum efficiency [3.90, 3.91].

3.3.2.2 Experimental Techniques for Optoacoustic Spectroscopy

The experimental arrangement for the optoacoustic measurement of gaseous species is shown schematically in Figure 3.6. The laser, generally operating in a cw mode, is tuned to overlap a vibrational-rotational transition of the molecular species to be measured and is directed through the sample cell. The laser is amplitude modulated at an acoustic frequency by a mechanical chopper, and the optoacoustic signal is detected by a sensitive capacitor microphone. The electrical signal from the microphone is demodulated by a lock-in amplifier and is normalized to the exciting laser intensity.

The detection limit for optoacoustic spectroscopy is generally set by the background signal level due to absorption in the windows and walls of the cell which is usually about two orders of magnitude larger than the Brownian noise level [3.86, 3.92]. This relatively constant background signal must be subtracted from the total measured signal to determine the signal arising from the molecular species of interest. In principle the wavelength independent background can be minimized by either frequency modulating the laser source or using a two-cell detection technique [3.88]. In this latter technique the laser beam passes through the sample cell and an identical reference cell containing the same gas composition as the sample cell minus the constituents to be measured. A transducer connected between the two cells measures the pressure difference which is proportional to the concentration of the desired measurement species.

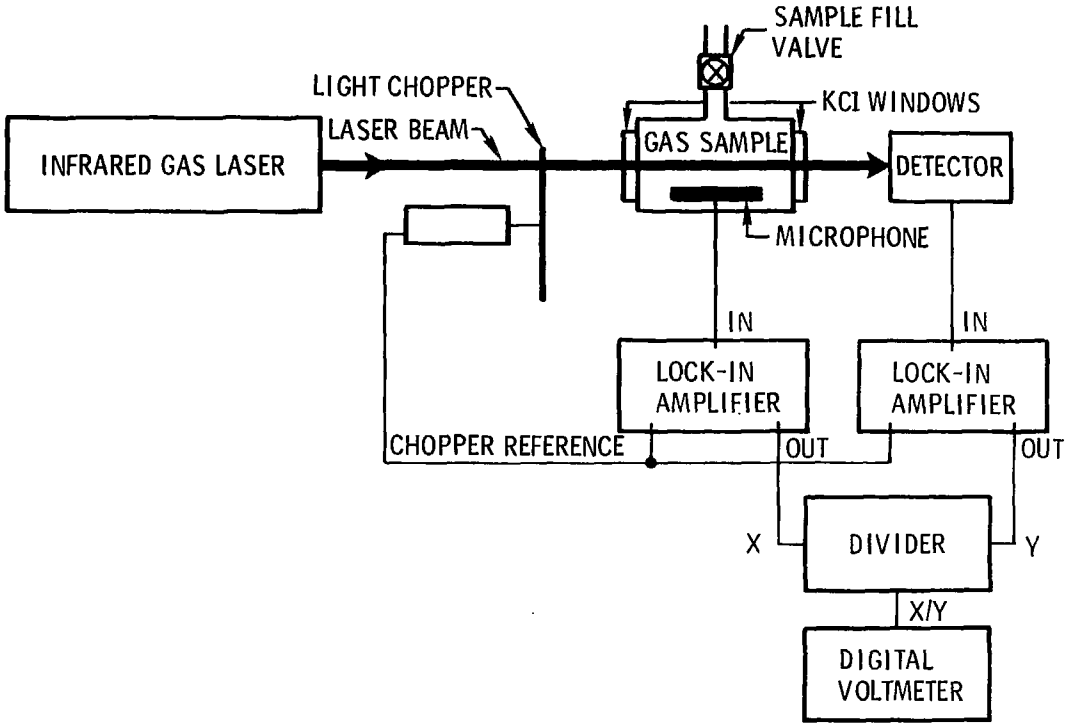

Figure 3.6. Experimental apparatus for optoacoustic spectroscopy.

For trace gas measurements, the optoacoustic signal level can be increased through the use of acoustical and/or optical enhancement techniques. Acoustical enhancement of the detected signal can be achieved by modulating the laser intensity at a frequency which is identical to a natural resonant acoustic frequency of the sample cell [3.88, 3.93 - 3.95]. A Q of 890 has been reported using a cylindrical sample chamber (5.3 cm radius and 10 cm length) designed to operate at the first order radial resonance frequency at $\sim$ 4 KHz [3.88]. Operation of an acoustically resonant cell at a very large Q factor, however, requires an extremely stable chopping frequency since any small frequency variations will cause a large change in the detected signal level. Therefore, for good signal stability it is often preferable to use a lower Q ($\sim$ 100) and further increase the signal level using optical enhancement techniques [3.91]. An optical enhancement of the detected signal by a factor of 10-100 can be achieved by propagating the laser beam back and forth through the sample cell many times with either a multiple-pass arrangement [3.91] or by placing the sample cell within the cavity of the exciting laser [3.95]. With these resonant enhancement techniques it is possible to detect gaseous species at concentrations of several ppb or lower over a 10 cm path length.

Measurements of molecular species in liquid solutions can also be made with optoacoustic spectroscopy. However, due to the presence of absorption by the solvert, frequency-switching techniques are generally used whereby the sample solution is irradiated alternately at two different wavelengths from the exciting laser [3.89, 3.96]. These wavelengths are chosen so that the solvent absorption remains relatively constant while the analyte absorption is highly different at the two wavelengths.

3.3.2.3 Use of Optoacoustic Spectroscopy for Quantitative Analysis

The reported use of optoacoustic spectroscopy for quantitative analysis has dealt primarily with the measurement of gaseous species and to a lesser extent with molecular species in binary liquid solutions. The gas phase measurements are summarized in Table 3.10. The measurements made using cw laser sources indicate that concentrations on the order of 10^{11} mol-cm^{-3} can be detected at atmospheric pressure for a number of molecular species.

Optoacoustic measurements of species in aqueous solution with an infrared laser source are complicated by the strong background absorption of water. In the measurement of aqueous ammonium sulfate with a cw CO_2 laser, a frequency-switching technique was used whereby the sample was alternately irradiated at 9.25 and 10.675 μm corresponding to regions of strong and weak absorption of the analyte species [3.96]. The relative amplitudes of the laser output at the two wavelengths were then adjusted to give a constant background signal due to absorption by the water in the cell. With this background nulling technique it has been possible to measure on the order of 100 mg-ℓ$^{-1}$ of $(NH_4)_2SO_4$ in solution. A similiar frequency-switching technique has been used in the visible with an argon ion laser to detect β-carotene in chloroform at concentrations as low as 0.08 μg-ℓ$^{-1}$ (9×10^{10} mol-cm^{-3}) [3.89].

3.3.3 Intracavity Absorption Spectroscopy

With intracavity absorption spectroscopy (IAS) the apparent absorption of a trace species can be increased by several orders of magnitude by placing it inside the cavity of a homogeneously broadened laser. This enhancement of IAS when compared with a single-pass external absorption

Table 3.10. Measurements of gaseous species by optoacoustic spectroscopy.

Analyte Species	Total Gas Pressure (torr)	Laser Type	Power (W)	Measurement Frequency(cm^{-1})	Absorption Pathlength(cm)	Resonance Enhancement	Minimum Detectable Concentration	Reference
HF	~ 760	pulsed HF	> 1 J/pulse	---	--	No	10 ppb	3.97
NO	--	pulsed HF	0.02 J/pulse	---	--	No	10 ppm	3.97
NO	~ 300	cw spin-flip Raman	0.015	1824.33	--	No	10 ppb[a]	3.98
NO	~ 15-20	cw spin-flip Raman	---	1887.6	--	No	1.5×10^{8} mol-cm^{-3}	3.99
H_2O	~ 15-20	cw spin-flip Raman	---	1889.6	--	No	~ 10^{11} mol-cm^{-3}	3.99
CO_2	~ 760	pulsed HF	5×10^{-6} J/pulse	3644.24	--	No	10^{3} ppm	3.97
CO_2	~ 760	pulsed CO_2	1 J/pulse	944.2	--	No	1 ppm	3.97
NO_2	10	cw dye	0.25	580-610 nm	10	Yes	20 ppb[a]	3.90
SO_2	~ 760	frequency-doubled cw dye	0.001	300.05 nm	10	Yes	0.12 ppb	3.91
CH_4	~ 760	Zeeman-tuned cw He-Ne	0.015	~ 2950	5	No	10 ppb	3.100
C_2H_4	500	cw CO_2	~ 1	949.43	--	No	5 ppb	3.92
C_2H_4	---	cw CO_2	~ 1	949.43	--	Yes	0.3 ppb	3.95

a. Estimated.

measurement has been attributed to the multiple passes of the laser beam through the absorbing medium as well as to the strong competition of simultaneously oscillating modes for the available energy of the homogeneously broadened gain medium [3.101-3.103]. To date IAS has been used to study atomic and molecular species in the vapor phase, in liquid solutions, and in a flame containing the atomized solution. The technique is extremely sensitive and shows great promise for use in trace gas analysis.

3.3.3.1 Explanation of Method

The sensitivity of an absorption measurement can be increased by placing the absorbing sample within the cavity of a homogeneously broadened laser (e.g. a dye laser) and observing the effect of the absorption on the spectral distribution of the laser output. In the case of a pulsed flashlamp-pumped dye laser the observed enhancement in sensitivity is typically a factor of 100, whereas for cw dye lasers enhancement factors of 10^3 - 10^5 have been reported [3.102, 3.104]. This large enhancement in sensitivity can be qualitatively understood since the introduction of an absorbing species into the cavity of a laser will produce an additional wavelength-dependent loss and therefore reduce the net gain at the absorption wavelength. This small decrease in gain will in turn result in a dramatic change in the spectral distribution of the laser output.

To date, no closed form theory has been formulated for the intracavity absorption process due to its extremely complicated nature. It involves the interaction of an inhomogeneously broadened absorber with a number of effects occurring in the laser: (1) a "resonator effect" resulting from the repeated passes of the laser beam through the absorbing medium, (2) the threshold nature

of the laser process, and (3) the strong mode competition for the available energy of the homogeneously broadened gain medium [3.104]. The simplified rate equation models which have been developed so far are incapable of explaining many of the details of the intracavity absorption process but do show the intracavity absorption to be greatest for the following laser characteristics: (1) operation close to threshold, (2) strong mode competition, (3) large spatial relaxation constant, and (4) many lasing modes or broadband operation [3.105].

The greatest area of development of intracavity absorption spectroscopy to date has been in the visible region of the spectrum using dye lasers although the method has also been demonstrated in the infrared with Nd:glass and spin-flip Raman lasers. Two other types of widely tunable homogeneously broadened lasers which should be investigated for their potential for IAS in the infrared are F-center lasers and parametric oscillators.

3.3.3.2 Experimental Techniques for Intracavity Absorption Spectroscopy

A schematic diagram of the experimental apparatus used for intracavity absorption measurements of molecular iodine using a cw dye laser is shown in Figure 3.7. In this arrangement, an iodine vapor cell is placed inside the cavity of a broadband (0.2-0.5 nm) cw dye laser and the iodine vapor pressure is regulated by means of a cold finger on the cell. In principle, the sealed vapor cell could be replaced by a flowing gas cell for on-line measurements.

The effect of the absorption of the intracavity sample can be monitored by observing the fluorescence from an evacuated monitor cell containing the gaseous species to be measured [3.102]. This external fluorescence detection provides a quantitative measure of the concentration of the intracavity

absorber while being much more sensitive and considerably simpler than other techniques which record the output spectrum of the laser. In addition, the use of photon counting electronics provides a fast (~ 1s), direct readout of the IAS signal and increases the concentration range over which intracavity absorption measurements can be made.

Pulsed dye lasers have also been used for IAS although the sensitivity is lower than that observed with cw dye lasers. The detection techniques generally employed with pulsed lasers rely on observing the laser output spectrum with a high resolution spectrometer or a Fabry-Perot etalon. The spectrum can be recorded on film or by means of a multi-channel detector array.

3.3.3.3 Use of Intracavity Absorption Spectroscopy for Quantitative Analysis

The experimental work on intracavity absorption spectroscopy has been concerned primarily with characterizing the process and determining the enhancement in sensitivity over that obtained in a single-pass external absorption measurement; and little work has been performed on the development of IAS as a quantitative analytical method. As a result, although the minimum detectable concentrations of a number of species in the vapor phase and in solution have been measured, few quantitative data have been presented in the sense of an analytical curve relating the enhanced or apparent absorption to the concentrations of the absorbing species placed in the laser cavity.

The experimental results for the detection of a number of gaseous species are summarized in Table 3.11. The IAS method is most sensitive using dye lasers (cw and flashlamp-pumped) and to date they have been used almost exclusively for quantitative IAS measurements. The minimum detectable concentrations of atomic species are several orders of magnitude lower than those for molecular

Table 3.11. Measurements of gaseous species by intracavity absorption spectroscopy.

Analyte Species	Total Gas Pressure(torr)	Laser Type	Output Power(W)	Measurement Wavelength(nm)	Laser Bandwidth(nm)	Absorption Pathlength(cm)	Minimum Detectable Concentration	Reference
Na	E[a]	cw dye	$\sim 5\times10^{-4}$	589.0	$\sim 6\times10^{-4}$	15	5×10^{5} atoms-cm^{-3}	3.106
Na	few torr (Ne)	pulsed dye	---	589.0	---	1.8	8.0×10^{8} atoms-cm^{-3}	3.107
Cs	E	pulsed dye	---	455.5	18.5	4	2×10^{-8} torr (7×10^{8} atoms-cm^{-3})	3.108
NO	10	cw CO		1884.37 cm^{-1}	---	60	1 ppb	3.109
NO	$\sim$ 300 (He)	cw CO	0.1-0.15	1900.08 cm^{-1}	---	15	$\sim 7.6\times10^{-4}$ torr (3×10^{13} mol-cm^{-3})	3.110
NO_2	E	pulsed dye	---	450, 490, 590	---	50	5×10^{-3} torr (2×10^{14} mol-cm^{-3})	3.111
I_2	E	cw dye	0.20	---	$\leq$ 0.05	26	$\leq 10^{-5}$ torr (4×10^{11} mol-cm^{-3})	3.104
I_2	E	cw dye	0.005-0.250	551.6, 589.0	0.2-0.5	5	5.4×10^{11} mol-cm^{-3}	3.112
I_2	E	cw dye	---	$\sim$ 600	$\sim$ 3.0	1.9	$< 4.4\times10^{-5}$ torr (2×10^{12} mol-cm^{-3})	3.102
I_2	E	pulsed dye	> 1J/pulse	$\sim$ 584	> 3	10	$\leq 10^{-4}$ torr (4×10^{12} mol-cm^{-3})	3.104

a. Cell evacuated prior to filling with measurement species.

species due primarily to the much larger absorption cross-section of electronic transitions. The molecular species which has been examined to the greatest extent with IAS is iodine, for which concentrations as low as 5.4×10^{11} mol-cm^{-3} have been measured over a 5 cm absorption cell pathlength [3.112].

Analytical calibration curves for intracavity absorption measurements of sodium and iodine in a cw dye laser are shown in Figures 3.8 and 3.9 [3.112, 3.113]. In generating these analytical curves the external fluorescence detection technique was used and the concentration of the intracavity absorber (contained in a 5 cm absorption cell) was varied by changing the cell temperature (for sodium) or the temperature of a cold finger on the cell (for iodine). The analytical curves obtained in this manner generally exhibit a linear region over several orders of magnitude change in absorber concentration and flatten out at both very low and very high absorber concentrations. The nonlinear behavior at low concentrations is thought to be due to a bleaching of the absorption whereas at high concentrations it is due to quenching of the laser action [3.105]. The exact shape of the analytical curve depends upon the experimental parameters of the laser.

A number of rare earth compounds in solution have been detected at concentrations as low as $\sim 10^{-4}$M using flashlamp-pumped dye lasers. These solution measurements are summarized in Table 3.11. Measurements were made with rare earth compounds which exhibit sharp absorption spectra since, when observing the spectral distribution of the laser output, it is very difficult to obtain quantitative information if the intracavity absorber has a complex absorption spectrum. The measured enhancement in sensitivity for IAS measurements in solution was 30-35 [3.115]; and the detection limits reported for $HoC\ell_3$ and $PrC\ell_3$ in Table 3.12 are about two orders of magnitude lower than those for direct spectrophotometry of the solutions [3.114].

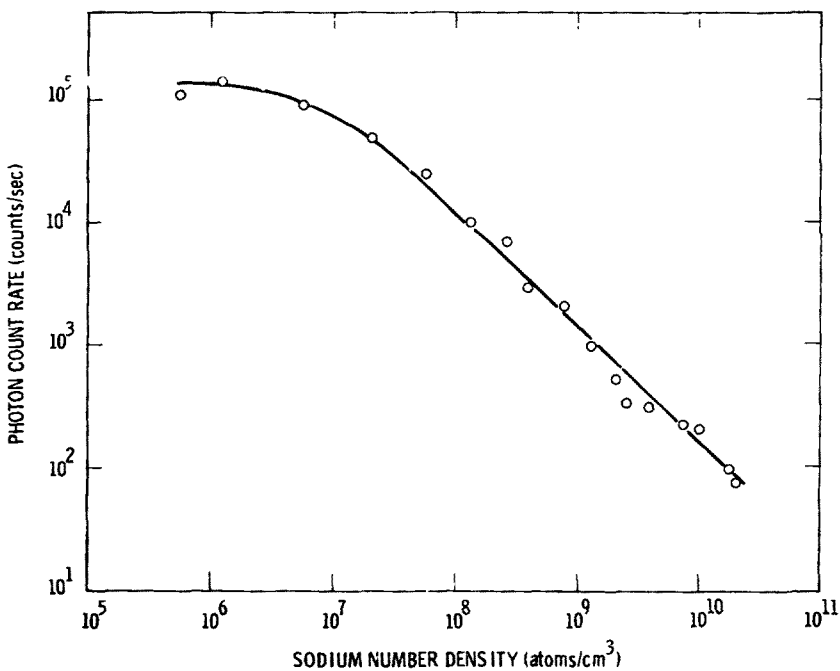

Figure 3.8. Analytical calibration curve for the measurement of sodium by intracavity absorption spectroscopy [3.112].

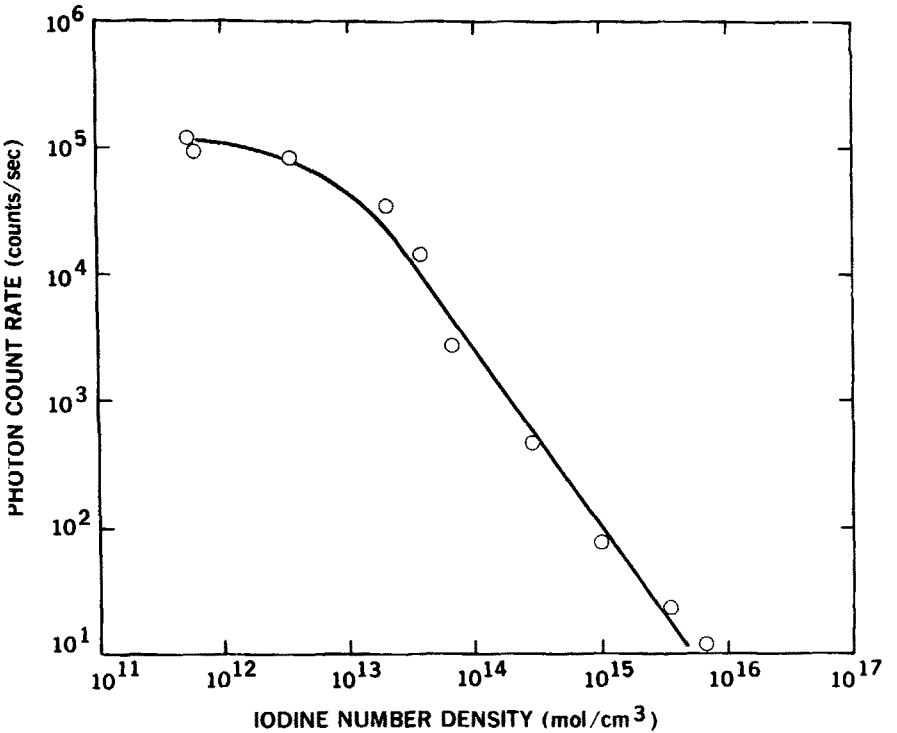

Figure 3.9. Analytical calibration curve for the measurement of iodine by intracavity absorption spectroscopy [3.112].

Table 3.12. Measurements of species in solution by intracavity absorption spectroscopy.

Analyte Species	Solvent	Laser Type	Measurement Wavelength(nm)	Laser Bandwidth(nm)	Absorption Pathlength(cm)	Minimum Detectable Concentration(M)	Reference
$HoCl_3$	0.1N HCl	pulsed dye	450.4	--	1	$\sim 1 \times 10^{-4}$M (27 mg-l^{-1})	3.114
$PrCl_3$	0.1N HCl	pulsed dye	588.3	--	1	$\sim 1 \times 10^{-4}$M	3.114
$Pr(NO_3)_3$	H_2O	pulsed dye	482.5	10-20	2	$< 6 \times 10^{-4}$M	3.115
$Eu(NO_3)_3$	Methanol	pulsed dye	579	10-20	2	$< 2.4 \times 10^{-3}$M	3.115
$NdCl_3$	H_2O	pulsed dye	575.5	10-20	2	$< 8 \times 10^{-3}$M	3.115
p-Benzoquinone	Hexane	pulsed dye	454	--	-	$< 5 \times 10^{-4}$M	3.116

3.3.4 Evaluation of Absorption Spectroscopy for Use in Nuclear Fuel Processing Plants

3.3.4.1 Previous Use in the Nuclear Fuel Cycle

External absorption spectroscopy using a tunable diode laser source and a long path absorption cell is being investigated for possible development of a $^{14}CO_2$ monitor [3.81, 3.117]. Accurate wavelength measurements have been made for lines in the ν_3 band of $^{14}CO_2$ at 4.5 μm (~ 2226 cm^{-1}) [3.118] and it is estimated that concentrations of $^{14}CO_2$ as low as ~ 10^8 mol-cm^{-3} could be measured (see Table 3.7) [3.82].

Intracavity absorption measurements of iodine isotopes (I-127 and I-129) have been made to demonstrate the isotopic selectivity of the technique and also to determine the minimum detectable concentration. With a 5 cm evacuated iodine cell contained in the cavity of a cw dye laser, the minimum detectable iodine concentration was 5.4 x 10^{11} mol-cm^{-3} [3.112]. This corresponds to an iodine-129 activity of ~ 3 x 10^{-14} Ci-cm^{-3}. The measurement of lower radioiodine activities should be possible by increasing the sampled intracavity volume (absorption cell length and laser beam diameter).

3.3.4.2 Possible Measurement Species

Laser absorption spectroscopy has proved to be a very sensitive technique for the measurement of gaseous species and shows great promise for monitoring many of the molecular species present in the off-gases in a nuclear-fuel processing plant. In general, molecular concentrations on the order of 1-100 ppb or lower can be measured with the various laser absorption methods. The species NO_2, HTO, $^{14}CO_2$, and $^{129}I_2$ are expected to exist in concentrations within or above this range at a number of locations in the off-gas filtration system of a

fuel processing plant (see Tables 1.6-1.9). In addition, organic iodides and tributyl phosphate vapors will be present at significant levels in the vessel off-gases, and ^{106}Ru will be present in the waste solidification off-gases.

Measurements of NO_2 at concentration levels below that expected at the main stack in a fuel processing plant ($\sim$ 5 ppm) have been reported for both external absorption and optoacoustic spectroscopy [3.81, 3.90]. With external absorption spectroscopy with a tunable diode laser source and a multipass sampling cell ($\sim$ 100 m pathlength) it has been estimated that $^{14}CO_2$ could be measured with a minimum detectable concentration of $\sim 10^{8}$-10^{9} mol-cm^{-3} [3.77, 3.82, 3.83]. This would permit the measurement of $^{14}CO_2$ in the dissolver off-gas filtration system at all points before the rare gas recovery stage where the $^{14}CO_2$ is expected to be trapped (see Table 1.6). Intracavity absorption spectroscopy has been used to detect iodine concentrations below 10^{12} mol-cm^{-3} with a cw dye laser [3.104, 3.112], and it is expected that the minimum detectable iodine concentration for this method could be reduced by 2-3 orders of magnitude by increasing the sampled gas volume which presently is $\leq$ 0.01 cm^{-3} [3.112].

Water vapor has been detected at concentrations of $\sim 10^{11}$ mol-cm^{-3} by optoacoustic spectroscopy using a cw spin-flip Raman laser source [3.99], and a detection limit of 50 ppb ($\sim 10^{12}$ mol-cm^{-3}) has been estimated for an external absorption measurement using a tunable diode laser [3.77]. To date no reported measurements have been made with the strong fundamental absorption bands of H_2O. In the case of HTO measurements, the ν_1 band at 2365 cm^{-1} ($\sim$ 4.23 μm) [3.119] could be used for increased sensitivity. With laser absorption spectroscopy it should be possible to monitor HTO in the dissolver

and waste solidification off-gases at the levels listed in Tables 1.6 and 1.7 ($\sim 10^{-10}$-10^{-12} mol-cm^{-3}).

The measurement of TBP and other hydrocarbon vapors in the off-gases is also possible with laser absorption spectroscopy by detecting the C-H stretching bands in the 3-4 μm region. In the case of $CH_3{}^{129}I$ present in the vessel off-gases the C-I absorption bands can be detected. Additionally it may be possible to detect ^{106}Ru present in the waste solidification off-gases by detecting the ν_3 band of RuO_4 at 920 cm^{-1} (10.9 μm) [3.120].

The minimum detectable concentration levels which have been reported for laser absorption measurements of solution species are $\sim 10^{-4}$ M in both the infrared and visible regions of the spectrum. This level of detection is comparable to or slightly better than that achieved for Raman scattering. The species which should be considered for measurement by the laser absorption methods are generally the same as those for Raman scattering (see Section 3.2.4.2). The use of absorption spectroscopy, however, is expected to reduce the problems encountered in Raman scattering due to sample fluorescence and scatteri by suspended solids. On the other hand, with absorption spectroscopy it will not be possible to simultaneously measure a large number of species as in Raman scattering, and possible problems for absorption measurements may arise from strong solvent absorption in the infrared.

The measurement of uranium, plutonium, and thorium nitrates by laser absorption spectroscopy is possible with a tunable dye laser since these species have well-defined absorption spectra in the visible and near-infrared regions of the spectrum. The absorption spectra of plutonium in its various

oxidation states are shown in Figures 3.10-3.12. These spectra have formed the basis for plutonium concentration and valence determinations using conventional absorption spectrophotometers [3.121-3.123]. The use of laser sources for these measurements should permit the detection of lower concentration levels and also provide the possibility for on-line monitoring of these species.

3.3.4.3 Isotope and Molecule Specificity

The laser absorption methods will be isotope specific for the vapor phase species of interest in a fuel processing plant due to the large isotope shifts in the vibrational spectra of these molecules as well as the small bandwidths available with tunable lasers [3.82, 3.112, 3.118, 3.124]. The absorption methods are also molecule specific and any interference from overlapping lines from other molecular species can generally be eliminated by making measurements at a reduced pressure ($\sim$ 10 torr) or through the selection of another vibration-rotation transition on which to make a measurement.

The broadening of the spectral lines in solution will prevent any isotope measurements on the heavy elements such as the actinides. However, the absorption methods retain their molecule specificity for solution measurements as can be seen for plutonium in Figs. 3.10-3.12.

3.3.4.4 Sensitivity to Matrix Variations

Matrix effects in off-gas measurements in a fuel processing plant could possibly arise from overlapping pressure-broadened absorption bands of atmospheric constituents (e.g. H_2O, CO_2). These effects, however, can be eliminated by: (1) proper selection of the measurement wavelength, (2) measurement at a reduced pressure with a narrowband laser source, and (3) evacuation of the space between the laser source, the sample cell, and the detector.

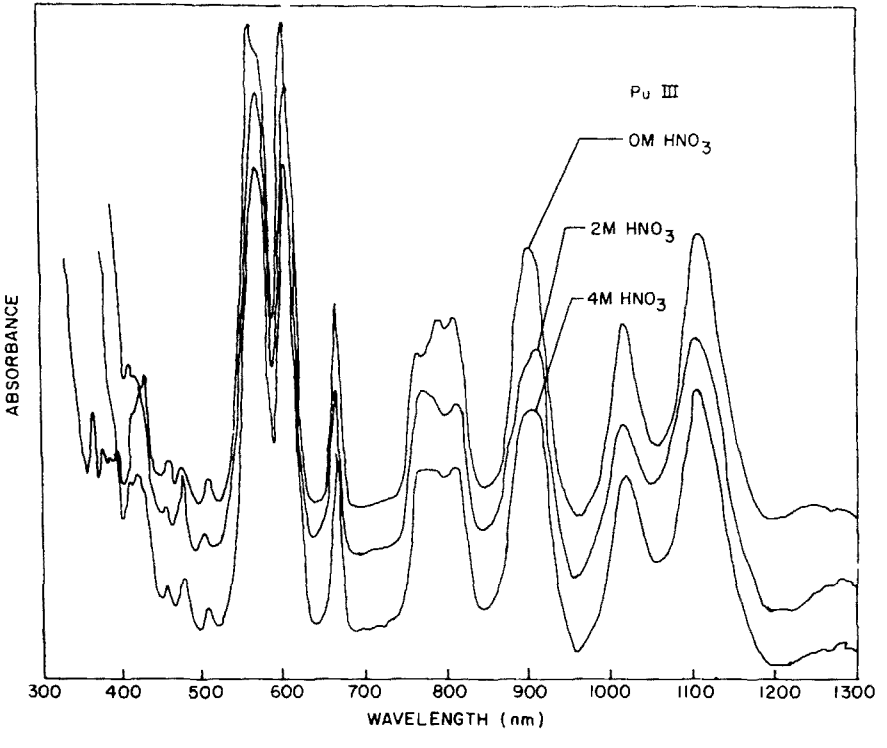

Figure 3.10. Absorption spectra of plutonium III in 0M, 2M, and 4M HNO_3. Reproduced from [3.121] with permission.

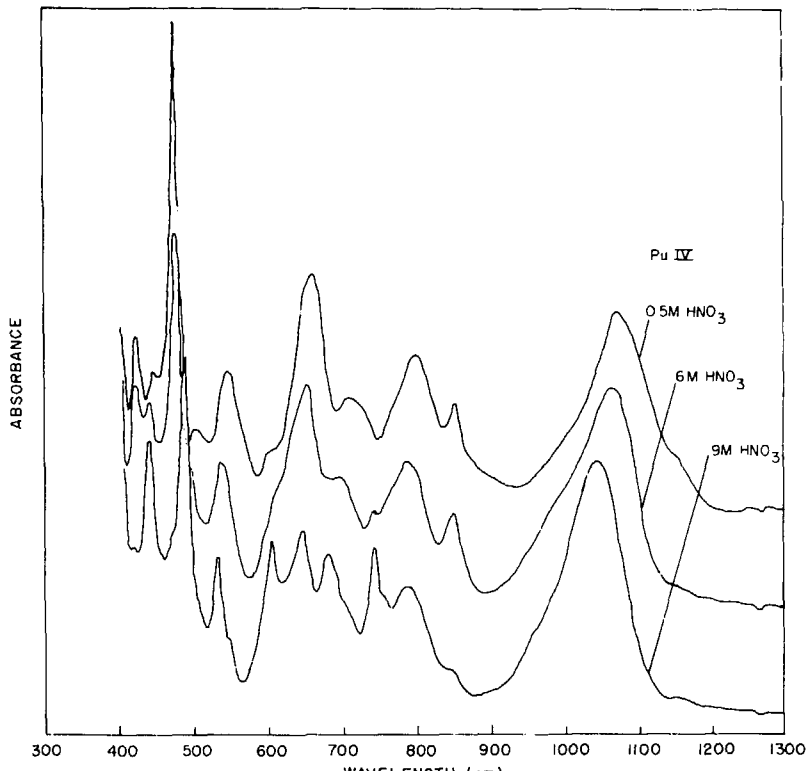

Figure 3.11. Absorption spectra of plutonium IV in 0.5M, 6M, and 9M HNO_3. Reproduced from [3.121] with permission.

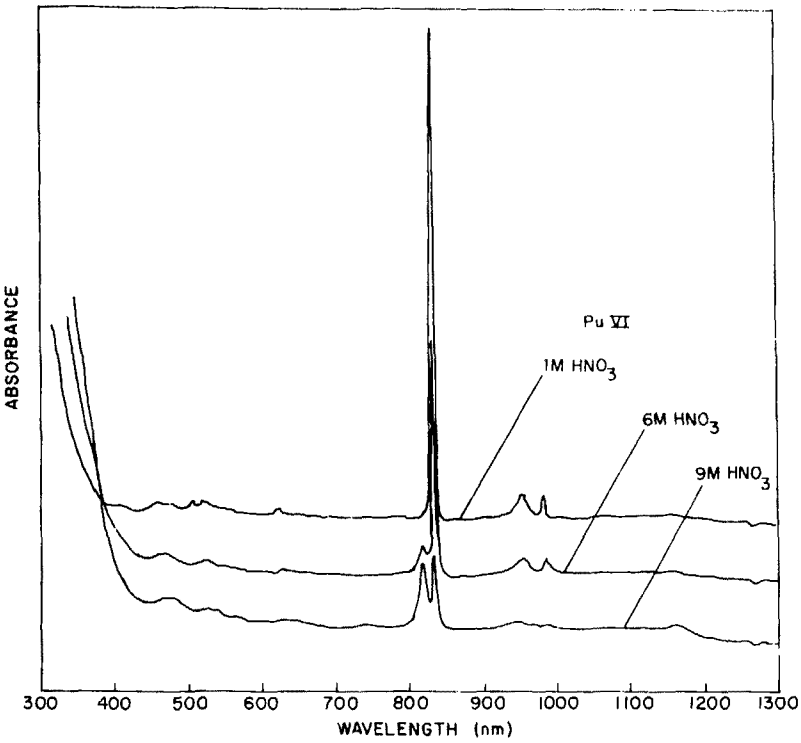

Figure 3.12. Absorption spectra of plutonium VI in 1M, 6M, and 9M HNO_3. Reproduced from [3.121] with permission.

In solutions, matrix effects will be evidenced by a slight shift in the shape and location of the absorption bands and the value of the absorptivity. These effects in solution measurements can be minimized through a proper solution of the measurement wavelength(s), the use of "peak-to-valley" or frequency-switching measurement techniques, and the preparation of absorption standards which closely resemble the sample composition.

3.3.4.5 Measurement Precision and Accuracy

As in the case of Raman scattering measurements, the precision and accuracy of laser absorption measurements will depend upon the availability of suitable standardization procedures and the factors which affect the detected signal level. The principal source of noise in laser absorption measurements will be laser source instabilities. For continuous monitoring of vapor phase species, techniques have been developed to actively stabilize the frequency of cw lasers and lock them to atomic and molecular transitions [3.125-3.128]. In addition the amplitude instabilities in cw lasers can be reduced to well below 1% with active feedback techniques or an electro-optic noise reduction system [3.129].

Pulse-to-pulse amplitude fluctuations of at least 5% will occur in the output from pulsed lasers. This source of noise is generally minimized by normalizing the detected signal to the laser intensity, or alternatively averaging the measurement over a large number of laser pulses.

Suspended solids are expected to be present in process and waste solutions and will attenuate the laser beam in an absorption measurement. These suspended solids can be removed by pre-filtering the sample solution, or else their effect can be minimized through the use of differential absorption measurement techniques (e.g. "peak-to-valley" or frequency-switching techniques).

The measurement precision for the laser absorption methods is expected to be in the range of 1-10% RSD for measurements at concentrations larger than ten times the limit of detection. This level of precision is probably more than adequate for off-gas monitoring and should prove useful for on-line monitoring for process control and liquid waste monitoring. These absorption methods should also be considered for continuous on-line SNM accountability measurements, with high accuracy measurements made off-line using conventional analytical methods. In the measurement of SNM in solution by absorption spectroscopy, consideration should be given to the large number of molecular forms in which plutonium and uranium can exist including the possibility of colloidal plutonium polymer formation at low acid concentrations (< 0.5M HNO_3) [3.130].

3.3.4.6 Standardization Procedures

The standardization procedures for laser absorption spectroscopy are expected to resemble those used in conventional absorption spectrophotometry. In the case of external absorption spectroscopy, dual beam measurement techniques can be used to minimize the effects of source instabilities and improve the measurement precision. The absorption standard can be in the form of a known species composition and concentration contained in a sealed cell. In the case of long path absorption measurements for trace gases, a short pathlength ($\sim$ 1-10 cm) cell containing a high species concentration ($\sim$ 1000 ppm) can be used [3.77]. At this relatively high species concentration, conventional methods for gas analysis can be used to characterize the composition of the standard cell. These short pathlength gas standard cells could also be used for intracavity absorption measurements although it will no longer be possible to use dual beam measurement techniques within the laser cavity.

For optoacoustic spectroscopy, it is possible to construct a dual beam instrument with two chambers (sample and reference standard) separated by a common pressure transducer [3.88]. This technique should work for both gas and solution measurements; although it may be difficult to obtain well characterized standard gases at the concentration levels (ppb) required for trace gas analysis by optoacoustic spectroscopy.

3.3.4.7 Measurement Time and On-Line Capability

The time required for laser absorption measurements will depend upon the particular measurement circumstances and the desired measurement precision. With electronic wavelength scanning techniques it has been possible to scan a cw dye laser over a range of 12.5 nm every 10 μs [3.87], and diode lasers are commercially available which can scan a range of 1 cm^{-1} in 0.1 ms with a laser linewidth of $< 10^{-4}$ cm^{-1} [3.131]. Single pulse absorption measurements may also be made with a time resolution defined by the duration of the laser pulse [$\sim 10^{-8}$-10^{-6}s]. However, for greatest measurement precision it is generally necessary to average the measurement over a longer time scale (typically several seconds).

The absorption methods are capable of making rapid on-line or off-line measurements for both gaseous and solution species. In the case of trace gas measurements in the infrared, the measurement should be made at a reduced pressure ($\sim$ 10 torr) to minimize any potential interference from other atmospheric constituents. The sample pressure can be reduced by expanding the sampled gas volume. Alternatively, for continuous monitoring a differential pressure system may be used to generate a constant gas flow through the sample chamber at a reduced pressure.

The use of an acoustically resonant sample chamber for optoacoustic spectroscopy will permit flowing gas measurements to be made if the gas inlet and outlet ports are located at the nodes of the acoustic standing wave [3.88, 3.95]. Resonant optoacoustic sample cells can also be operated without any windows thus allowing continuous air sampling [3.96]. Continuous on-line measurements are also possible with intracavity absorption spectroscopy [3.102, 3.112].

3.3.4.8 Capability for Automated Operation

Measurements of NO and H_2O concentrations in the stratosphere have been made using completely automated external absorption and optoacoustic spectrometers mounted on a balloon platform [3.99, 3.132]. The laser source for these measurements was a spin-flip Raman laser; and the data gathering system consisted of lock-in amplifiers and a minicomputer. The minicomputer also controlled the details of the experiment, averaged the data over a preset number of scans of the laser wavelength, and periodically transmitted the data to the base station on the ground.

Microprocessor- and calculator-controlled tunable laser sources offer the possibility of completely automated wavelength scanning for absorption measurements. Digital data collection and analysis can be used for absorption measurements in such the same way as it has been used for Raman scattering measurements (see Sec. 3.2.4.8).

3.3.4.9 Summary of the Principal Advantages and Disadvantages of the Absorption Methods

The principal advantages and disadvantages of the absorption methods for quantitative analysis are summarized in Tables 3.13-3.15.

Table 3.13. Summary of external absorption spectroscopy.

Advantages:

1. The external absorption signal is imposed on a coherent laser beam which permits measurements over a long sample path length for gaseous species or alternatively permits a large spatial separation between the laser source, sample cell, and detector. The signal collection efficiency of this coherent beam is essentially unity.

2. Dual beam and "peak-to-valley" measurement techniques can be used for standardization and also to compensate for variations in experimental parameters.

3. The absorption methods permit on line non-destructive assay (NDA) or off-line measurements using small sample sizes.

4. The absorption methods are molecule specific and are also isotope specific for vibrational transitions in molecules involving light atoms.

5. The sample absorbance in an external absorption measurement scales linearly with analyte concentration, absorption cross-section, and path length so that interpretation of the data is straightforward.

6. The external absorption method has a high sensitivity for long path measurements of gaseous species at a reduced pressure ($\sim$ 1-100 ppb at $\sim$ 10 torr pressure).

Disadvantages:

1. The strong infrared absorption in liquid solutions requires the use of a high power laser or a very short path length sample cell. The minimum detectable concentrations in solution are in the range $\sim 10^{-4}$-10^{-3}M.

2. The absorption bands in solution are broad; and overlapping bands can interfere with a measurement. Other possible sources of interference in solutions can arise from the dependence of the sample absorption on temperature, solvent effects, the shifting of chemical equilibria, scattering of the laser beam, and instrumental factors.

3. The absorption methods measure the average species concentration over the laser path length and thus are generally not useful for applications requiring spatial resolution.

Table 3.14. Summary of optoacoustic spectroscopy.

Advantages:

1. In the small signal approximation, the detected signal scales linearly with analyte concentration, path length, and laser power. Enhancement of the optoacoustic signal is possible using resonant acoustic and optical techniques.

2. Optoacoustic spectroscopy has a high sensitivity for the measurement of gaseous species ($\sim$ 1-100 ppb with a cw laser and an acoustically resonant sample chamber.)

3. Dual beam measurements are possible for standardization and also to compensate for variations in experimental parameters. Frequency-switching techniques allow measurements in liquid solutions with a minimum detectable concentration of $\leq 10^{-3}$M.

4. In optoacoustic spectroscopy a non-optical signal is generated thereby eliminating the need for a cooled detector in the infrared.

Disadvantages:

1. For greatest sensitivity in optoacoustic spectroscopy a relatively high power tunable cw laser ($\geq$ 1 mW) is required.

2. A synchronous background signal is generated by absorption of the laser light by the cell windows, walls, and by gaseous impurities present in the sample cell. A background level is also generated by acoustic noise. The relatively large synchronous background level must be subtracted from the measured signal to obtain the signal generated by the analyte species.

Table 3.15. Summary of intracavity absorption spectroscopy.

Advantages:

1. The intracavity absorption method provides an enhancement in sensitivity of $\sim 10^2$-10^5 over external absorption spectroscopy depending upon the particular laser type used. The method has a very high sensitivity for the measurement of vapor phase species ($\sim 5 \times 10^5$ atoms-cm^{-3} for Na; $\sim 5 \times 10^{11}$ mol-cm^{-3} for I_2).

2. The detected signal scales linearly with analyte concentration and path length over a range of several orders of magnitude.

3. The external fluorescence detection technique provides a quantitative measurement of the change in the laser spectrum with analyte concentration. This external fluorescence detection technique allows the measurement of all absorption lines lying within the laser bandwidth and permits the independent and simultaneous measurement of a number of intracavity absorbing species including iodine isotopes.

Disadvantages:

1. The intracavity absorption method relies in part on the mode competition in a homogeneously broadened laser, and the largest enhancement in sensitivity has been achieved with cw dye lasers which operate in the visible. The enhancement in sensitivity is much lower with inhomogeneous lasers (e.g. CO) operating in the infrared thus limiting the usefulness of the technique for most molecular species.

2. Intracavity absorption spectroscopy is not generally applicable to measurements in liquid solutions with the exception of rare earth compounds which exhibit sharp absorption spectra.

3.4 Fluorescence Spectroscopy

Fluorescence spectroscopy can be used to measure those atomic and molecular species in which the absorption of light is accompanied by a radiative relaxation of the excited state. In contrast, the basis for the opto-acoustic (absorption) method is the nonradiative conversion of the excitation energy into heat. Thus the two methods are complimentary and, in principle at least, can be applied together to measure any type of atomic or molecular transition [3.133].

The use of lasers as the excitation sources for fluorescence spectroscopy has greatly increased the sensitivity for both vapor phase and solution measurements. Laser-excited atomic fluorescence spectroscopy has been used to detect sodium in the vapor phase at concentrations as low as 100 atoms-cm^{-3} [3.134]; and thallium, when atomized from solution, has been detected at concentrations as low as 0.5 ppt (parts-per-trillion) corresponding to $\sim 7 \times 10^{7}$ atoms in the 50 $\mu\ell$ sample volume [3.135]. Laser-excited molecular fluorescence spectroscopy has been nearly as sensitive, with reported detection limits of 5×10^{4} mol-cm^{-3} for BaO in the vapor phase [3.136] and 0.39 ppt ($\sim 8 \times 10^{-13}$M) for the organic dye Rhodamine 6G in solution [3.137].

The requirements for a radiative relaxation channel and a sensitive photodetector to measure the emitted light have generally limited the analytical use of fluorescence spectroscopy to electronic transitions in the ultraviolet and visible regions of the spectrum. However, when applicable the sensitivity of the fluorescence methods is several orders of magnitude greater than that of the absorption methods. In addition, the fluorescence methods have a very high spatial resolution (up to $10\lambda^{3}$ [3.133]), whereas the absorption methods measure the average species concentration over the laser path.

3.4.1 Atomic Fluorescence Spectroscopy

Atomic fluorescence spectroscopy (AFS) is the most sensitive of the laser-based analytical methods, capable of detecting sodium at concentrations corresponding to less than one atom on the average within the probe volume of a focused cw dye laser [3.134, 3.138]. This extreme sensitivity is made possible by the short upper-state lifetime of the sodium D_2 transition (16 ns) which permits the absorption and emission of $\times 10^7$ photons per second by a single atom when the incident resonance laser radiation equals the saturation intensity (21 $mW\text{-}cm^{-2}$) [3.139]. Since atomic transition lifetimes are typically 10^{-8} s, equally sensitive measurements should be possible for other elements under saturation conditions.

Atomic fluorescence measurements can be made for vapor phase species and also for species atomized from aqueous solutions with either flame or non-flame atomizers. The use of atomic fluorescence spectroscopy as a quantitative analytical technique was first introduced in 1964 [3.140]; and since that time, AFS has been developed into a reliable method for the analysis of trace metals in solution using flame atomizers and conventional light sources. The use of tunable dye laser excitation sources and non-flame atomizers in recent years, however, has increased the sensitivity of the method by several orders of magnitude. In addition, the possibility of obtaining saturation conditions with lasers will allow fluorescence measurements to be made independent of the source intensity and quenching collisions, thereby obtaining the maximum fluorescence emission while minimizing the effect of source instabilities on the measurement [3.141].

A number of reviews on laser-excited fluorescence spectroscopy have been published in recent years [3.1, 3.4-3.6, 3.8, 3.133, 3.139, 3.142]. Reviews have also appeared on the use of non-flame atomizers for improved atomization efficiency in AFS measurements [3.143, 3.144].

3.4.1.1 Explanation of Method

Atomic fluorescence is a complex phenomenon to interpret since it involves both the absorption and emission of radiation. In addition, during its lifetime (typically 10^{-8}s) an excited atom will undergo a number of collisions with foreign gas molecules which can lead to the quenching of its fluorescence by nonradiative collisional energy transfer to the foreign gas molecules.

In atomic fluorescence spectroscopy, radiation from a spectral source is absorbed according to Beer's law (Eqn. 3.14) resulting in the excitation of atoms to higher energy states. A fraction of these atoms subsequently decay by the emission of radiation which is detected. If a line source is used for excitation, the intensity of the fluorescence, I_F, emitted by a weakly absorbing atomic vapor is proportional to the species concentration and the intensity of the exciting radiation [3.145]:

$$I_F = KI_o N\sigma L \tag{3.16}$$

where K is a proportionality constant taking into account the geometrical factors, wavelength, transition probability, Doppler width of the absorbing line, and fluorescence quantum efficiency,

I_o is the integrated intensity of the narrow line excitation source,

N is the concentration of the absorbing atomic species,

σ is the absorption cross-section,

and L is the absorption path length viewed by the fluorescence collection optics.

There are basically five different types of atomic fluorescence transitions: resonance fluorescence, in which the same lower and upper levels are involved in the excitation-deexcitation process; direct-line fluorescence, in which a single upper level and two or more lower levels are involved in the excitation-deexcitation process; stepwise-line fluorescence, in which a

single lower level and two or more upper levels are involved; sensitized fluorescence, in which one species is excited and transfers some or all of its excitation energy to an atom of the same or another species, either of which emits fluorescence upon relaxing to a lower level; and multi-photon fluorescence, in which two or more photons excite an atom which then is deexcited by the emission of fluorescence [3.146]. The first three types of fluorescence transitions defined above are commonly used in AFS and are illustrated in Figure 3.13. Multi-photon fluorescence is a nonlinear process and will be covered in Section 3.5.

3.4.1.2 Experimental Techniques for Atomic Fluorescence Spectroscopy

A schematic diagram illustrating the experimental apparatus used for laser-excited atomic fluorescence spectroscopy is shown in Figure 3.14. The frequency-doubled output from a nitrogen (N_2) pumped tunable dye laser is used as the excitation source for the analyte species which is atomized from solution by means of a non-flame atomizer. The analyte vapor is excited by the incident laser light and its fluorescence emission is detected normal to the laser beam. A narrowband interference filter is used to spectrally filter the fluorescence while a variable slit acts as a spatial filter to minimize the amount of continuum radiation from the high temperature atomizer which reaches the PMT. A boxcar integrator is used to process the detected signal, and the time history of the fluorescence from the atomized sample is recorded on a chart recorder. A heated monitor cell containing the analyte element is used to tune the laser to the excitation wavelength and to adjust the boxcar integrator sampling gate width and position. In addition the signal from this monitor cell can be used to measure the amplitude and frequency stability of the laser.

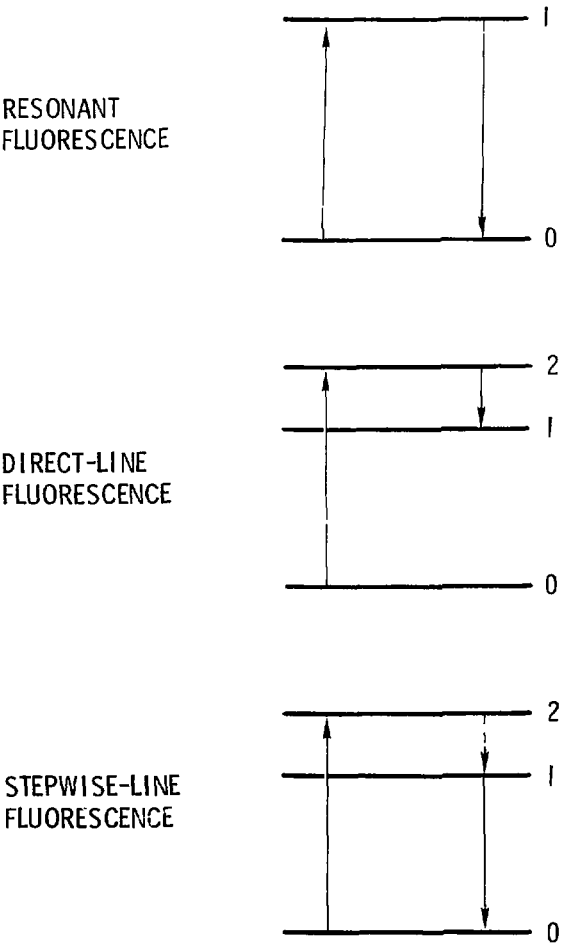

Figure 3.13. Types of atomic fluorescence transitions.

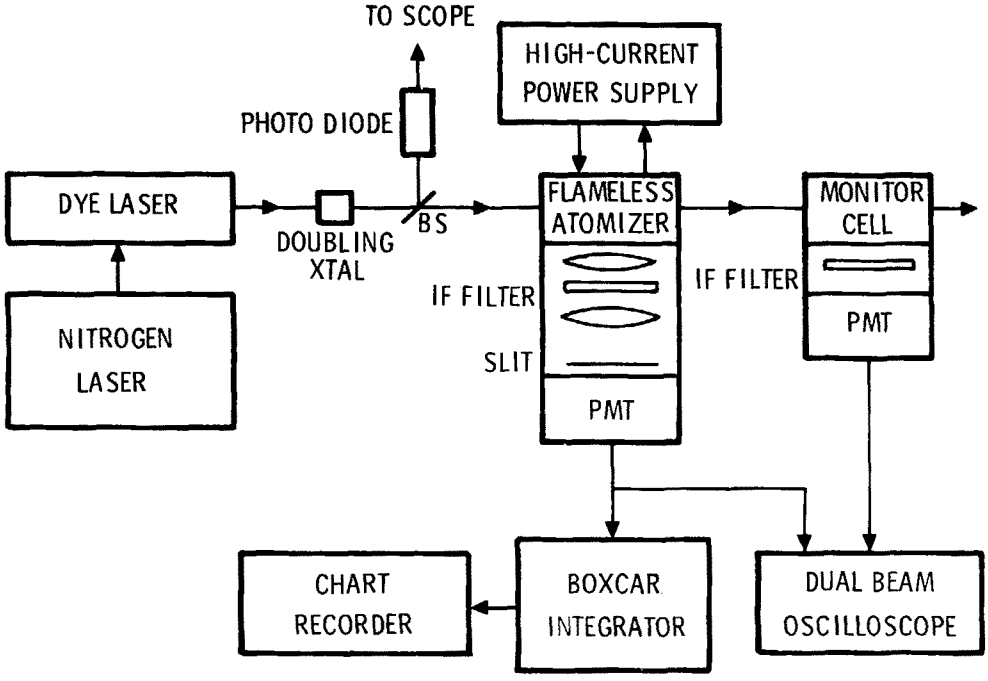

Figure 3.14. Experimental apparatus for laser-excited atomic fluorescence spectroscopy using a non-flame atomizer [3.135].

Although other types of pulsed and cw dye lasers have been used for AFS, N_2 laser pumped dye lasers have offered the greatest utility for AFS due to their wide wavelength range, high peak power, moderate repetition rate, and short pulse time duration. These dye lasers are tunable over the entire wavelength range 360-950 nm and can be frequency doubled to extend their operation to wavelengths below 220 nm [3.147-3.150]. This frequency doubling capability permits the excitation of the most sensitive lines, which for most elements lie in the ultraviolet. The short time duration ($\leq 10^{-8}$s) output from these lasers permits the fluorescence signal to be processed using time-gating techniques which effectively discriminate against the many sources of background noise in AFS (e.g. PMT dark current, emission from the high temperature atomizer, and emission by the analyte species) [3.151].

The use of a non-flame atomizer has a number of advantages over the conventional flame atomizers for use in atomic fluorescence spectroscopy [3.135, 3.143]. The non-flame atomizer produces a denser atomic vapor with increased sample residence time, and is free from the chemiluminescence and thermal emission found in the flame gases. Its atomization efficiency can approach 100%. It can be operated in an inert gas environment to minimize fluorescence quenching and metal-oxide formation, and it has a lower level of ionization for the alkali metals. Finally, small sample sizes (including solid samples) can be used. As a result of these factors, much lower limits of detection have been obtained for most metals with non-flame atomizers. An electrically heated non-flame atomizer designed for laser-excited AFS is shown in Figure 3.15.

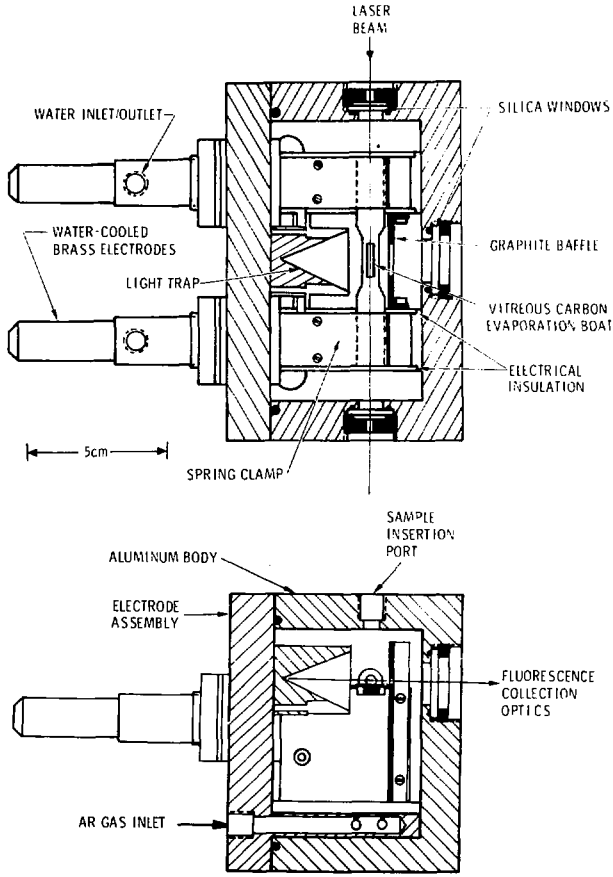

Figure 3.15. Non-flame atomizer for laser-excited atomic fluorescence spectroscopy [3.135].

The detection of non-resonant fluorescence (i.e. direct-line or stepwise-line fluorescence) in atomic fluorescence spectroscopy is desirable since it eliminates the strong Rayleigh and Mie scattering of the laser light which otherwise generally limits the detection to relatively high concentrations. This detection of non-resonant fluorescence also eliminates self-absorption in the sample and increases the analytically useful concentration range over which measurements can be made ($> 10^6$) [3.135].

Saturation of the fluorescence emission can be achieved with the high spectral irradiance from tunable dye lasers. This provides a fluorescence signal many orders of magnitude larger than could be achieved using conventional light sources. Under saturation conditions, Beer's law is no longer valid and the fluorescence emission shows relatively little dependence upon fluctuations in the laser intensity or variations in the collisional quenching [3.141]. However, if the analyte concentration is small, the fluorescence intensity still retains its linear concentration dependence. The advantages of saturating the fluorescence are generally offset by the increase in scattered light when resonance fluorescence is detected; and this generally results in higher detection limits when scattered light is the primary source of noise [3.152]. Thus the advantages of saturation conditions are best utilized when non-resonant fluorescence is detected.

3.4.1.3 Use of Atomic Fluorescence Spectroscopy for Quantitative Analysis

Atomic fluorescence spectroscopy has been used to measure a number of species present in the vapor phase; but its greatest utility as an analytical tool has been in the analysis of trace metals in solution. The reported measurements of vapor phase species by AFS are summarized in Table 3.16. To date,

Table 3.16. Measurements of vapor phase species by laser-excited atomic fluorescence spectroscopy.

Analyte Species	Total Gas Pressure (Torr)	Dye Laser Parameters: Type	Power (W)	Bandwidth (nm)	Wavelength (nm)	Detection Wavelength (nm)	Minimum Detectable Concentration ($atoms\text{-}cm^{-3}$)	Reference
Na	-	cw	3×10^{-6}	3×10^{-4} (250 MHz)	589.0	589.0	10^{2}	3.134
Na	~ 760 (Ar)	cw	0.400	9×10^{-3} (8 GHz)	589.6	589.0	10^{b}	3.138
Na	F[a]	flashlamp-pumped	--	0.05	589.0	589.0	1.8×10^{8}	3.153
U	E	cw	5×10^{-3}	2×10^{-3}	591.54	591.54	3×10^{3}	3.154

a. Vapor cell evacuated prior to filling with the analyte species.

b. Calculated

relatively few quantitative measurements of vapor phase atomic species have been reported in the literature. However, the minimum detectable concentration for the reported measurements has been extremely small, especially when a cw dye laser has been used as the excitation source. In the case of sodium, less than one atom on the average has been detected within the probe volume of a focused laser beam [3.134, 3.138].

A large number of elements in solution have been measured by AFS when atomized from solution using a flame or non-flame atomizer. These measurements are summarized in Table 3.17 with the best reported sensitivity for each analyte species listed for each type of dye laser excitation source. The large majority of the reported laser-excited AFS measurements have been made using N_2 pumped dye laser sources and flame atomizers. Whenever non-flame atomizers have been used, however, much lower limits of detection have been reported.

Although attempts have been made to apply atomic fluorescence spectroscopy from an absolute standpoint, it is very difficult to accurately estimate the many parameters which must be accurately known for this approach to succeed [3.164]. For this reason, the analytical use of AFS has been based on a much simpler empirical approach involving the generation of analytical calibration curves (fluorescence signal vs analyte concentration) with standard samples. From these calibration curves the concentrations of unknown samples can be interpolated. An analytical calibration curve for laser-excited AFS measurements of thallium with a frequency doubled N_2 pumped dye laser is shown in Figure 3.16. In general, the analytical curves generated with laser sources are linear over a range of 3-6 orders of magnitude, becoming nonlinear at high concentrations due to the strong absorption of the laser light and/or the resonance fluorescence of the analyte species [3.135].

Table 3.17. Laser-excited AFS measurements of elements atomized from solution.

Analyte Species	Atomization Cell	Laser Type	Excitation Wavelength(nm)	Detection Wavelength(nm)	Minimum Detectable Concentration ($ng\text{-}ml^{-1}$)	Reference
Ag	F[a]	ND[b]	328.1	328.1	4	3.155
Al	F	N[c]	394.4	396.1	0.6	3.155
Ba	F	CW	553.5	553.5	2	3.156
Ba	F	N	553.7	553.7	8	3.155
Bi	F	ND	306.8	306.8	3	3.155
Ca	F	N	422.7	422.7	0.08	3.155
Cd	F	ND	228.8	228.8	8	3.155
Ce(ion)	F	N	371.64	393.92	500	3.157
Co	F	N	347.4	357.5	200	3.158
Cr	F	N	359.3	359.3	1	3.155
Cs	NF[d]	N	455.5	852.1	0.02 (1.2 pg)	3.159
Cu	F	ND	324.7	324.7	1	3.155
Dy(ion)	F	N	364.54	353.60	300	3.157
Er	F	N	400.80	400.80	500	3.157
Eu	F	N	459.40	462.72	20	3.157
Fe	F	ND	296.7	373.5	30	3.155
Ga	F	N	403.3	417.2	0.9	3.155
Gd(ion)	F	N	376.84	336.22	800	3.157
Hf	F	N	368.24	377.76	1.0×10^5	3.160
Ho	F	N	405.39	410.38	150	3.157
In	F	N	410.4	451.1	0.2	3.155
Li	F	N	670.8	670.8	0.5	3.155
Lu	F	N	465.80	513.51	3.0×10^3	3.157
Mg	F	ND	285.2	285.2	0.2	3.155
Mg	F	FD[e]	285.2	285.2	0.3	3.161
Mn	F	ND	279.5	279.5	0.4	3.155
Mo	F	N	390.3	390.3	12	3.155
Na	F	CW	589.5	589.5	0.1	3.162
Na	F	FL[f]	589.0	589.0	0.2	3.163
Na	F	N	589.0	589.0	0.1	3.155
Nb	F	N	405.89	407.97	1.5×10^3	3.160
Nd	F	CW	562.0	562.0	2.0×10^3	3.162
Nd	F	N	463.42	489.69	2.0×10^3	3.157
Ni	F	FD	305.1	305.1	100	3.161
Ni	F	N	361.0	352.4	2	3.155
Os	F	N	442.05	426.08	1.5×10^5	3.160
Pb	NF	FD	283.3	405.8	0.04 (0.2 pg)	3.152
Pb	F	ND	283.3	405.8	13	3.155
Pr(ion)	F	N	427.23	430.58	1.0×10^3	3.157
Rh	F	N	369.24	350.2, 402.04	150	3.160
Ru	F	N	372.8	349.89	500	3.160
Sc	F	N	391.18	402.37	10	3.160
Sm(ion)	F	N	366.14	373.91	150	3.157
Sr	F	N	460.7	460.7	0.3	3.155
Tb(ion)	F	N	370.28	350.92	500	3.157
Ti	F	N	399.9	399.9	0.3	3.155
Tl	NF	ND	276.8	351.9, 352.9	0.005 (0.025 pg)	3.135
Tm	F	N	371.79	409.42	100	3.157
U	F	CW	591.5	591.5	5.0×10^5	3.162
V	F	CW	609.0	609.0	300	3.162
V	F	N	370.4	411.2	30	3.155
Yb	F	N	398.80	346.44	10	3.157

a. Flame atomizer.
b. Frequency-doubled N_2 pumped dye laser.
c. N_2 pumped dye laser.
d. Non-flame atomizer.
e. Frequency-doubled flashlamp pumped dye laser.
f. Flashlamp pumped dye laser.

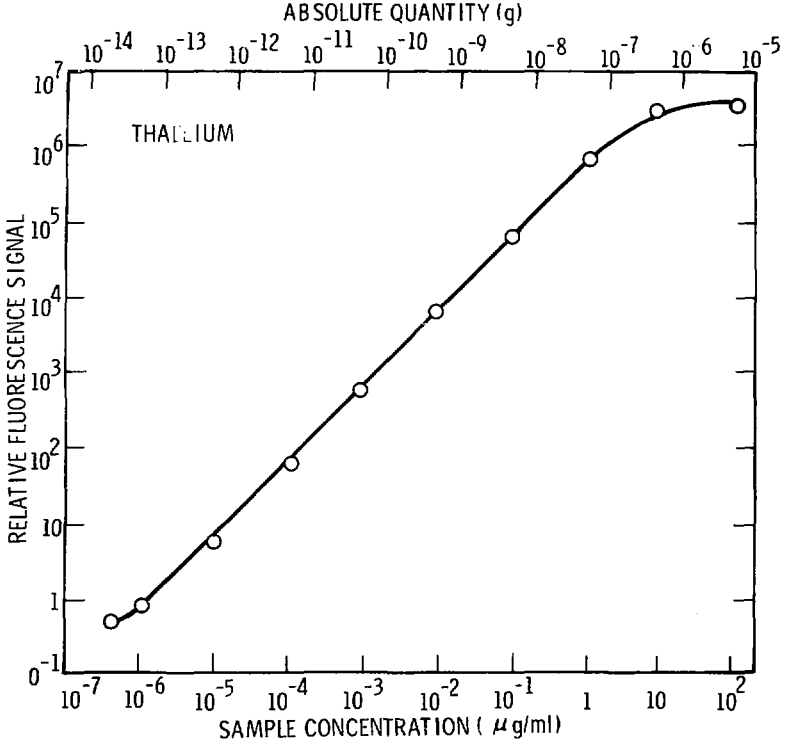

Figure 3.16. Analytical calibration curve for laser-excited AFS measurements of thallium [3.35].

3.4.2 Molecular Fluorescence Spectroscopy

The sensitivity of laser-excited molecular fluorescence spectroscopy (MFS) for gaseous species is lower than that of atomic fluorescence spectroscopy. This can be attributed to a number of factors: the presence of vibrational structure in the ground electronic state reduces the fraction of molecules in resonance with the narrowband exciting laser radiation; the lifetime of molecular states is much longer than that of excited electronic states, resulting in a lower transition rate for excited molecules and increased fluorescence quenching; and the molecular fluorescence consists of a progression of vibrational-rotational lines spread over a large portion of the spectrum, decreasing the signal to noise ratio in the detection system. The areas of applicability of MFS are also more limited than those of AFS since the large majority of molecular species are de-excited by nonradiative processes and therefore do not fluoresce. However, for those species for which it can be used, laser-excited MFS has been a very sensitive method with reported detection limits on the order of parts-per-billion or lower for many gaseous and solution species. The progress in the development and applications of laser-excited MFS has been reviewed often in recent years [3.1, 3.4-3.6, 3.8, 3.133, 3.139, 3.142, 3.165-3.168].

3.4.2.1 Explanation of Method

The signal expression for molecular fluorescence spectroscopy is identical to that of atomic fluorescence spectroscopy (Eqn. 3.16). Molecular fluorescence is Stokes shifted from the wavelength of the exciting laser light. In solution, the fluorescence is in the form of one or more broad bands, whereas in gases a progression of vibration-rotation lines is observed (P, Q, and R branches).

3.4.2.2 Experimental Techniques for Molecular Fluorescence Spectroscopy

The experimental apparatus for laser-excited MFS is similar to that shown for AFS in Figure 3.14. Due to the broad absorption bands of molecules, a greater degree of freedom exists in the choice of the laser excitation source for MFS. A number of molecular fluorescence measurements have been reported with fixed frequency gas lasers (argon, He-Ne, He-Cd, and N_2) as well as tunable dye lasers. In general, however, an order of magnitude improvement in sensitivity has been obtained with tunable dye laser sources as opposed to fixed frequency lasers [3.169].

In a molecular fluorescence experiment, the Stokes-shifted sidelight is filtered to reject the resonantly scattered laser light and also the Raman scattered light from the solvent or the major constituents in gas samples (e.g. N_2, O_2, H_2O for atmospheric measurements). This can be done with a spectrometer or an interference filter, although often a long-pass color glass filter is used. The fluorescence light is detected with a PMT and processed with a boxcar integrator or a lock-in amplifier depending on whether a pulsed or a modulated cw laser is used as the excitation source.

The specificity of molecular fluorescence for species in solution is generally poor due to their broad emission bandwidth. However, it can be greatly improved through the use of certain separation techniques. High-pressure liquid chromatography has been used to separate a number of aflatoxins prior to their measurement by MFS [3.170]. This has permitted the detection of these aflatoxins in quantities as low as 0.75 pg in a 4 $\mu\ell$ suspended droplet of solvent eluting from the separation column. Another technique used to increase the specificity of MFS involves cooling aromatic solutions to liquid nitrogen

temperatures to obtain sharp emission spectra (< 0.1 nm half-width) [3.171]. Using this Shpol'skii effect, it has been possible to simultaneously measure fifteen different polynuclear aromatic hydrocarbons (PAH) in a single sample at concentrations of 10^{-10} - 10^{-8} g-mℓ^{-1} with a conventional spectral source [3.172]. The use of laser excitation has improved by several orders of magnitude the sensitivity for detecting PAH compounds [3.167].

3.4.2.3 Use of Molecular Fluorescence Spectroscopy for Quantitative Analysis

The use of MFS for the quantitative analysis of gases has been primarily concerned with those species of interest in air analysis. The localized MFS measurements are summarized in Table 3.18. In Table 3.18, the measurement of NO was accomplished by first oxidizing it to NO_2 [3.173]. The lower sensitivity for formaldehyde at atmospheric pressure is due to fluorescence quenching which reduces the fluorescence quantum efficiency to $\sim 10^{-4}$ [3.174]. Similarly, in the case of I_2, the fluorescence signal at atmospheric pressure (air) was measured to be $\sim$ 130 times smaller than that for measurements under evacuated conditions [3.175].

The use of molecular fluorescence spectroscopy for the analysis of elements in solution is almost entirely limited to molecular complexes and metal chelate systems [3.180]. With only a few exceptions (e.g. rare earth compounds and uranium salts) metallic elements require complexation with an organic molecule to become fluorescent. Furthermore the fluorescence of organic molecules in solution generally occurs only in those molecules having cyclic conjugated bond systems (e.g. benzene, naphthalene, anthracene).

Table 3.18. Measurements of gaseous species by laser-excited molecular fluorescence spectroscopy.

Analyte Species	Total Gas Pressure (torr)	Laser Type	Excitation Wavelength(nm)	Detection Wavelength(nm)	Minimum Detectable Concentration	Reference
BaO	$\sim 10^{-3}$	N_2 pumped dye	--	--	5×10^{4} mol-cm^{-3}	3.136
CH	~ 760	frequency-doubled dye	282.58	309	5×10^{6} mol-cm^{-3}	3.176
CH	~ 1	frequency-doubled N_2 pumped dye	--	290-400	$\sim 10^{9}$ mol-cm^{-3}	3.177
I_2	--	cw argon	514.5	--	5×10^{8} mol-cm^{-3}	3.133
I_2	~ 760	cw He-Ne	632.8	> 660	$\sim 2 \times 10^{11}$ mol-cm^{-3} [a]	3.175
NO	~ 760	cw argon	488.0	--	< 10 ppb	3.173
NO_2	~ 760	cw He-Cd	441.6	> 550	0.6 ppb ($\sim 2 \times 10^{10}$ mol-cm^{-3})	3.179
NO_2	~ 760	cw argon	488.0	--	3 ppb ($\sim 8 \times 10^{10}$ mol-cm^{-3})	3.173
NH_2	~ 1 (Ar)	cw dye	570.3	--	$\leq 2 \times 10^{-6}$ torr ($\leq 7 \times 10^{12}$ mol-cm^{-3})[a]	3.179
H_2CO (Formaldehyde)	750	frequency-doubled flashlamp pumped dye	326	~ 400	50 ppb ($\sim 1 \times 10^{12}$ mol-cm^{-3})	3.174

a. Estimated.

The reported measurements of solution species by laser-excited molecular fluorescence spectroscopy are listed in Table 3.19. The majority of these measurements have been made using pulsed laser excitation in the ultraviolet. Many of these solution species have been measured at concentrations below 10 ppt; and the most sensitive of these measurements have detection limits corresponding to about 10^7 analyte molecules within the probe volume of the excitation laser [3.169, 3.170].

Analytical calibration curves are used for molecular fluorescence measurements of solution species in a manner similar to that reported for atomic fluorescence measurements (see Section 3.4.1.3). These analytical curves have a linear range of 3-7 orders of magnitude change in analyte concentration, and become nonlinear at high analyte concentrations due to self-quenching and reabsorption of the fluorescence emission [3.184]. The concentration of an unknown sample is determined by interpolation from these analytical curves or by using other standardization techniques (e.g. internal standards and constant addition techniques).

3.4.3 Evaluation of Fluorescence Spectroscopy for Use in Nuclear Fuel Processing Plants

3.4.3.1 Previous Use in the Nuclear Fuel Cycle

Laser-excited fluorescence spectroscopy has only recently been applied for the quantitative analysis of species of interest in the nuclear fuel cycle. Atomic fluorescence measurements of uranium atomized from solution have been made using a cw dye laser, but have shown a relatively poor limit of detection (500 $\mu g\text{-}m\ell^{-1}$) [3.162]. Similar resonance fluorescence measurements of uranium

Table 3.19. Measurements of solution species by laser-excited molecular fluorescence spectroscopy.

Analyte Species	Solvent	Laser Type	Excitation Wavelength(nm)	Detection Wavelength(nm)	Minimum Detectable Concentration (g cm^{-3})	Reference
Benzene	H_2O	frequency-doubled N_2 dye	259.95	273, 302	19 ($2.5x10^{-7}$ M)	3.169
Naphthalene	H_2O	frequency-doubled N_2 dye	273.0	340, 360	$1.3x10^{-3}$ ($1x10^{-1}$ M)	3.169
Anthracene	H_2O	frequency-doubled N_2 dye	254.0	404	< $4.4x10^{-3}$ (< $2.5x10^{-11}$ M)	3.169
	Cyclohexane	N_2	337	397	0.01	3.181
Fluoranthene	H_2O	frequency-doubled N_2 dye	287.0	450	$1x10^{-3}$ ($5x10^{-13}$ M)	3.169
	Cyclohexane	N_2	337	460	0.01	3.181
Phenanthene	Cyclohexane	N_2	337	400	0.05	3.181
Pyrene	H_2O	frequency-doubled N_2 dye	273.0	395	$5x10^{-4}$ ($2.5x10^{-12}$ M)	3.169
	Cyclohexane	N_2	337	390	0.02	3.181
Chrysene	Cyclohexane	N_2	337	388	0.03	3.181
Acridine	Ethanol	N_2	337	415	0.05	3.181
	Ethanol	N_2 dye	365	415	0.1	3.181
Acridine Yellow	---	pulsed argon	515	---	6 ($1.9x10^{-8}$ M)	3.182
Acridine Red	---	pulsed argon	515	---	0.8 ($2.3x10^{-9}$ M)	3.182
Quinine	1M H_2SO_4	N_2	337	456	0.01	3.181
	1M H_2SO_4	N_2 dye	365	456	0.03	3.181
Quinine Sulfate	0.1 N H_2SO_4	N_2 dye	365	454	0.011	3.183
Rubrene	---	pulsed argon	515	---	0.5 ($1x10^{-9}$M)	3.182
Tryptophane	---	frequency doubled argon	257	---	$2.4x10^{3}$ ($5.4x10^{-6}$ M)	3.152
Fluorescein	H_2O	N_2 dye	470	514	$2x10^{-3}$ ($5x10^{-12}$ M)	3.184
	H_2O	N_2	337	514	0.03	3.181
Rhodamine 6G	H_2O	N_2	337.1	355-700	$6.2x10^{-4}$ ($1.3x10^{-12}$ M)	3.137
	Ethanol	N_2	337.1	355-700	$3.9x10^{-4}$ ($8.2x10^{-13}$ M)	3.137
Rhodamine B	---	pulsed argon	515	---	0.1 ($1.6x10^{-10}$ M)	3.182
Riboflavin	---	N_2 dye	375	540	$4.7x10^{-4}$ ($1.25x10^{-12}$ M)	3.185
Aflatoxin B_1	Ethanol	N_2	337.1	345-650	$2.5x10^{-3}$ ($7.8x10^{-12}$ M)	3.137
	---	cw He-Cd	325	---	0.75 pg	3.170
Aflatoxin B_2	---	cw He-Cd	325	---	0.75 pg	3.170
Aflatoxin G_1	---	cw He-Cd	325	---	0.75 pg	3.170
Aflatoxin G_2	---	cw He-Cd	325	---	0.75 pg	3.170

in the vapor phase have been extremely sensitive, with a detection limit of 3×10^3 atoms-cm^{-3} corresponding to about 10 atoms within the probe volume of the laser [3.154]. Thus the low sensitivity of the solution measurement is likely due to one or more of the following factors related to the flame atomizer: a low atomization efficiency, fluorescence quenching and/or a high scattered light level due to the flame gases, or a significant thermal depopulation of the uranium ground state in the nitrous oxide-acetylene flame (at 2500°K, 40% of the uranium atoms will be in the 620 cm^{-1} level which is inaccessible to the laser tuned to excite the 591.5 nm transition [3.186]).

Laser-excited molecular fluorescence spectroscopy is also being developed as a technique for monitoring airborne iodine-129 in the nuclear fuel cycle. To date, measurements of iodine concentrations as low as 4×10^{-10} g-cm^{-3} (9.3×10^{11} mol-cm^{-3}) have been made with evacuated vapor cells; and it is expected that airborne iodine concentrations of 10^{-10} g-cm^{-3} (2.3×10^{11} mol-cm^{-3}) or lower could be detected [3.175].

3.4.3.2 Possible Measurement Species

Laser-excited molecular fluorescence spectroscopy should be considered as a method for monitoring NO_2 and $^{129}I_2$ present in the off-gases in a nuclear-fuel processing plant. Laser-excited MFS has been used to measure NO_2 in air at concentrations far below those which are expected to be present in the off-gases from a fuel processing plant. The measurement of airborne $^{129}I_2$ by MFS is presently being investigated; and at the anticipated level of sensitivity, this method should permit the measurement of $^{129}I_2$ in the dissolver and high level liquid waste (HLLW) solidification off-gas control systems at all points prior to the iodine adsorbers.

Laser-excited atomic fluorescence spectroscopy has proven to be a very sensitive method for the measurement of species atomized from liquid solutions. AFS is capable of measuring most of the elements which are present as fission products in the HLLW stream. Of the actinide elements present in the HLLW stream, so far only uranium has been measured by AFS. The emission spectra of the actinides have been measured, and with the exception of americium are quite complex, containing large numbers of lines of low and relatively uniform intensity [3.187]. The average line intensities for thorium and protactinium are higher than that of uranium, while those of neptunium and plutonium are lower. The average line intensities of the actinides have been compared with those of the rare earths and show a similar pattern. Thus it should be possible to measure the actinides with a sensitivity comparable to that obtained for measurements of the rare earths ($< 1\ \mu g\text{-}m\ell^{-1}$). In the case of americium a much lower detection limit is expected.

The fluorimetric determination of uranium in a sodium fluoride flux by ultraviolet excitation (365 nm mercury line) is an extremely sensitive method but requires considerable sample preparation [3.122, 3.123]. However, with the much higher irradiance from laser sources, it may be possible to make direct on-line fluorimetric measurements in process solutions. A number of lasers emit in the ultraviolet and could be used as excitation sources. These include cw helium-cadnium (325 and 442 nm), cw argon (334, 351, and 364 nm), and pulsed N_2 lasers (337 nm). The possibility of observing fluorescence from plutonium in solution has been investigated over the entire wavelength range 300-800 nm but with no fluorescence observed from plutonium in any of its oxidation states [3.188].

3.4.3.3 Isotope and Molecule Specificity

In laser-excited atomic fluorescence spectroscopy, the spectral resolution is generally dependent on the bandwidth of the laser rather than that of the detection system [3.155]. Therefore when using a narrowband laser as the excitation source, AFS will be element specific or can always be made element specific through the proper choice of the excitation wavelength. Any spectral interferences from flame emission of other elements in the sample will be negligible when a gated detection system is used. Thus the only source of spectral interference in laser-excited AFS with gated detection is expected to come from molecular species formed in the atomizer (e.g. flame gases) and excited by the laser. This source of interference can be minimized through the use of a non-flame atomizer.

In atomic fluorescence spectroscopy, the lines from individual isotopes will generally not be resolvable due to the presence of Doppler and collisional broadening. To date no isotope specific measurements have been made with AFS; although in principle the method could be made isotope specific by utilizing a narrowband dye laser in conjunction with a nonlinear spectroscopic method such as intermodulated fluorescence spectroscopy [3.159].

The ability of laser-excited molecular fluorescence spectroscopy to discriminate between the stable isotope $^{127}I_2$ and the radioisotope $^{129}I_2$ has been demonstrated [3.175]. However, to date no measurements have been r with the heteronuclear molecule $^{127}I^{129}I$ which is expected to be present in significant quantities in the off-gases from a fuel processing plant. In gas phase measurements the fluorescence bands from different molecules may overlap, but by carefully selecting the excitation and detection wavelengths it is expected that this source of interference can be eliminated.

Molecular fluorescence spectroscopy will not be isotope specific for solution measurements; and the molecule specificity of this method will depend upon the composition of the sample solution and the measurement circumstances. If a number of species are present in solution with overlapping fluorescence bands, MFS will in most cases not be molecule specific. However, in the case of aromatic hydrocarbons in solution it has been possible to cool the sample to liquid nitrogen temperatures to obtain sharp emission spectra and thus independently measure a number of species in the sample [3.171]. In other instances, the analyte species may be the only source of fluorescence in the sample solution.

3.4.3.4 Sensitivity to Matrix Variations

Discussions of the matrix effects in fluorescence spectroscopy have appeared in the various textbooks and reviews of the fluorescence methods [3.144, 3.189-3.194]. With the exception of fluorescence quenching the matrix effects for fluorescence measurements will be very similar to those encountered in absorption spectroscopy.

In the case of atomic fluorescence spectroscopy the presence of matrix effects reduces the number of free atoms which can fluoresce and also reduces the fluorescence intensity from the excited analyte atoms. The physical and chemical interferences which arise from interactions with the matrix components include incomplete dissociation and atomization of the analyte compound, partial ionization of the analyte atoms, and the formation of compounds (e.g. metal oxides) with other species present in the sample or the atomization system.

A partial ionization of the analyte species will occur if the atomization temperature is too high; whereas the other sources of interferences above will occur for too low an atomization temperature [3.189]. Both types of interferences

have the effect of reducing the measured fluorescence signal. In many cases, these sources of interferences can be minimized by increasing the atomization temperature to provide an acceptable level of dissociation and atomization while adding a large amount of an easily ionized element (e.g. an alkali metal) to the sample solution to suppress the ionization of the analyte species [3.195]. The use of a non-flame atomizer will increase the atomization efficiency while reducing the other sources of interference [3.135, 3.143].

Fluorescence quenching is produced by collisional deactivation of the excited analyte atoms. In the case of flame atomizers, the quenching rate depends upon the composition of the flame gases and is least for a low temperature stoichiometric hydrogen-oxygen flame diluted with an inert gas such as argon [3.196]. However, for most elements an air-acetylene or nitrous oxide-acetylene flame is required to achieve an acceptable atomization efficiency and freedom from interference even though the fluorescence quenching is more severe with these types of flames [3.144]. The fluorescence quenching effect can be minimized by using a non-flame atomizer which operates in an inert gas environment or by saturating the absorption of the analyte species [3.143, 3.144].

For measurements of airborne molecular gases by laser-excited fluorescence spectroscopy, the fluorescence quenching rate will be relatively constant and the major sources of interference are expected to come from fluorescence (of the walls and windows of the sample chamber, from aerosols, and from other fluorescent gases in the sample) and also from Raman scattered light (from N_2, O_2, and H_2O [3.167, 3.173, 3.176, 3.178]. The interference from other fluorescing gases the sample can be eliminated by a careful selection of the excitation and detection wavelengths, while the wavelength independent aerosol fluorescence

can be discriminated against by measuring the total fluorescence signal with lasers tuned on and off the analyte absorption line [3.167]. If the wavelength separation in the above frequency switching technique is smaller than the band-pass of the detection system, this technique can also be used to discriminate against Raman scattered light.

In solution measurements, matrix effects will be evidenced by shifts in the peak fluorescence wavelength and changes in the fluorescence intensity. Since the fluorescence bands in solution are generally very broad, the most serious problem in solution measurements will be fluorescence quenching. The fluorescence intensity of a solution species depends upon a number of factors: temperature, viscosity, pH, and the composition of the solution [3.191-3.194]. The fluorescence intensity usually increases as the temperature of the sample is lowered or as the viscosity of the sample is increased. In both instances, the collisional deactivation of the excited analyte molecules is reduced thereby increasing the fluorescence efficiency.

Very dramatic changes in the fluorescence intensity and spectrum have been observed for some types of molecules in solution when the pH of the solution is varied [3.194]. In fact, some substances are so sensitive to pH that they are used as fluorescence indicators in acid-base titrations of colored solutions.

The presence of fluorescence quenching agents in the sample solution will generally have the greatest effect upon the fluorescence intensity of the analyte species. These quenching agents can be classed as nonresonant (transparent) quenchers (e.g. dissolved oxygen and potassium iodide) and resonant (absorbing) quenchers [3.193]. The quenching effect will be greatest for the resonant

quenching agents since they also absorb to a certain extent both the exciting and fluorescent light ("light filter effect"). Self-quenching can also occur at high analyte concentrations when the absorption and fluorescence bands of the analyte species overlap. Presently there are no techniques available for eliminating the quenching effects in solution, so they must be taken into account when making solution measurements.

3.4.3.5 Measurement Precision and Accuracy

As with all the laser-based analytical methods, the precision and accuracy of the atomic and molecular fluorescence measurements will depend upon the availability of suitable standardization procedures and the factors which will affect the fluorescence signal level. The principal source of noise in the fluorescence methods will usually come from instabilities (amplitude and frequency) in the laser. However, by saturating the absorption of the analyte species in AFS this source of noise can be minimized [3.141]; and the predominant source of noise remaining will be scattering of the laser radiation by particles and optical inhomogeneities in the atomizer.

The measurement precision in AFS is usually higher when flame atomizers are used; and measurments using a N_2 laser pumped dye laser as the excitation source have been made with a precision in the range of 5-8% RSD for analyte concentrations 10X the limit of detection (LOD), and 2-3% RSD for concentrations 1000X the LOD [3.151, 3.158]. With a non-flame atomizer, the best reported precision for comparable measurement circumstances has been 9% RSD at 20X the LOD, increasing to 4% RSD at 2000X the LOD [3.135]. The lower precision obtained using a non-flame atomizer can be attributed in part to sampling errors associated with the small sample size used ($\sim$ 50 $\mu\ell$). In

laser-excited MFS measurements of solution species with a cw helium-cadmium laser, a measurement precision in the range of 0.7-6% RSD has been reported [3.197].

At the relatively high concentration levels of the elemental species present in the HLLW stream in a fuel processing plant, a measurement precision in the range of 2-5% RSD could probably be realized with AFS using a N_2 laser pumped dye laser source. The measurement precision for uranium in process streams could probably be made as high as 1-2% RSD using an amplitude stabilized fixed-frequency cw laser (e.g. He-Cd or argon) and the precision would be somewhat poorer when using an unstabilized pulsed N_2 laser. This level of precision should be more than adequate for continuous on-line monitoring for process control and secondary accountability.

3.4.3.6 Standardization Procedures

The standardization procedure which is used for atomic fluorescence spectroscopy involves the generation of an analytical calibration curve with standard samples which have been serially diluted to lower and lower concentrations. From this calibration curve the concentration of unknown samples can be interpolated.

For fluorescence measurements of gases such as NO_2, the standardization procedure generally involves the use of a calibrated permeation tube [3.178]. In the case of measurements of airborne I_2, it may be possible to compare the fluorescence of the air sample with that from a sealed vapor cell containing I_2 at atmospheric pressure (N_2). The iodine fluorescence intensity from this reference cell could be varied to match that of the unknown sample by varying the temperature of a cold finger on the cell. And from the vapor pressure curves for I_2, the concentration of the air sample could be determined.

In the case of solution measurements, the recommended standardization procedures involve the use of analytical calibration curves, internal standards, and a constant addition method [3.192]. The use of an internal standard is particularly applicable for measurements at a reduced sample temperature for which the fluorescence bands are sharp [3.172]. In the use of the constant addition method, a known concentration of the analyte species in the same chemical form as the sample is added to one sample aliquot while an identical volume of solvent is added to a second aliquot [3.198]. The fluorescence signals from the two adjusted samples are then measured and are used to calculate the concentration of the original sample. A multiple-addition adaptation of this method can be used when the analytical calibration curve is nonlinear. The analyte addition method is the only standardization procedure which compensates for multiplicative interferences when the sample matrix is unknown or varies from sample to sample [3.198].

3.4.3.7 Measurement Time and On-Line Capability

Laser-excited atomic fluorescence spectroscopy is an off-line method with a measurement time determined by the type of laser source and atomization system used. With a N_2 pumped dye laser operating at a pulse repetition rate of 10-100 s^{-1}, the time required for a single sample and blank determination will range from 2-5 minutes with a flame atomizer and 5-10 minutes for a non-flame atomizer. The longer measurement time for the non-flame atomizer is required to carefully dry the liquid sample, then reduce any combustable (organic) materials in the sample to ash, and finally atomize the sample.

After the atomization stage, 1-2 minutes are allowed for the graphite or vitreous carbon evaporation boat to cool down to room temperature prior to inserting the blank. Although the measurement time is longer with non-flame atomizers, they can be operated in a sealed environment with a small sample size for the analysis of radioactive species.

For measurements of airborne NO_2 by laser-excited MFS, flowing gas measurements can be made with a measurement time determined by the integration time constant of the detection system (100 s at 0.9 ppb NO_2 concentration) [3.167, 3.173, 3.178]. MFS measurements of free radicals such as OH and NH_2 have also been made under flowing conditions [3.177, 3.179]. And although flowing gas measurements of I_2 have not been demonstrated to date, no problems are anticipated in making such measurements.

Laser-excited MFS can also be used for off-line or on-line non-destructive assay (NDA) of solution species. For off-line measurements sample sizes as small as 4 $\mu\ell$ have been reported [3.120]; and with analog detection electronics measurement times of several seconds have been reported [3.169]. On-line NDA measurements have been made in standard stopped-flow absorption cells (30-60 $\mu\ell$ volume) with front-surface illumination and fluorescence detection [3.197]. Continuous-flow measurements have not been reported but should be possible for real time on-line monitoring of the analyte concentration.

3.4.3.8 Capability for Automated Operation

Microprocessor- and calculator-controlled N_2 pumped dye lasers are availabl for use in fluorescence measurements [3.75, 3.199]. For molecular fluorescence measurements fixed-frequency gas lasers can be used in many cases as the

excitation source. The operation of non-flame atomizers for AFS can be automated; and automated samplers are available for use with non-flame atomizers [3.200]. Digital data collection and analysis can be used for fluorescence measurements in much the same way as it has been used for Raman scattering measurements (see Section 3.2.4.8).

3.4.3.9 Summary of the Principal Advantages and Disadvantages of the Fluorescence Methods

The principal advantages and disadvantages of the fluorescence methods for quantitative analysis are summarized in Tables 3.20 and 3.21.

Table 3.20. Summary of atomic fluorescence spectroscopy.

Advantages:

1. AFS is an element specific method which can be used to measure a large number of elements in solution (one at a time) with very few spectral interferences.

2. The measured fluorescence signal scales linearly with analyte concentration over a large concentration range; and reliable standardization procedures (analytical calibration curve) have been developed.

3. AFS is extremely sensitive, permitting the detection of many atomic species at sub-part-per-billion levels. Saturation of the absorption of the analyte species will minimize the effects of laser instabilities and fluorescence quenching while non-resonant fluorescence detection will eliminate self-absorption and scattered laser light.

4. The fluorescence methods have a very high spatial resolution (up to 10 λ^3).

5. There is a possibility of extending AFS to the detection of isotopes by using nonlinear fluorescence spectroscopy (e.g. intermodulated fluorescence spectroscopy).

Disadvantages:

1. AFS is an off-line measurement in which the sample is destroyed. Several minutes are required for each elemental determination.

2. Multi-element analysis by AFS is difficult and time consuming. The experimental parameters must be readjusted for each element.

Table 3.21. Summary of molecular fluorescence spectroscopy.

Advantages:

1. MFS can be used for on-line non-destructive assay (NDA) or off-line measurements using small samples (10-100 $\mu\ell$) contained in sealed cells.

2. The measured fluorescence signal scales linearly with analyte concentration over a large concentration range; and reliable standardization procedures (internal standard and constant addition) have been developed.

3. MFS is extremely sensitive and has a very high spatial resolution.

4. Fixed-frequency lasers can often be used for MFS measurements. Frequency-switching techniques have been developed to discriminate against aerosol fluorescence and Raman scattering for gaseous measurements.

Disadvantages:

1. Few molecular species exhibit fluorescence, thus limiting the utility of the method.

2. The molecule specificity in solution will depend upon the measurement circumstances and the presence of other species which fluoresce or quench the fluorescence of the analyte species.

3. In solution, the analyte fluorescence is sensitive to changes in temperature, viscosity, pH, and the presence of fluorescence quenching agents.

3.5 Nonlinear Spectroscopy

Atoms and molecules in the gas phase at a low pressure undergo random thermal motion with a velocity distribution dependent upon the gas temperature and the mass of the individual particles. This velocity distribution is the source of Doppler broadening which at room temperature produces a linewidth in atomic and molecular transitions many times larger than the natural linewidth which is determined by the lifetime of the excited state. In most atomic species the hyperfine structure and isotope shifts of electronic transitions cannot be resolved using linear absorption and fluorescence spectroscopy because of the Doppler effect.

A number of techniques have been developed to remove the restriction of the Doppler effect on optical spectroscopy [3.5]. These techniques include atomic and molecular beams, microwave-optical double resonance spectroscopy, level crossing spectroscopy, and quantum beat spectroscopy. The availability of narrowband tunable lasers has led in recent years to the development of a number of nonlinear spectroscopic methods, two of which can be used to virtually eliminate the effect of Doppler broadening thereby attaining a spectral resolution limited only by the laser linewidth and/or the natural transition linewidth. The two principal methods of nonlinear laser spectroscopy which are essentially free of Doppler broadening are saturation spectroscopy which is based upon the changes produced in the velocity distribution of atoms or molecules when excited by an intense coherent light beam, and two-photon spectroscopy which is based on the simultaneous absorption of photons by an atom or molecule from two laser beams similar in frequency but propagating in opposite directions [3.5].

Although the use of these nonlinear spectroscopic methods for quantitative analysis has received little attention to date, they are considered in this report since they offer unprecedented spectral resolution for the detection of isotopes and are applicable over a very wide spectral range (ultraviolet, visible, and infrared). In addition, two-photon spectroscopy permits the study of species having energy levels at twice the photon energy thus extending the wavelength range of nonlinear laser spectroscopy to the vacuum ultraviolet. And furthermore, two-photon spectroscopy can be used for measurements in an environment for which a single photon would be strongly absorbed (e.g. the measurement of the rare gases in the atmosphere).

The field of nonlinear laser spectroscopy is rapidly growing and has been reviewed frequently in recent years [3.1, 3.3, 3.5, 3.8, 3.139, 3.201-3.209]. A bibliography on the optical isotope shifts of atoms has also been compiled [3.210].

3.5.1 Saturation Spectroscopy

When a gas is excited by the intense coherent radiation from a laser, the optical pumping of the atoms or molecules into an excited state can proceed faster than the competing relaxation processes (e.g. spontaneous emission and collisional relaxation) thereby saturating the absorbing transition [3.1]. Saturation will occur, however, only for those atoms or molecules which are Doppler-shifted into resonance with the exciting laser radiation. Therefore, in the excited state there will be an excess population with the resonant axial velocity; whereas in the lower level there will be a deficiency.

These changes in the velocity distribution can produce narrow resonant changes in the absorption which can then be probed by a second laser beam of identical frequency but traveling in the opposite direction [3.3]. If the common frequency of the two laser beams (pump and probe) does not coincide with the center frequency of the atomic or molecular transition, the oppositely directed beams will interact with two velocity groups having exactly opposite velocities because of the Doppler effect. In this case the absorption of the weak probe beam will be unaffected by the presence of the intense pump beam. On the other hand, if the laser frequency is tuned to the center of the Doppler profile, both beams will interact with the same velocity group, namely those having essentialy zero axial velocity. In this case the probe beam will interact with the velocity group whose absorption has been saturated by the pump beam, and thus the absorption of the probe beam will be decreased. Therefore as the laser frequency is tuned across the Doppler profile the absorption of the probe beam will exhibit a resonant "dip" exactly at the center of the Doppler profile with a width equal to the homogeneous linewidth (determined by the natural linewidth, collisional broadening, and laser linewidth).

3.5.1.1 Explanation of Method

The saturation of an atomic or molecular transition can be described by an intensity- and frequency-dependent absorption coefficient, $\alpha(\nu,I)$ [3.211]:

$$\frac{dI}{I} = \alpha(\nu,I)dz. \tag{3.17}$$

In the case of a homogeneously broadened transition

$$\alpha(\nu,I) = \frac{\alpha_o(\nu)}{1 + I/I_s}$$

with

$$\alpha_o(\nu) = \frac{\alpha_o}{\pi} \frac{\Delta\nu/2}{(\Delta\nu/2)^2 + (\nu - \nu_o)^2}$$

where I_s is the saturation intensity of the transition,

α_o is the absorption at line center,

and $\Delta\nu$ is the homogeneous linewidth of the transition.

With a moderate laser intensity ($I \ll I_s$), Eqn. 3.17 can be approximated as

$$\alpha(\nu,I) \approx \alpha_o(\nu)[1 - I/I_s]$$

In a saturated absorption experiment, the change in intensity of a weak probe beam caused by an intense pump beam which is turned on and off is measured [3.211]. The change in intensity of the probe beam is given by

$$\left[\frac{dI}{I}\right]_{I=0} - \left[\frac{dI}{I}\right]_I \approx \alpha_o(\nu)\, L\, \frac{I}{I_s}$$

where L is the interaction path length in the absorbing medium.

Alternate methods for saturation spectroscopy measure the change in fluorescence intensity of a gas upon saturation (intermodulated fluorescence spectroscopy [3.212]) or the change in polarization of the probe beam (polarization spectroscopy [3.213]).

3.5.1.2 Experimental Techniques for Saturation Spectroscopy

The experimental apparatus used for a saturation absorption experiment is shown schematically in Figure 3.17. A strong pump beam and a weak probe beam are obtained from a tunable cw laser and are oppositely directed through a sample cell containing an absorbing gas at a low pressure ($\sim$ 0.1 - 1 torr) [3.214]. A slight crossing angle ($<$ 2 mrad) of the two beams is used to prevent feedback into the laser. The saturating pump beam is chopped and the resultant modulation of the probe beam due to the nonlinear interaction in the absorbing gas is measured.

As the laser is tuned to the center of the Doppler-broadened absorption line in the gas, both laser beams interact with the same group of atoms or molecules, namely those having essentially zero axial velocity. This produces an absorption spectrum with a spectral resolution determined by the laser linewidth and the homogeneous linewidth of the gas. If the laser linewidth is small and the gas maintained at a low pressure ($\sim$ 0.1 torr) to reduce collisional broadening, a resolution nearly equal to the natural linewidth can be obtained. This permits the observation of hyperfine structure and isotope shifts in atoms and molecules. Saturated absorption measurements can also be made with a narrowband pulsed tunable dye laser [3.215].

Saturated absorption spectroscopy can provide a spectral resolution much higher than that of the external absorption method which is Doppler-limited [3.216]. However, this increase in spectral resolution is at the expense of an equally large decrease in sensitivity. Therefore for the trace analysis of isotopes with the use of nonlinear laser spectroscopy it is preferable, when possible, to use intermodulated fluorescence spectroscopy which provides

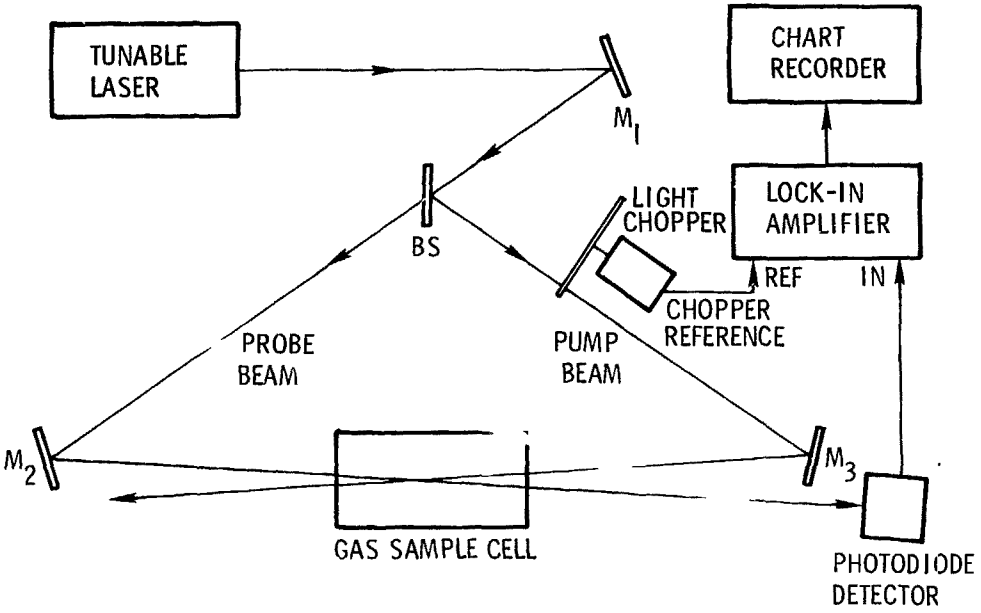

Figure 3.17. Experimental apparatus for saturated absorption spectroscopy [3.214].

both a high spectral resolution and a high sensitivity. In a fluorescing gas, whenever the absorption is reduced by saturation so also is the fluorescence.

A schematic diagram of the experimental apparatus for intermodulated fluorescence spectroscopy is shown in Figure 3.18. In order to detect the fluorescence, the two laser beams are adjusted to be of nearly equal intensity and are modulated at different frequencies. The nonlinear interaction of the two beams produces fluorescence components at the sum and difference frequencies which can then be detected using a PMT and a lock-in amplifier.

3.5.1.3 Use of Saturation Spectroscopy for Quantitative Analysis

To date, the emphasis with saturation spectroscopy has been placed entirely on its use as a Doppler-free method for studying the hyperfine structure and isotope shifts in atomic and molecular species with the result that it has yet to be used for quantitative analysis. Theoretical studies of the sensitivity of saturation absorption spectroscopy, however, have indicated that at a gas pressure of 10^{-2} torr this method will have a detection limit 2 to 3 orders of magnitude higher than external absorption spectroscopy [3.216]. Saturated absorption measurements of the sodium hyperfine structure and isotope shifts have been made at concentrations of $\sim 8 \times 10^{9}$ atoms-cm^{-3} using a N_2 pumped dye laser [3.215] and 2×10^{9} atoms-cm^{-3} using a cw dye laser [3.217]. The sensitivity of intermodulated fluorescence spectroscopy (IMF) is expected to be much higher than that of saturation absorption spectroscopy [3.216]; and IMF measurements of the hyperfine structure of iodine have been possible at vapor pressures as low as 2×10^{-4} torr ($\sim 8 \times 10^{12}$ mol-cm^{-3}) [3.212].

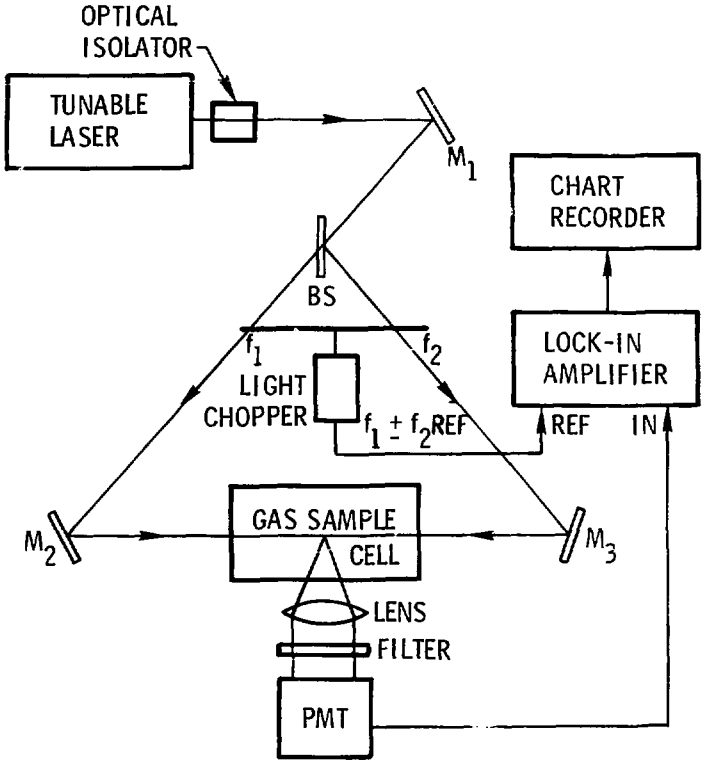

Figure 3.18. Experimental apparatus for intermodulated fluorescence spectroscopy [3.212].

3.5.2 Two-Photon Spectroscopy

The simultaneous absorption of photons by an atom or molecule from two laser beams similiar in frequency but propagating in opposite directions form the basis for Doppler-free two-photon spectroscopy (TPS). Two-photon spectroscopy allows the investigation of forbidden transitions and, in this respect, compliments saturation spectroscopy as a method for high resolution spectroscopy. In addition, TPS can be used to study levels having an energy twice as large as the photon energy, thereby extending the range of nonlinear laser spectroscopy to the vacuum ultraviolet.

3.5.2.1 Explanation of Method

To understand Doppler-free two-photon spectroscopy, consider an experiment in which an atom is present in a vapor cell and traveling with an axial velocity component v_z [3.218]. If two laser beams of frequency ν are directed through the cell in opposite directions, the frequencies of these beams as seen by the atom will be $\nu\left(1 - \frac{v_z}{c}\right)$ and $\nu\left(1 + \frac{v_z}{c}\right)$. Therefore if the atom undergoes a two-photon transition by absorbing one photon from each of the two counter-propagating laser beams, the Doppler-shift will be cancelled since

$$\nu\left(1 - \frac{v_z}{c}\right) + \nu\left(1 + \frac{v_z}{c}\right) = 2\nu. \qquad (3.18)$$

From Eqn. 3.18 it can be seen that each atom or molecule in a gas, regardless of its thermal velocity, can participate in the two-photon absorption process in which one photon is taken from each of the two counterpropagating beams.

Since it is also possible for an atom to absorb two photons which are traveling in the same direction, the profile of a two-photon absorption line

will in general be the sum of a wide Doppler-broadened profile and a narrow Doppler-free profile. However, by using circularly polarized laser beams it is possible to select a two-photon transition for which the Doppler-broadened profile is completely eliminated (e.g. S to S transitions for which the selection rule is $\Delta m = 0$) [3.219].

Two-photon spectroscopy can also be performed with two laser beams of different frequencies. The ability to arbitrarily select one of the laser frequencies allows the use of a resonant intermediate level which will greatly increase the two-photon absorption cross-section. In the case of sodium, the use of a resonant intermediate level increased the two-photon absorption cross-section by over seven orders of magnitude [3.220]. The induced cross-section for the sodium 3S-4D transition is intensity dependent, being on the order of $(5 \times 10^{-14})I_2$ cm^2 where I_2 (W - cm^{-2}) is the intensity of the laser beam at the resonance frequency ν_2. Thus by focusing the cw dye laser beam in the sample, the two-photon absorption cross-section of sodium can easily be made comparable to the single photon absorption cross-section of the 3S-3P resonance transition which is $\sim 3 \times 10^{-10}$ cm^2.

The use of two distinct laser frequencies in a two-photon measurement will also result in a residual Doppler shift. This residual Doppler shift will be reduced from the normal Doppler shift by the factor $(\nu_1 - \nu_2)/(\nu_1 + \nu_2)$ where ν_1 and ν_2 are the frequencies of the two laser beams [3.218].

3.5.2.3 Experimental Techniques for Two-Photon Spectroscopy

A schematic diagram of the experimental apparatus for two-photon spectroscopy of sodium is shown in Figure 3.19. The sodium vapor cell is placed in a

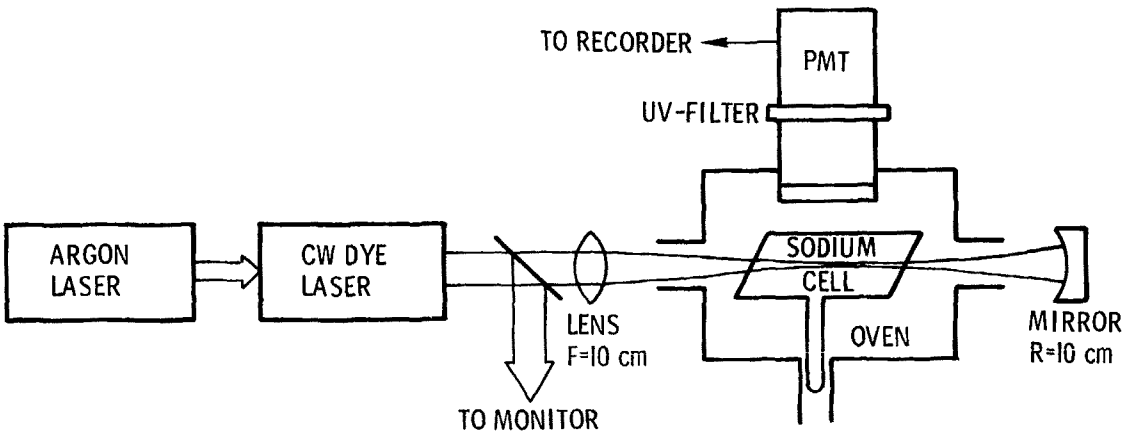

Figure 3.19. Experimental apparatus for two-photon laser spectroscopy of sodium [3.221].

standing wave field outside the cavity of a continuously tunable single mode cw dye laser. By tuning the dye laser to half the transition wavelength (578.732 nm) approximately 10% of the sodium atoms could be excited to the 3s → 4d two photon transition with a laser power of 30-50 mw [3.221]. The two-photon absorption is detected by observing the resultant fluorescence decay from the 4p → 3s transition at 330.2 nm. At a concentration of $\sim 10^{10}$ atoms-cm^{-3} the detected fluorescence light corresponded to 6×10^{7} photons-s^{-1} thereby allowing the two-photon absorption spectrum of sodium to be recorded directly by a chart recorder.

Doppler-free two-photon spectroscopy has also been performed on transitions that would be in the vacuum ultraviolet (VUV) (e.g. 1S → 2S transitions in atomic hydrogen and deuterium [3.222]). The experimental arrangement used in these measurements was similar to that shown in Figure 3.19 except that a frequency-doubled N_2-pumped dye laser (243.0 nm) was used as the excitation source. The ground state H and D atoms were produced by the dissociation of H_2 and D_2 in a Wood-type discharge tube (typically 0.1-0.5 torr pressure). Collisional transfer from the 2S to 2P levels permitted the two-photon absorption to be monitored by observing the 2P → 1S fluorescence at the L_α wavelength (121.5 nm).

VUV multi-photon spectroscopy has also been performed on xenon, hydrogen, and deuterium that was not Doppler-free. The $^1S_0 \rightarrow {}^1D_2$ transition in xenon at 126.2 nm was studied with a frequency-doubled N_2-pumped dye laser [3.223]. The xenon two-photon absorption was detected by observing the fluorescence decay of the $^3P_2$ state in the near-infrared. Three-photon ionization of atomic hydrogen and deuterium with a resonant two-photon intermediate state has been used as a sensitive means of detecting these atoms [3.224]. Concentrations of H and D as low as 4×10^{9} atoms-cm^{-3} could be detected in

the presence of 10^{17} atoms-cm^{-3} of buffer gas using this method. Isotopically selective excitation of the 1S → 2S two-photon transitions in H and D was possible using the fourth harmonic of a Q-switched Nd:YAG laser (266 nm) and the frequency-doubled and -summed output from a second harmonic Nd:YAG-pumped dye laser (224 nm). Ionization of the excited atoms was produced by an additional photon from the frequency-quadrupled Nd:YAG laser.

The use of ion detection techniques in multi-photon spectroscopy can be extremely sensitive. By saturating an intermediate one- or two-photon transition essentially the entire quantum-selected population can be ionized and detected with a gas proportional counter or an evacuated electron multiplier [3.225]. This detection technique has permitted the detection of single atoms of cesium [3.225-3.227]. In making these measurements, a flashlamp-pumped dye laser was used to excite the cesium $6^2S_{1/2} \rightarrow 7^2P_{3/2}$ transition at 455.5 nm with additional photons from the same laser ionizing the excited cesium atoms [3.225]. With a laser fluence of 100 mJ-cm^{-2}, 90% of the ground state cesium atoms were ionized in these measurements. A gas proportional counter (P-10 counting gas) was used to detect single cesium atoms in an environment of 10^{19} atoms-cm^{-3} of counting gas. This technique has also been used to measure the density fluctuations of cesium atoms [3.226], and to detect single cesium atoms formed from the spontaneous fission decay of ^{252}Cf [3.227].

3.5.2.3 Use of Two-Photon Spectroscopy for Quantitative Analysis

When fluorescence detection is used, the sensitivity of two-photon spectroscopy will be comparable to or better than that of saturation spectroscopy. Doppler-free two-photon measurements of sodium have been made at a concentration level of 10^{10} atoms-cm^{-3} with a signal-to-noise

ratio of ~ 100 thus indicating a detection limit on the order of 10^{7} atoms-cm^{-3} [3.221].

When two-photon ionization is used with saturation of the intermediate state, it has been possible to detect single atoms of cesium in a gas proportional counter [3.225-3.227]. In the case of saturated three-photon ionization, discharge-produced H and D have been detected at concentrations as low as 4×10^{9} atoms-cm^{-3} [3.224]. In this latter case, the ionization signal was linear with concentration up to 1.5×10^{14} atoms-cm^{-3}.

3.5.3 Evaluation of Nonlinear Spectroscopy for Use in Nuclear-Fuel Processing Plants

3.5.3.1 Previous Use in the Nuclear Fuel Cycle

Nonlinear laser spectroscopy has yet to be used as an analytical method in the nuclear fuel cycle.

3.5.3.2 Possible Measurement Species

The nonlinear spectroscopic methods could be used to make isotope specific measurements of species present in nuclear-fuel processing plants. The species which could possibly be measured with these methods include isotopes of uranium and plutonium and fission products. In the case of metallic elements in solution, the use of a non-flame atomizer would provide an atomic vapor which could be probed to make an isotope-specific measurement.

Fission product gases such as ^{85}Kr, HTO, and $^{14}CO_2$ could also be detected by the nonlinear spectroscopic methods. Saturated multi-photon spectroscopy may provide a very sensitive means for the detection of these gaseous species.

3.5.3.3 Isotope and Molecule Specificity

The nonlinear spectroscopic methods can attain a spectral resolution nearly equal to the natural linewidth of atomic and molecular transitions, and, thus, these methods will be both isotope and molecule specific. The shifts in the D_1 lines of sodium-22 and -23 and those in the 556 and 557 nm lines of the even isotopes of neutral krypton have been measured by saturation spectroscopy [3.217, 3.228, 3.229]. Two-photon spectroscopy has been used to make isotope selective measurements of hydrogen and deuterium [3.222, 3.224] and of rubidium-85 and -87 [3.230].

3.5.3.4 Sensitivity to Matrix Variations

The sensitivity of the nonlinear spectroscopic methods to matrix effects should be similar to that reported for absorption and fluorescence spectroscopy (see Sections 3.3.4.4 and 3.4.3.4).

3.5.3.5 Measurement Precision and Accuracy

No measurements of the precision and accuracy of the nonlinear methods have been made although they should be comparable to those reported for atomic fluorescence spectroscopy (see Sec. 3.4.3.5).

3.5.3.6 Standardization Procedures

The standardization procedures for the measurement of isotopes in solution would be based on the use of an analytical calibration curve in a manner similar to that reported for atomic fluorescence spectroscopy (see Sec. 3.4.3.6).

3.5.3.7 Measurement Time and On-Line Capability

For the measurement of species atomized from solution with a non-flame atomizer the measurement time and on-line capability of the nonlinear methods

will be identical to that reported for atomic fluorescence spectroscopy (see Sec. 3.4.3.7).

3.5.3.8 Capability for Automated Operation

The nonlinear spectroscopic methods could be automated in a manner similar to that reported for the fluorescence methods (see Sec. 3.4.3.8).

3.5.3.9 Summary of the Principal Advantages and Disadvantages of the Nonlinear Spectroscopic Methods

The principal advantages and disadvantages of the nonlinear spectroscopic methods for quantitative analysis are summarized in Tables 3.22 and 3.23.

Table 3.12. Summary of saturation spectroscopy.

Advantages:

1. Saturation spectroscopy is a Doppler-free method which permits the attainment of a spectral resolution limited only by the laser linewidth and/or the homogeneous linewidth of atomic and molecular transitions. This will permit isotope specific measurements in most atomic and molecular species.

2. The use of fluorescence detection in saturation spectroscopy greatly increases the sensitivity of the method. To date, high spectral resolution measurements have been made on sodium at concentrations as low as 2×10^{7} atoms-cm^{-3} and on iodine at concentrations as low as $\sim 8 \times 10^{10}$ molecules-cm^{-3}.

Disadvantages:

1. Saturation spectroscopy requires that measurements be made at a reduced pressure to reduce the effect of collisional broadening.

Table 3.13. Summary of two-photon spectroscopy.

Advantages:

1. Doppler-free two-photon spectroscopy can be performed using counter-propagating circularly polarized laser beams. This will permit isotope specific measurements in most atomic and molecular species.

2. The sensitivity of two-photon spectroscopy can be very high since the use of counter-propagating laser beams allows interaction with the entire velocity distribution. The use of a resonant intermediate state provides an intensity-dependent two-photon absorption cross-section which can be made comparable to a single photon absorption cross-section. Doppler-free TPS measurements of sodium have been possible at concentrations as low as $\sim 10^3$ atoms-cm^{-3}. Doppler-broadened two-photon ionization has permitted the detection of single cesium atoms in a gas proportional counter.

3. Two-photon spectroscopy allows the measurement of species having energy levels at twice the photon energy, thereby extending the wavelength range of nonlinear laser spectroscopy to the vacuum ultraviolet. TPS can be used for measurements in an environment for which a single photon would be strongly absorbed.

Disadvantages:

1. Resonantly-enhanced TPS generally requires the use of two lasers.

2. Doppler-free TPS measurements must be made at a reduced pressure to reduce the effect of collisional broadening. Doppler-broadened two-photon ionization measurements must be made in an evacuated electron multiplier or a gas proportional.

4. A Comparison of the Laser-Based and Conventional Analytical Methods for Use in Nuclear-Fuel Processing Plants

In this chapter, the laser-based analytical methods will be compared to the conventional analytical methods presently in use at fuel processing plants or proposed for use at such plants. By comparing the various methods for the measurement of specific species at specific locations in a fuel processing plant, the promising areas for the development of the laser-based methods can be identified.

4.1 Introduction

The conventional analytical methods used in the nuclear fuel cycle are in many cases extremely precise and accurate, and have proven very reliable over many years of use. However, the majority of these conventional methods must be used off-line and require a chemical separation of the analyte species from other interfering species by solvent extraction and/or ion exchange techniques. This chemical separation from interfering species and subsequent manipulations of the sample required with many of the conventional methods are time consuming and result in a low sample through-put.

The development of at-line and on-line non-destructive assay (NDA) methods in recent years has eliminated the need for chemical separations and sample handling while still providing, in many cases, a high degree of precision and accuracy. These NDA methods can substantially reduce the measurement time, and, in many cases, permit continuous on-line monitoring of selected species. The NDA methods, however, have been developed primarily for the measurement of uranium and plutonium and are not as widely applicable as the off-line chemical methods. In addition, the NDA methods are in certain cases susceptible

to interferences from other species in solution. The use of passive NDA methods (e.g. alpha, beta, gamma, and neutron counting) which measure decay radiation will also require a long counting time when the analyte species has either a very long half-life or is present in the sample at a very low concentration.

Although, in most cases, the reported precision and accuracy of the laser-based analytical measurements has been poorer than that attained using many of the conventional methods, techniques are now available which promise to greatly improve the precision and accuracy of the laser-based measurements. In addition the high spectral irradiance of lasers permits a greatly reduced measurement time and/or an increased sensitivity for low-level measurements. A number of the laser-based methods show promise for the at-line or on-line measurement of specific species for accountability, process control, and effluent control. Other laser-based methods can be used for off-line measurements with very small sample sizes (~ 1-50 μℓ) thereby minimizing the problem of handling highly radioactive samples. For the off-line laser-based methods minimal sample preparation, if any, is expected to be required.

In the case of long-lived radioisotopes, the laser-based methods have an inherent advantage over the passive counting methods. The total ensemble of atoms or molecules present in the probe volume in the sample can potentially contribute to the detected optical signal, whereas only those atoms which decay can be detected by the counting methods. This higher sensitivity of the laser-based methods will permit the real-time on-line monitoring of HTO, $^{129}I_2$ and $^{14}CO_2$ and possibly ^{85}Kr in the off-gases in a fuel processing plant.

4.2 A Comparison of Methods for SNM Accountability

The measurement of uranium and plutonium in the input accountability tank in a fuel processing plant requires the use of methods which are highly accurate and precise. In addition a highly accurate measurement of the isotopic abundances of uranium and plutonium is required at this point in order to calculate the effective atomic weights for later use with element specific measurement methods. At present, the laser-based methods cannot provide the degree of accuracy and precision required for these measurements: however, the nonlinear laser spectroscopic methods are element and isotope specific and thus would eliminate the source of interference in mass spectrometry from ions having the same m/e ratio (e.g. ^{238}U and ^{238}Pu, ^{241}Am and ^{241}Pu, ^{232}Th and ^{232}U).

In the product storage tanks, highly accurate accountability measurements are again required. However, in this case only the concentrations of uranium and plutonium must be determined. A number of conventional methods (isotope-dilution mass spectrometry, titrimetry, gravimetry, absorption-edge densitometry, and spectrophotometry) can be used for these measurements. These conventional methods offer a higher degree of accuracy than could be presently achieved with the laser-based methods. The conventional methods above, absorption-edge densitometry and spectrophotometry are presently being considered for on-line accountability measurements of the product solutions.

A number of NDA methods can also be used for accountability measurements in process streams. These include alpha spectrometry and gamma-ray spectrometry (which are both isotope specific) and absorption edge densitometry and spectrophotometry (which are both element specific). The laser-

based methods which should be considered for accountability in process streams are Raman scattering, external absorption spectroscopy, and molecular fluorescence spectroscopy. These methods can provide a faster measurement time and a higher sensitivity than the conventional methods although presently at the expense of a lower degree of precision and accuracy. The laser-based methods are therefore most appropriate on those process streams where the SNM concentration is low, where a more rapid measurement is required, or where interferences prevent the use of the conventional NDA methods. When "spiked" or Civex fuel cycles are considered, the much higher background radiation levels in these cycles may allow the element specific laser-based methods to successfully compete with the conventional NDA methods.

A number of conventional methods have been used for measurements of uranium and plutonium in waste streams: alpha spectrometry, spectrophotometry, and fluorimetry. The use of alpha spectrometry for these measurements requires a counting time of at least several minutes; while spectrophotometry and fluorimetry require that the sample be chemically separated from interfering species and either complexed or fused prior to a measurement. The use of laser-based methods such as resonant Raman scattering, external absorption spectroscopy, and molecular fluorescence spectroscopy should permit rapid on-line measurements of SNM in these waste streams. In addition, atomic fluorescence spectroscopy could be used as a rapid at-line measurement method for uranium and plutonium in both the high level liquid waste (HLLW) streams and the low activity waste (LAW) streams.

4.3 A Comparison of Methods for Process Control

On-line laser-based analytical methods are available which offer a rapid response time for process control. Laser-excited resonant Raman spectroscopy, external absorption spectroscopy, and molecular fluorescence spectroscopy should be considered as possible methods for measuring the loss of uranium and especially plutonium to the aqueous waste streams. These measurements of plutonium will provide the first indication of improper operation of the separation banks. The use of the laser-based methods should provide a much faster measurement than would be possible with any of the conventional methods.

Raman scattering and external absorption spectroscopy are molecule specific and thus can be used to determine the relative abundance of plutonium in its various oxidation states. This measurement is required at the various points in the solvent extraction process where plutonium is to be extracted into or out from aqueous solution. Laser Raman scattering can also be used for the simultaneous determination of the concentration of the oxidant (NO_2^-) or reductant (ferrous sulfamate, hydroxylamine nitrate, or U(IV)) which must be added for proper valence adjustment of plutonium. Presently, spectrophotometry is used to measure the nitrite ion concentration indirectly by monitoring the NO_2 concentration in air which is sparged through the process solution.

Raman scattering and possibly external absorption spectroscopy could be used as an alternative to gas chromatography for the measurement of solvent degradation products in process and acid wash streams. Gas chromatography is time consuming since the solvent degradation products must be chemically pretreated to convert them into volatile methyl derivatives prior to injection

into the gas chromatograph. Sample preparation should be minimized with the laser-based methods. Raman scattering could also be used to monitor the presence of solvents in the aqueous waste streams.

Atomic fluorescence spectroscopy provides a very sensitive method for the measurement of plutonium and neptunium in the process streams in the second uranium cycle and the measurement of uranium in the second plutonium cycle. Similarly thorium and protactinium could be measured in the Thorex process. The valence of neptunium and protactinium could possibly be measured in the first cycle feed adjustment tank using resonant Raman scattering or external absorption spectroscopy. This measurement would permit a proper valence adjustment of these species to ensure that the product solutions meet the required alpha decontamination specifications.

4.4 A Comparison of Methods for Effluent Control

Conventional methods have been developed for real-time on-line measurements of NO_2 (chemiluminescence NO_x analyzer), tributyl phosphate vapors (photometric phosphorous gas analyzer) and krypton-85 (gamma-ray counting). However, on-line real-time monitoring methods either do not exist or suffer serious interferences when used to detect HTO, $^{129}I_2$, and $^{14}CO_2$. The high sensitivity of the laser-based methods should permit real-time on-line measurements of these and other gases. External absorption spectroscopy could be used for on-line real-time monitoring of HTO, $^{14}CO_2$, and $CH_3{}^{129}I$ at selected points in the off-gas control system, while molecular fluorescence spectroscopy or intracavity absorption spectroscopy could be used to monitor $^{129}I_2$. Two-photon spectroscopy should be considered as a sensitive off-line method for the measurement of ^{85}Kr, HTO, and $^{14}CO_2$.

If unforseen problems arise with the conventional methods for monitoring NO_2 and tributyl phosphate (TBP) vapors, laser-based methods also exist for these species. Molecular fluorescence spectroscopy could be used to monitor NO_2, while external absorption spectroscopy is capable of monitoring both NO_2 and TBP vapors.

Laser-excited atomic fluorescence spectroscopy could be used to measure specific fission products and actinide elements present in the liquid waste streams (HLLW and SAW). When coupled with a nonlinear spectroscopic method such as intermodulated fluorescence spectroscopy, it should be possible to determine the concentration of specific isotopes in these waste streams. Laser Raman spectroscopy has already been used to measure the concentrations of the various anions present in the high level liquid waste from a fuel processing plant.

Atomic emission spectroscopy is a conventional method which can be used to simultaneously determine the many elements present in the waste streams. However, this method is in general not isotope specific and it lacks the sensitivity of laser-excited atomic fluorescence spectroscopy. The counting methods, on the other hand, are isotope specific but require a chemical separation of the analyte species from the highly radioactive waste streams and thus are time consuming.

4.5 Conclusion

The high sensitivity, selectivity, and speed of the laser-based analytical methods have been demonstrated in numerous applications outside of the nuclear fuel cycle. The application of these methods to measurements in nuclear-fuel processing plants will greatly improve the response times for critical process and effluent control measurements, improve dynamic accountability

measurements at secondary process and waste streams, and improve the measurement sensitivity for low-level species in gaseous and liquid effluent streams. The use of active stabilization and/or parallel data acquisition techniques should permit these measurements to be made with a precision and accuracy comparable to that of the conventional analytical methods. Thus the laser-based analytical methods offer exciting possibilities for an improved measurement capability in nuclear-fuel processing plants and elsewhere in the nuclear fuel cycle.

REFERENCES

1.1 W. E. Siri, et.al., "Study of Nuclear Material Accounting," NUREG-0290 (Vol. 2), (1977).

1.2 C. J. Rodden, ed., "Selected Measurement Methods for Plutonium and Uranium in the Nuclear Fuel Cycle," TID-7029 (2nd Ed.), (1972).

1.3 H. Sorantin, Determination of Uranium and Plutonium in Nuclear Fuels, (Verlag Chemie, Weinheim, W. Ger., 1975).

1.4 "Savannah River Laboratory, Quarterly Report, Alternate Fuel Cycle Technologies, April-June 1977," DPST-AFCT-77-1-2 (1977), p. 138.

1.5 W. E. Siri, T. Gozani, and J. Maly, "Study of Nuclear Material Accounting," NUREG-0290 (Vol. 3), (1977).

1.6 D. D. Jackson, J. E. Rein, and G. R. Waterbury, "Chemical Assay of Plutonium for Safeguards," Nucl. Technol., 23, 132 (1974).

1.7 M. V. Ramaniah, P. R. Natarajin, and P. Venkataramana, "Chemical Methods for the Determination of Uranium and Plutonium," Radiochim. Acta 22, 199 (1975).

1.8 E. A. Hakkila, et.al., "Coordinated Safeguards for Materials Management in a Fuel Reprocessing Plant," LA-6881, Vol. 2 (1977).

1.9 C. D. Bingham and M. W. Lerner, "Uranium Assay Requirements of Nuclear Accountability and Safeguards," Nucl. Technol., 23, 106 (1974).

1.10 "Savannah River Laboratory, Quarterly Report, Light Water Reactor Fuel Recycle, April-June 1976," DPST-LWR-76-1-2 (1976), p. 9.

1.11 F. E. Driggers and T. T. Thompson, eds., "Program Plan for Research and Development in Support of Thorium Fuel Cycle Technologies," DPST-TFCT-77-100 (1977).

1.12 W. E. Prout and A. E. Symonds, "Recovery of Thorium and Uranium-233 from Irradiated Thorium Oxide and Metal," DP-1036 (1967).

1.13 F. E. Driggers, "Reference Thorium Fuel Cycle," DPST-TFCT-77-101 (1977).

1.14 "Savannah River Laboratory, Quarterly Report, Light Water Reactor Fuel Recycle, October-December 1976," DPST-LWR-76-1-4 (1977), p. 32.

1.15 Reference 1.., p. 85.

1.16 "Savannah River Laboratory, Quarterly Report, Light Water Reactor Fuel Recycle, July-September 1976," DPST-LWR-76-1-3 (1976), pp. 33, 38.

1.17 "Savannah River Laboratory, Quarterly Report, Light Water Reactor Fuel Recycle, January-March 1977," DPST-LWR-77-1-1 (1977), p. 32.

1.18 "Composite Quarterly Report, Light Water Reactor Fuel Recycle," DPST-LWR-77-2-1 (1977), pp. 33, 34.

1.19 Reference 1.15, p. 53.

1.20 Reference 1.17, p. 46.

1.21 Reference 1.4, p. 84.

1.22 M. C. Thompson, Separations Chemistry Division, Savannah River Laboratories, private communication.

1.23 Reference 1.17, pp. 46, 52, 53.

1.24 Reference 1.14, p. 47.

1.25 Reference 1.4, pp. 10, 11.

1.26 R. B. Hower, B. Hekkala, and D. T. Pence, "Radioactive Airborne Effluent Measurement and Monitoring Survey of Reprocessing and Waste Treatment Facilities," SAI-77-863-LJ (1977).

1.27 "Savannah River Laboratory, Composite Quarterly Report, Light Water Reactor Fuel Recycle," DPST-LWR-76-2-3 (1976), p. 76.

1.28 J. F. Kordas and P. L. Phelps, "A Review of Monitoring Instruments for Transuranics in Fuel Fabrication and Reprocessing Plants," UCRL-52123 Rev. 1 (1977).

1.29 "Savannah River Laboratory, Quarterly Report, Alternate Fuel Cycle Technologies, April-June 1977," DPST-AFCT-77-1-2, p. 102.

1.30 R. W. Lynch, ed., "Sandia Solidification Process, Cumulative Report, July 1974 - January 1976," SAND-76-0105 (1976), p. III.A.2.a-2.

2.1 C. J. Rodden, ed., "Selected Measurement Methods for Plutonium and Uranium in the Nuclear Fuel Cycle," TID-7029 (2nd Ed.), (1972).

2.2 R. G. Gutmacher, F. Stephens, K. Ernst, J. E. Harrar, and J. Magistad, "Methods for the Accountability of Plutonium Nitrate Solutions," WASH-1282 (1974).

2.3 D. D. Jackson, J. E. Rein, and . . Waterbury, "Chemical Assay of Plutonium for Safeguards," Nucl. Technol., 23, 132 (1974).

2.4 H. Sorantin, Determination of Uranium and Plutonium in Nuclear Fuels, (Verlag, Weinheim, W. Ger., 1975).

2.5 M. V. Ramaniah, P. R. Natarajan and P. Venkataramana, "Chemical Methods for the Determination of Uranium and Plutonium," Radiochim. Acta, 22, 199 (1975).

2.6 W. E. Siri, T. Gonzani, and J. Maly, "Study of Nuclear Material Accounting, Final Report, July 1, 1976 - April 1, 1977," NUREG-0290 (Vol. 3), (1977).

2.7 E. A. Hakkila, "A Critical Review of Conventional Analytical Techniques for Fissile Materials," in 'Coordinated Safeguards for Materials Management in a Fuel Reprocessing Plant, Vol. 2, Appendix,' LA-6881, Vol. 2 (1977).

2.8 D. C. Camp, "A Review of LLL-Developed Instruments, Techniques and Methods Applicable to Alternative Fuel Cycle Technologies," UCRL-52326 (1977).

2.9 "Instrumentation for Environmental Monitoring, Radiation," LBL-1, Vol. 4 (1972).

2.10 R. J. Budnitz, "Plutonium: A Review of Measurement Techniques for Environmental Monitoring," IEEE Trans. Nucl. Sci., NS-21, 430 (1974).

2.11 J. F. Kordas and P. L. Phelps, "A Review of Monitoring Instruments for Transuranics in Fuel Fabrication and Reprocessing Plants," UCRL-52123 Rev. 1 (1977).

2.12 R. B. Hower, B. Hekkala, and D. T. Pence, "Radioactive Airborne Effluent Measurement and Monitoring Survey of Reprocessing and Waste Treatment Facilities," SAI-77-863-LJ (1977).

2.13 R. Gunnink, J. B. Niday, and P. D. Siemens, "A System for Plutonium Analysis by Gamma Ray Spectrometry, Part 1: Techniques for Analysis of Solutions," UCRL-51577, Pt. 1 (1974).

2.14 E. A. Hakkila, "Analytical Chemistry Needs For Nuclear Safeguards in Nuclear Fuel Reprocessing," in Analytical Chemistry in Nuclear Fuel Reprocessing, W. S. Lyon, ed. (Science Press, Princeton, N. J., 1978), pp. 24-31.

2.15 C. D. Bingham and M. W. Lerner, "Uranium Assay Requirements of Nuclear Accountability and Safeguards," Nucl. Technol., 23, 106 (1974).

2.16 K. Lewis, D. L. Colwell, C. G. Goldbeck, and J. E. Harrar, "An Evaluation of an Automated Titration System for the Determination of Uranium," in Analytical Chemistry in Nuclear Fuel Processing, W. S. Lyon, ed. (Science Press, Princeton, N. J., 1978), pp. 134-141.

2.17 R. Gunnink and J. F. Tinney, "Total Fissile Content and Isotopic Analysis of Nuclear Materials by Gamma-Ray Spectrometry," UCRL-73274 (1971).

2.18 R. Gunnink, "A System for Plutonium Analysis by Gamma Ray Spectrometry, Part 2: Computer Programs for Data Reduction and Interpretation," UCRL 51577, Pt. 2 (1974).

2.19. T. R. Canada, D. G. Langner, J. L. Parker, and E. A. Hakkila, "Gamma- and X-Ray Techniques for the Nondestructive Assay of Special Nuclear Material in Solution," in 'Coordinated Safeguards for Materials Management in a Fuel Reprocessing Plant, Vol. 2, Appendix,' LA-6881, Vol. 2 (1977).

2.20 T. R. Canada, J. L. Parker, and T. D. Reilly, "Total Plutonium and Uranium Determination by Gamma-Ray Densitometry," Trans. Am. Nucl. Soc., 22, 140 1975).

2.21 R. Gunnink and J. E. Evans, "In-Line Measurement of Total and Isotopic Plutonium Concentrations by Gamma-Ray Spectrometry," UCRL-52220 (1977).

2.22 R. B. Walton, et.al., "Non-Destructive Analytical Techniques for Materials in the Nuclear Fuel Cycle," in Analytical Methods in the Nuclear Fuel Cycle (International Atomic Energy Agency, Vienna, 1972), pp. 353-372.

2.23 D. D. Jackson, R. M. Hollen, S. F. Marsh, M. R. Ortiz, and J. E. Rein, "Determination of Submilligram Amounts of Uranium with the LASL Automated Spectrophotometer," in Analytical Chemistry in Nuclear Fuel Processing, W. S. Lyon, ed. (Science Press, Princeton, N. J., 1978), pp. 126-133.

2.24 P. G. Hagan and F. J. Miner, "Spectrophotometric Determination of Plutonium III, IV, and VI in Nitric Acid Solutions," RFP-1391 (1969).

2.25 E. W. Baumann, "Determination of Trace Uranium in Purex Aqueous Waste with Arsenazo III," DP-1458 (1977).

2.26 G. R. Price, R. J. Ferretti, and S. Schwartz, "Fluorophotometric Determination of Uranium," Anal. Chem., 25, 322 (1953).

2.27 "Savannah River Laboratory, Quarterly Report Alternate Fuel Cycle Technologies, April-June 1977," DPST-AFCT-77-1-2, p. 137.

2.28 "Composite Quarterly Report, Light Water Reactor Fuel Recycle July-September 1976," DPST-LWR-76-2-3, p. 73-76.

2.29 "Instrumentation for Environmental Monitoring, Air," LBL-1, Vol. 1 (1972).

2.30 "Composite Quarterly Report, Light Water Reactor Fuel Recycle, January-March 1977," DPST-LWR-77-2-1, p. 60.

2.31 Meloy Laboratories, Inc., Model PA-460 Phosphorous Gas Detector/Analyzer Data Sheet.

2.32 Reference 2.30, p. 125.

2.33 B.-G. Brodda, "In-Line and Off-Line Destruction Chemical Analysis in Fuel Reprocessing," in Analytical Chemistry in Nuclear Fuel Processing, W. S. Lyon, ed. (Science Press, Princeton, N. J., 1978), pp. 191-198.

2.34 R. D. Dierks and J. L. Russel, "2AF Sodium Nitrite Monitor: Interim Report," BNWL-CC-2396 (1970).

2.35 W. L. Belew, G. A. Huff, and L. F. Sears, "The Remote Sampling System and On-Line Analytical Monitors in the Barnwell Nuclear Fuels Reprocessing Plant," in Analytical Chemistry in Nuclear Fuel Processing, W. S. Lyon, ed. (Science Press, Princeton, N. J., 1), pp. 213-222.

3.1 W. Demtröder, Laser Spectroscopy, Topics in Current Chemistry, Vol. 17 (Springer-Verlag, New York, 1973).

3.2 F. P. Schöfer, ed., Dye Lasers, Topics in Applied Physics, Vol. 1 (Springer-Verlag, New York, 1973).

3.3 M. S. Feld and V. S. Letokhov, "Laser Spectroscopy," Sci. Amer., 229, 69 (1973).

3.4 J. I. Steinfeld, "Tunable Lasers and Their Application in Analytical Chemistry," CRC Crit. Rev. in Anal. Chem., 5, 225 (1975).

3.5 V. S. Letokhov, "Problems in Laser Spectroscopy," Sov. Phys. Usp., 19, 109 (1976).

3.6 H. Walther, ed., Laser Spectroscopy of Atoms and Molecules, Topics in Applied Physics, Vol. 2 (Springer-Verlag, New York, 1976).

3.7 A. Mooradian, T. Jaeger, and P. Stokseth, eds., Tunable Lasers and Applications, Springer Series in Optical Sciences, Vol. 3 (Springer-Verlag, New York, 1976).

3.8 S. Kimel and S. Speiser, "Lasers and Chemistry," Chem. Reviews, 77, 437 (1977).

3.9 J. Kuhl and W. Schmidt, "Tunable Coherent Light Sources," Appl. Phys., 3, 251 (1974).

3.10 A. Mooradian, "Laser Raman Spectroscopy," Science, 169, 20 (1970).

3.11 C. T. Walker, "Applications of Raman Spectroscopy to Molecular Physics," in Laser Photochemistry, Tunable Lasers, and Other Topics, S. F. Jacobs, M. Sargent, III, M. O. Scully, and C. T. Walker, eds. (Addison-Wesley, Reading, Ma., 1976)pp.145-195.

3.12 D. E. Irish and H. Chen, "The Application of Raman Spectroscopy to Chemical Analysis," Appl. Spectrosc., 25, 1 (1971).

3.13 Y. S. Bobovich, "Laser Spectroscopy Utilizing Spontaneous Raman Scattering of Weakly Interacting Molecules and its Applications," Sov. Phys. Usp., 15, 671 (1973).

3.14 W. L. Grossman, "Raman Spectroscopy, "Anal. Chem., 46, 345R (1974); 48, 261R (1976).

3.15 P. J. Hendra, "Laser Raman Spectroscopy," in Vibrational Spectra and Structure, Vol. 2, J. R. Durig, ed. (Marcel Delcker, Inc., New York, 1975) pp. 135-383.

3.16 J. M. Cherlow and S. P. S. Porto, "Laser Raman Spectroscopy of Gases," in Ref. 3.6, pp. 253-282.

3.17 H. A. Szymanski, ed., Raman Spectroscopy, Theory and Practice (Plenum Press, New York, 1967).

3.18 H. A. Szymanski, ed., Raman Spectroscopy, Theory and Practice, Vol. 2 (Plenum Press, New York, 1970).

3.19 T. R. Gilson and P. J. Hendra, Laser Raman Spectroscopy (Wiley-Interscience New York, 1970).

3.20 M. Tobin, Laser Raman Spectroscopy (Wiley-Interscience, New York, 1971).

3.21 S. K. Freeman, Applications of Laser Raman Spectroscopy, (John Wiley and Sons, New York, 1974).

3.22 A. Owyoung, "The Application of Third Order Nonlinear Optical Techniques to the Diagnosis of Combusting Media," SAND-77-0005 (1977).

3.23 G. T. McNice, "Raman Spectroscopy with a Tunable Dye Laser and a Narrowband Filter," Appl. Opt. 11, 699 (1972).

3.24 [illegible]ger, R. P. English, and R. J. D. Smith, "Laser Raman Spectrometer [illegible]ess Control," Appl. Opt., 12, 2083 (1973)

3.25 S. K. Freeman, "Small Sample Handling in Laser Raman Spectroscopy," Anal. Chem., 41, 398 (1969).

3.26 A. L. Marston, "Analysis of Radioactive Waste Supernate by Laser-Raman Spectrometry," Nucl. Technol., 25, 576 (1975).

3.27 A. G. Miller, "Laser Raman Spectrometric Determination of Oxyanions in Nuclear Waste Materials," Anal. Chim., 49, 2044 (1977).

3.28 R. A. Hill and D. L. Hartley, "Focused, Multiple-Pass Cell for Raman Scattering," Appl. Opt., 13, 186 (1974).

3.29 F. G. Ullman, "Investigation of Laser Raman Spectroscopy for Analysis of Water Quality," PB-261 238 (1976).

3.30 K. M. Cunningham, M. C. Goldberg, and E. R. Weiner, "Investigation of Detection Limits for Solutes in Water Measured by Laser Raman Spectrometry Anal. Chem., 49, 70 (1977).

3.31 S. I. Baldwin and C. W. Brown, "Detection of Ionic Water Pollutants by Laser Excited Raman Spectroscopy," Water Research, 6, 1601 (1972).

3.32 A. B. Harvey, J. R. McDonald and W. M. Tolles, "Analytical Applications of a New Spectroscopic Tool: Coherent Anti-Stokes Raman Spectroscopy (CARS)," in Progress in Analytical Chemistry, Vol. 8, I. L. Simmons and G. W. Ewing, eds. (Plenum Press, New York, 1976), pp. 211-238.

3.33 W. M. Tolles and R. D. Turner, "A Comparative Analysis of the Analytical Capabilities of Coherent Anti-Stokes Raman Spectroscopy (CARS) Relative to Raman Scattering and Absorption Spectroscopy," Appl. Spectrosc., 31, 96 (1977).

3.34 T. Hirshfeld, "Elimination of Fluorescence in Raman Spectroscopy," J. Opt. Soc. Am., 63, 1309 (1973).

3.35 J. Funfschilling and D. F. Williams, "cw Laser Wavelength Modulation in Raman and Site Selection Fluorescence Spectroscopy," Appl. Spectrosc., 30, 445 (1976).

3.36 F. L. Galeener, "FM Spectroscopy: Raman Scattering and Luminescence," Chem. Phys. Lett., 48, 7 (1977).

3.37 J. M. Harris, R. W. Chrisman, F. E. Lytle, and R. S. Tobias, "Sub-Nanosecond Time-Resolved Rejection of Fluorescence from Raman Spectra," Anal. Chem., 48, 1937 (1976).

3.38 W. Kiefer, "Laser-Excited Resonance Raman Spectra of Small Molecules and Ions - A Review," Appl. Spectrosc., 28, 115 (1974).

3.39 R. F. Begley, A. B. Harvey, and R. L. Byer, "Coherent Anti-Stokes Raman Spectroscopy," Appl. Phys. Lett., 25, 387 (1974).

3.40 R. F. Begley, A. B. Harvey, R. L. Byer, and B. S. Hudson, "A New Spectroscopic Tool, Coherent Anti-Stokes Raman Spectroscopy," Am. Lab., 6, 11 (Nov. 1974).

3.41 M. Maier, "Applications of Stimulated Raman Scattering," Appl. Phys., 11, 209 (1976)

3.42 L. A. Rahn, "Coherent Anti-Stokes Raman Spectroscopy," SAND77-8229 (1977).

3.43 M. D. Levenson, "Coherent Raman Spectroscopy," Phys. Today, 30, 44 (May 1977).

3.44 A. C. Eckbreth, P. A. Bonczyk, and J. F. Verdieck, "Review of Laser Raman and Fluorescence Techniques for Practical Combustion Diagnostics," PB-269 653 (1977).

3.45 J. J. Song, G. L. Eesley, and M. D. Levenson, "Background Suppression in Coherent Raman Spectroscopy," Appl. Phys. Lett., 29, 567 (1976).

3.46 R. F. Begley, A. B. Harvey, R. L. Byer, and B. S. Hudson, "Raman Spectroscopy with Intense, Coherent, Anti-Stokes Beams," J. Chem. Phys., 61, 2466 (1974).

3.47 P. R. Régnier, F. Moya, and J. P. E. Taron, "Gas Concentration Measurement by Coherent Raman Anti-Stokes Scattering," AIAA J., 12, 826 (1974).

3.48 L. B. Rogers, J. D. Stuart, L. F. Goss, T. B. Malloy, Jr., and L. A. Carreria, "Micro Sampling and the Use of a Flow Cell for Coherent Anti-Stokes Raman Spectroscopy," Anal. Chem., 49, 959 (1977).

3.49 J. Nestor, T. G. Spiro, and G. Klauminzer, "Coherent Anti-Stokes Raman Scattering (CARS) Spectra, with Resonance Enhancement of Cytrochrome C and Vitamin B_{12} in Dilute Aqueous Solution," Proc. Natl. Acad. Sci. USA, 73, 3329 (1976).

3.50 I. Chabay, G. K. Klauninzer, and B. S. Hudson, "Coherent Anti-Stokes Raman Spectroscopy (CARS): Improved Experimental Design and Observation of New Higher-Order Processes," Appl. Phys. Lett., 28, 27 (1976).

3.51 B. Attal, O. O. Schnepp, and J. P. E. Taron, "Resonant CARS in I_2 Vapor," Opt. Comm., to be published.

3.52 L. A. Carreira, T. C. Maguire, and T. B. Malloy, Jr., "Excitation Profiles of the Coherent Anti-Stokes Resonance Raman Spectrum of β-Carotene," J. Chem. Phys., 66, 2621 (1977).

3.53 L. A. Carreira, L. P. Goss, and T. B. Malloy, Jr., "Comparison of Coherent Anti-Stokes and Coherent Stokes Raman Lineshapes of the ν_1 Line of β-Carotene near a One Photon Resonance," J. Chem. Phys., to be published.

3.54 W. J. Jones and B. P. Stoicheff, "Inverse Raman Spectra: Induced Absorption at Optical Frequencies," Phys. Rev. Lett., 13, 657 (1964).

3.55 W. Wernche, A. Lau, M. Pfeiffer, H. J. Weigmann, G. Hunsalz, and K. Lenz, "Inverse Resonance Raman Scattering and Resonance Raman Amplification," Opt. Comm., 16, 128 (1976).

3.56 A. Owyoung, "Sensitivity Limitations for cw Stimulated Raman Spectroscopy," Opt. Comm., 22, 323 (1977).

3.57 A. Owyoung and E. D. Jones, "Stimulated Raman Spectroscopy Using Low-Power cw Lasers," Opt. Lett., 1, 152 (1977).

3.58 W. Wernche, J. Klein, A. Lau, K. Lang, and G. Hurnsalz, "Investigation of Inverse Raman Scattering Using the Method of Intra-Cavity Spectroscopy," Opt. Comm., 11, 159 (1974).

3.59 V. M. Baev, W. Wernche, and E. A. Sviridenkov, "Detection of Raman Amplification Lines by Intraresonator Laser Spectroscopy," Sov. J. Quant. Electron., 5, 477 (1975).

3.60 A. Lau, W. Wernche, M. Pfeiffer, K. Lenz, and H. J. Weigmann, "Inverse Raman Scattering," Sov. J. Quant. Electron., 6, 402 (1976).

3.61 Adelbert Owyoung, Sandia Laboratories, private communication.

3.62 "Savannah River Laboratory, Quarterly Report, Alternate Fuel Cycle Technologies, April-June 1977," DPST-AFCT-77-1-2 (1977), pp. 67-70.

3.63 "Savannah River Laboratory, Quarterly Report, Light Water Fuel Recycle, January-March 1977," DPST-LWR-77-1-1 (1977) p. 48.

3.64 D. Kato, "Isotopic Analysis by a Raman-Spectrophotometric Method," J. Appl. Phys., 47, 1072 (1976).

3.65 M. M. Sushchinskii, Raman Spectra of Molecules and Crystals, (Keter Inc., N. Y., 1972), p. 175.

3.66 B. Hudson, "Selection Rules for Coherent Anti-Stokes Raman Spectroscopy," J. Chem. Phys., 61, 5461 (1974).

3.67 L. A. Carreira, L. P. Goss, and T. G. Malloy, Jr., "Preresonance Enhancement of the Cohrent Anti-Stokes Raman Spectra of Fluorescent Compounds," Submitted to J. Chem. Phys.

3.68 B. Hudson, W. Hetherington III, S. Craver, I. Chabay, and G. K. Klauminger, "Resonance Enhanced Coherent Anti-Stokes Raman Scattering," Proc. Natl. Acad. Sci. USA, 73, 3798 (1976).

3.69 R. R. Alfano and N. Ockman, "Methods for Detecting Weak Light Signals," J. Opt. Soc. Am., 58, 90 (1968).

3.70 J. D. Winefordner, ed., Trace Analysis, Chemical Analysis, Vol. 46, (John Wiley and Sons, New York, 1976), pp. 9, 15-31.

3.71 M. Crunelle-Cros and J. C. Merlin," Application of Laser Raman Multichannel Spectroscopy to a Kinetic Study in the Liquid Phase," J. Raman. Spectrosc., 6, 261 (1977).

3.72 W. B. Roh, P. W. Schreiber, and J. P. E. Taran, "Single-pulse Coherent Anti-Stokes Raman Scattering," Appl. Phys. Lett., 29, 174 (1976).

3.73 C. H. Warren and L. Ramaley, "Digital Laser Raman Spectrophotometer System with On-Line Computer Control of Data Acquisition and Reduction," Appl. Opt., 12, 1976 (1973).

3.74 J. M. Kurepa, B. M. Parrić, and B. J. Levi, "An Automatic Spectroscopic Photon Counting Detector System," Spectrochim. Acta, 32B, 413 (1977).

3.75 Molectron Corporation, DL-II series N_2-pumped dye lasers with calculator-controlled wavelength scanning and synchronized frequency-doubling crystals.

3.76 E. D. Hinkley, R. T. Ku, and P. L. Kelley, "Techniques for Detection of Molecular Pollutants by Absorption of Laser Radiation," in Laser Monitoring of the Atmosphere, Topics in Applied Physics, Vol. 14, E. D. Hinkley, ed. (Springer-Verlag, New York, 1976), pp. 238-295.

3.77 J. Reid, J. Shewchun, B. K. Garside, and E. A. Ballik, "High Sensitivity Pollution Detection Employing Tunable Diode Lasers," Appl. Opt., 17, 300 (1978).

3.78 K. L. Cheng, "Absorptiometry," in Spectrochemical Methods of Analysis, Advances in Analytical Chemistry and Instrumentation, Vol. 9, J. D. Winefordner, ed. (Wiley-Interscience, New York, 1971), pp. 321-385.

3.79 G. Kraus and M. Maier, "Infrared Absorption Spectroscopy of Aqueous Solutions with a CO_2 Laser," Appl. Phys., 7, 287 (1975).

3.80 P. A. Bonczyk, "Apparatus for Local Sensing of Nitric Oxide as a Pollutant," Rev. Sci. Instrum., 46, 456 (1975).

3.81 S. M. Freund, D. M. Sweger, and J. C. Travis, "Quantitative Detection of Nitrogen Dioxide in Nitrogen Using Laser Magnetic Resonance at 1616 cm^{-1}," Anal. Chem., 48, 1944 (1976).

3.82 B. Lehmann, M. Wahlen, R. Zumbruman, H. Deschger, and W. Schnell, "Isotope Analysis by Infrared Laser Absorption Spectroscopy," Appl. Phys. 13, 153 (1977).

3.83 A. W. Mantz, J. F. Butler, and K. W. Nill, "Industrial Applications of Tunable Diode Lasers," Paper THGG4 presented at the IEEE/OSA Conference on Laser and Electro-Optical Systems, San Diego, Ca., 7-9 February 1978.

3.84 H. Gerlach, "Rapid Turning of a Dye Laser," Opt. Comm., 8, 41 (1973).

3.85 J. M. Telle and C. L. Tang, "New Method for Electro-Optical Tuning of Tunable Lasers," Appl. Phys. Lett., 24, 85 (1974).

3.86 L. D. Hutchison and R. S. Hughes, "Rapid Acoustooptic Tuning of a Dye Laser," Appl. Opt., 13, 1395 (1974).

3.87 J. M. Telle and C. L. Tang, "Direct Absorption Spectroscopy Using a Rapidly Tunable CW Dye Laser," Opt. Comm., 11, 251 (1974).

3.88 L. G. Rosengren, "Optimal Optoacoustic Detector Design," Appl. Opt., 14, 1960 (1975).

3.89 W. Lahmann, H. J. Ludewig, and H. Welling, "Opto-Acoustic Trace Analysis of Liquids with the Frequency-Modulated Beam of an Argon Ion Laser," Anal. Chem., 49, 549 (1977).

3.90 A. M. Angus, E. E. Mariner, and M. J. Colles, "Opto-Acoustic Spectroscopy with a Visible CW Dye Laser," Opt. Comm., 14, 223 (1975).

3.91 K. P. Koch and W. Lahmann, "Optoacoustic Detection of Sulphur Dioxide Below the Parts Per Billion Level," Appl. Phys. Lett. 32, 289 (1978).

3.92 L. B. Kreuger, N. D. Kenyan, and C. K. N. Patel, "Air Pollution: Sensitive Detection of Ten Pollutant Gases by Carbon Monoxide and Carbon Dioxide Lasers," Science, 177, 347 (1972).

3.93 C. F. Dewey, Jr., R. D. Kamm, and C. E. Hackett, "Acoustic Amplifier for Detection of Atmospheric Pollutants," Appl. Phys. Lett., 23, 633 (1973).

3.94 R. D. Kamm, "Detection of Weakly Absorbing Gases Using a Resonant Optoacoustic Method," J. Appl. Phys., 47, 3550 (1976).

3.95 S. Shtrikman and M. Slatkine, "Trace-Gas Analysis With a Resonant Optoacoustic Cell Operating Inside the Cavity of a CO_2 Laser," Appl. Phys. Lett., 31, 830 (1977).

3.96 P.-E. Nordal and S. O. Kanstad, "Photoacoustic Spectroscopy of Ammonium Sulphate and Glucose Powders and Their Aqueous Solutions Using a CO_2 Laser," Opt. Comm., 22, 185 (1977).

3.97 A. S. Gomenyuk, V. P. Zharov, D. D. Ogurok, E. A. Ryabov O. A. Tumanov, and V. O. Shaidurov, "Optoacoustic Detection of Low Concentrations of Hydrogen Fluoride, Nitric Oxide, and Carbon Dioxide in Gases Using Radiation of Pulsed Hydrogen Fluoride Laser," Sov. J. Quant. Electron., 4, 1001 (1975).

3.98 L. B. Kreuzer and C. K. N. Patel, "Nitric Oxide Air Pollution: Detection by Optoacoustic Spectroscopy," Science 173, 45 (1971).

3.99 C. K. N. Patel, E. G. Burkhardt, and C. A. Lambert, "Spectroscopic Measurements of Stratospheric Nitric Oxide and Water Vapor," Science, 184, 1173 (1974).

3.100 L. B. Kreuzer, "Ultralow Gas Concentration Infrared Absorption Spectroscopy," J. Appl. Phys., 42, 2934 (1971).

3.101 R. A. Keller, E. F. Zalewski and N. C. Peterson, "Enhancement of Absorption Spectra by Dye-Laser Quenching, II," J. Opt. Soc. Am., 62, 319 (1972).

3.102 T. W. Hänsch, A. L. Schawlow, and P. E. Toschek, "Ultrasensitive Response of a CW Dye Laser to Selective Extinction," IEEE J. Quant. Electron., QE-8, 802 (1972).

3.103 W. Brunner and H. Paul, "On the Theory of Selective Intracavity Absorption," Opt. Comm., 12, 252 (1974).

3.104. R. A. Keller, J. D. Simmons, and D. A. Jennings, "Enhancement of Absorption Spectra by Dye-Laser Quenching, III: Quantitative Aspects and a Comparison of Flashlamp-Pumped and CW Systems Under High Resolution," J. Opt. Soc. Am., 63, 1552 (1973).

3.105 K. Tohma, "Intracavity Absorption of Dye Lasers: A Rate-Equation Model," J. Appl. Phys., 47, 1422 (1976).

3.106 M. Maeda, F. Ishitsuka, M. Matsumoto, and Y. Miyazoe, "Quantitative Detection of Atomic Absorption by Intracavity Dye-Laser Quenching," Appl. Opt. 16, 403 (1977).

3.107 A. Dönszelmann, J. Neijzen, and H. Benschop, "Quenching of a Narrow-Band CW-Dye Laser," Physica 83C, 389 (1976).

3.108 W. J. Childs, M. S. Fred, and L. S. Goodman, "Ultrasensitive Detection of Cs Vapor by Intracavity Laser Quenching," Appl. Opt., 13, 2297 (1974).

3.109 A. Kaldor and B. W. Woodward, "Infrared Laser Monitoring Techniques for NO and NO_2," AICHE Symposium Series, 71, 183 (1974).

3.110. C. Chackerian, Jr. and M. F. Weisbach, "Amplified Laser Absorption: Detection of Nitric Oxide," J. Opt. Soc. Am., 63, 342 (1973).

3.111. G. H. Atkinson and T. N. Heimlich, "Quantitative Intracavity Laser Detection of NO_2 by Optical Multichannel Analysis," J. Chem. Phys., 66, 5005 (1977).

3.112. J. P. Hohimer and P. J. Hargis, Jr., "Intracavity Selective Absorption Spectroscopy as an Analytical Technique for Iodine Radicisotope Detection," Paper TuKK2 presented at the IEEE/OSA Conference on Laser and Electro-Optical Systems, San Diego, CA, 7-9 February 1978.

3.113. J. P. Hohimer and P. J. Hargis, Jr., Sandia Laboratories, unpublished data.

3.114. R. C. Spiker, Jr. and J. S. Shirk, "Quantitative Dye Laser Amplified Absorption Spectrometry," Anal. Chem., 46, 572 (1974).

3.115. G. Horlich and E. G. Codding, "Dye Laser Intra-Cavity Enhanced Absorption Measured Using a Photodiode Array Direct Reading Spectrometer," Anal. Chem., 46, 133 (1974).

3.116. H. W. Latz, H. F. Wyles, and R. B. Grun, "Atomic and Molecular Absorption Measurements by Intra-Cavity Quenching of Laser Fluorescence," Anal. Chem., 45, 2405 (1973).

3.117. K. W. Nill, Laser Analytics, Inc., private communication.

3.118. R. S. Eng, K. W. Nill, and M. Wahlen, "Tunable Diode Laser Spectroscopic Determination of ν_3 Band Center of $^{14}C^{16}O_2$ at 4.5 μm," Appl. Opt., 16, 3072 (1977).

3.119 W. F. Libby, "Vibrational Frequencies of the Isotopic Water Molecules; Equilibria with the Isotopic Hydrogens," J. Chem. Phys., 11, 101 (1943).

3.120 R. E. Dodd, "Infrared Spectra of Ruthenium and Osmium Tetroxides," Trans. Faraday Soc., 55, 1480 (1959).

3.121 P. G. Hagen and F. J. Miner, "Spectrophotometric Determination of Plutonium III, IV, and VI in Nitric Acid Solutions," RFP-1391 (1969).

3.122 C. J. Rodden, ed., "Selected Measurement Methods for Plutonium and Uranium in the Nuclear Fuel Cycle," TID-7029 (2nd Ed.), (1972).

3.123 H. Sorantin, Determination of Uranium and Plutonium in Nuclear Fuels, (Verlag Chemie, Weinhein, W. Ger., 1975).

3.124 A. S. Gomenyuk, V. P. Zharov, V. S. Letokhov, and E. A. Ryabov, "Laser Optoacoustic Method for Measuring Relative Isotopic Abundances of Molecules," Sov. J. Quant. Electron., 6, 195 (1976).

3.125 K. M. Baird and G. R. Hanes, "Stabilization of Wavelengths From Gas Lasers," Rep. Prog. Phys., 37, 927 (1974).

3.126 J. P. Hohimer, R. C.Kelley, and F. K. Tittel, "Frequency Stabilization of a High Power Argon Laser," Appl. Opt., 11, 626 (1972).

3.127 P. P. Sorokin, J. R. Lankard, V. L. Moruzzi, and A. Lurio, "Frequency-Locking of Organic Dye Lasers to Atomic Resonance Lines," Appl. Phys. Lett., 15, 179 (1969).

3.128 R. B. Green, R. A. Keller, G. G. Luther, P. K. Shenck, and J. C. Travis, "Use of an Opto-Galvanic Effect to Frequency-Lock a Continuous Wave Dye Laser," IEEE J. Quant. Electron., QE-13, 63 (1977).

3.129 Coherent Associates, Model 307 Laser Noise Reduction System Data Sheet.

3.130 C. A. Colvin, "Quantitative Determination of Plutonium Oxidation States in Variable Nitric Acid Solutions for Control Laboratories - Spectrophotometric," RL-SA-33 (1965).

3.131 Laser Analytics, Inc., Model LS-3 Laser Source Spectrometer Data Sheet.

3.132 C. K. N. Patel, "Spectroscopic Measurements of the Stratosphere Using Tunable Infrared Lasers," Opt. and Quant. Electron., 8, 145 (1976).

3.133 V. S. Letokhov, "Linear Laser Spectroscopy," Opt. and Laser Tech., 9, 263 (1977).

3.134 W. M. Fairbank, Jr., T. W. Hänsch, and A. L. Schawlow, "Absolute Measurement of Very Low Sodium-Vapor Densities Using Laser Resonance Fluorescence," J. Opt. Soc. Am., 65, 199 (1975).

3.135 J. P. Hohimer and P. J. Hargis, Jr., "Atomic Fluorescence Spectrometry of Thallium with a Frequency-Doubled Dye Laser and Vitreous Carbon Atomizer," Anal. Chim. Acta, 97, 43 (1978).

3.136 R. N. Zare and P. J. Dagdizian, "Tunable Laser Fluorescence Method for Product State Analysis," Science, 185, 739 (1974).

3.137 A. B. Bradley and R. N. Zare, "Laser Fluorimetry. Sub-Part-per-Trillion Detection of Solutes," J. Am. Chem. Soc., 98, 620 (1976).

3.138 J. A. Gelbwachs, C. F. Klein, and J. E. Wessel, "Single-Atom Detection by SONRES," IEEE J. Quant. Electron., QE-14, 121 (1978).

3.139 T. W. Hänsch, "Applications of Dye Lasers," in Dye Lasers, Topics In Applied Physics, Vol. 1, F. P. Schäfer, ed (Springer-Verlag, New York, 1973), pp. 205-274.

3.140 J. D. Winefordner and T. J. Vickers, "Atomic Fluorescence Spectrometry as a Means of Chemical Analysis," Anal. Chem., 36, 161 (1964).

3.141 E. H. Piepmeier, "Theory of Laser Saturated Atomic Resonance Fluorescence," Spectrochim. Acta, 27B, 431 (1972).

3.142 A. L. Robinson, "Analytical Chemistry: Using Lasers to Detect Less and Less," Science, 199, 1191 (1978).

3.143 G. F. Kirkbright, "The Application of Non-Flame Atom Cells in Atomic Absorption and Atomic Fluorescence Spectroscopy," Analyst, 96, 609 (1971).

3.144 R. F. Browner, "Atomic Fluorescence Spectrometry as an Analytical Technique," Analyst, 99, 617 (1974).

3.145 J. Kuhl and G. Marowsky, "Narrow-Band Dye Laser as a Light Source for Fluorescence Analysis in the Subnanogram Range," Opt. Comm., 4, 125 (1971).

3.146 N. Omenetto and J. D. Winefordner, "Types of Fluorescence Transitions in Atomic Fluorescence Spectrometry," Appl. Spectrosc., 26, 555 (1972).

3.147 R. S. Adhav and R. W. Wallace, "Second Harmonic Generation in 90° Phase-Matched KDP Isomorphs," IEEE J. Quant. Electron., QE-9, 855 (1973).

3.148 F. B. Dunning, E. D. Stokes, and R. F. Stebbings, "The Efficient Generation of Coherent Radiation Continuously Tunable from 2500 Å to 3250 Å," Opt. Comm., 6, 63 (1972).

3.149 F. B. Dunning, F. K. Tittel, and R. F. Stebbings, "The Generation of Tunable Coherent Radiation in the Wavelength Range 2300-3000 Å Using Lithium Formate Monohydride," Opt. Comm., 7, 181 (1973).

3.150 C. F. Dewey, Jr., W. R. Cook, Jr., R. T. Hodgson, and J. J. Wynne, "Frequency Doubling in $KB_5O_8 \cdot 4H_2O$ and $NH_4B_5O_8 \cdot 4H_2O$ to 217.3 nm," Appl. Phys. Lett., 26, 714 (1975).

3.151 L. M. Fraser and J. D. Winefordner, "Laser-Excited Atomic Fluorescence Flame Spectrometry," Anal. Chem., 43, 1693 (1971).

3.152 S. Neumann and M. Kriese, "Sub-Picogram Detection of Lead by Non-Flame Atomic Fluorescence Spectrometry with Dye Laser Excitation," Spectrochim. Acta, 29B, 127 (1974).

3.153 H. L. Brod and E. S. Yeung, "Atomic Fluorescence Spectrometry Using a Flashlamp-Pumped Dye Laser," Anal. Chem., 48, 344 (1976).

3.154 V. I. Balykin, V. S. Letokhov, V. I. Mishin, and V. A. Semchishen, "Laser Detection of Low Concentrations of Uranium Atoms Produced in a Chemical Reaction," JETP Lett., 24, 436 (1976).

3.155 S. J. Weeks, H. Haraguchi, and J. D. Winefordner, "Improvement of Detection Limits in Laser-Excited Atomic Fluorescence Flame Spectrometry," Anal. Chem., 50, 360 (1978).

3.156 R. B. Green and J. C. Travis, "Resonance Flame Atomic Fluorescence Spectrometry with Continuous Wave Dye Laser Excitation," Anal. Chem., 48, 1954 (1976).

3.157 N. Omenetto, N. N. Hatch, L. M. Fraser, and J. D. Winefordner, "Laser Excited Atomic and Ionic Fluorescence of the Rare Earths in the Nitrous Oxide-Acetylene Flame," Anal. Chem., 45, 195 (1973).

3.158 L. M. Fraser and J. D. Winefordner, "Laser-Excited Atomic Fluorescence Flame Spectrometry as an Analytical Method," Anal. Chem., 44, 1444 (1972).

3.159 J. P. Hohimer and P. J. Hargis, Jr., "Picogram Detection of Cesium in Aqueous Solution by Nonflame Atomic Fluorescence Spectroscopy with Dye Laser Excitation," Appl. Phys. Lett., 30, 344 (1977).

3.160 N. Omenetto, N. N. Hatch, L. M. Fraser, and J. D. Winefordner, "Laser Excited Atomic Fluorescence of Some Transition Elements in the Nitrous Oxide-Acetylene Flame," Spectrochim. Acta, 28B, 65 (1973).

3.161 J. Kuhl and H. Spitschan, "Flame-Fluorescence Detection of Mg, Ni, and Pb with a Frequency-Doubled Dye Laser as Excitation Source," Opt. Comm., 7, 256 (1973).

3.162 B. W. Smith, M. B. Blackburn, and J. D. Winefordner, "Atomic Fluorescence Flame Spectrometry with a Continuous Wave Dye Laser," Can. J. Spectrosc., 22, 57 (1977).

3.163 J. Kuhl, S. Neumann, and M. Kriese, "Influence of Saturation Phenomena on Laser-Excited Atomic Fluorescence Flame Spectrometry," Z. Naturforsch., 28a, 273 (1973).

3.164 V. Svoboda, R. F. Browner, and J. D. Winefordner, "Analytical Curves in Atomic Fluorescence Spectrometry," Appl. Spectrosc., 26, 505 (1972).

3.165 J. A. Hodgeson, W. A. McClenny, and P. L. Hanst, "Air Pollution Monitoring by Advanced Spectroscopic Techniques," Science, 182, 248 (1973).

3.166 R. N. Zare, "Laser Fluorimetry," in Laser Spectroscopy, Lecture Notes in Physics, Vol. 43, S. Haroche, J. C. Pebay-Peyroula, T. W. Hänsch, and S. E. Harris, eds. (Springer-Verlag, New York, 1975) pp. 112-120.

3.167 M. Birnbaum, "Laser-Excited Fluorescence Techniques in Air Pollution Monitoring," in Modern Fluorescence Spectroscopy, Vol. 1, E. L. Wehry, ed., (Plenum Press, New York, 1976) pp. 121-157.

3.168 C. M. O'Donnell and T. N. Solle, "Fluorometric and Phosphorometric Analysis," Anal. Chem., 48, 175R (1976).

3.169 J. H. Richardson and M. E. Ando, "Sub-Part-per-Trillion Detection of Polycyclic Aromatic Hydrocarbons by Laser Induced Molecular Fluorescence," Anal. Chem., 49, 955 (1977).

3.170 G. J. Diebold and R. N. Zare, "Laser Fluorimetry: Subpicogram Detection of Aflatoxins Using High-Pressure Liquid Chromatography," Science, 196, 1439 (1977).

3.171 G. F. Kirkbright and C. C. DeLima, "The Detection and Determination of Polynuclear Aromatic Hydrocarbons by Luminescence Spectrometry Utilizing the Shpol'skii Effect at 77K," Analyst, 99, 338 (1974).

3.172 T. Y. Gaevaya and A. Y. Khesina, "Quantitative Determination of Polycyclic Aromatic Hydrocarbons in Individual and Multicomponent Solutions From Their Quasilinear Fluorescence and Phosphorescence Spectra," J. Anal. Chem. (USSR), 29, 1913 (1974).

3.173 A. W. Tucker, A. B. Peterson, and M. Birnbaum, "Fluorescence Determination of Atmospheric NO and NO_2," Appl. Opt., 12, 2036 (1973).

3.174 K. H. Becker, U. Schurath, and T. Tatarczyk, "Fluorescence Determination of Low Formaldehyde Concentrations in Air by Dye Laser Excitation," Appl. Opt., 14, 310 (1975).

3.175 A. P. Baronavski and J. R. McDonald, "A Radioiodine Detector Based on Laser Induced Fluorescence," NRL Memorandum Report 3514 (1977).

3.176 C. E. Wang and L. I. Davis, Jr., "Measurement of Hydroxyl Concentrations in Air Using a Tunable uv Laser Beam," Phys. Rev. Lett., 32, 349 (1974).

3.177 M. A. A. Clyne, I. S. McDermid, and A. M. Curran, "The Spectroscopic Detection of Molecular Species Using a Scanning Narrow-Band Dye Laser," J. Photochem., 5, 201 (1976).

3.178 A. W. Tucker, M. Birnbaum, and C. L. Fincher, "Atmospheric NO_2 Determination by 442-nm Laser Induced Fluorescence," Appl. Opt., 14, 1418 (1975).

3.179 G. Hancock, W. Lange, M. Lenzi, and K. H. Welge, "Laser Fluorescence of NH_2 and Rate Constant Measurement of NH_2 + NO," Chem. Phys. Lett., 33, 168 (1975).

3.180 Reference 3.70, p. 214.

3.181 T. F. Van Geel and J. D. Winefordner, "Pulsed Nitrogen Laser in Analytical Spectrometry of Molecules in the Condensed Phase," Anal. Chem., 48, 335 (1976).

3.182 F. E. Lytle and M. S. Kelsey, "Cavity-Dumped Argon-Ion Laser as an Excitation Source in Time-Resolved Fluorimetry," Anal. Chem., 48, 855 (1974).

3.183 B. W. Smith, F. W. Plankey, N. Omenetto, L. P. Hart, and J. D. Winefordner, "Analytical Applications of Laser Excited Fluorimetry of Molecules in the Condensed Phase," Spectrochim. Acta, 30A, 1459 (1974).

3.184 T. Imasaka, H. Kadone, T. Ogawa, and N. Ishibashi, "Detection Limit of Fluorescein as Determined by Fluorometry with an Esculin Laser Source," Anal. Chem. 49, 667 (1977).

3.185 J. H. Richardson, B. W. Wallin, D. C. Johnson, and L. W. Hrubesh, "Sub-Part-Per-Trillion Detection of Riboflavin by Laser-Induced Fluorescence," Anal. Chim. Acta, 86, 263 (1976).

3.186 B. J. Snavely, "Separation of Uranium Isotopes by Laser Photochemistry," UCRL-75725 (1974), p. 6.

3.187 F. S. Tomkins and M. Fred, "The Spectra of the Heavy Elements," J. Opt. Soc. Am., 39, 357 (1949).

.188 M. A. Lyster, R. L. Fellows, and J. P. Young, "Search for Plutonium Fluorescence," CONF-750915-2 (1975).

3.189 R. Smith, "Flame Fluorescence Spectrometry," in Spectrochemical Methods of Analysis, Advances in Analytical Chemistry and Instrumentation, Vol. 9, J. D. Winefordner, ed. (Wiley-Interscience, New York, 1971) pp. 235-282.

3.190 V. Sychra, V. Svoboda, and I. Rubeska, Atomic Fluorescence Spectroscopy (Van Nostrand Reinhold Co., New York, 1975).

3.191 B. L. Van Duuren and T. L. Chan, "Fluorescence Spectrometry," in Spectrochemical Methods of Analysis, Advances in Analytical Chemistry and Instrumentation, Vol. 9, J. D. Winefordner, ed. (Wiley-Interscience, New York, 1971) pp. 387-450.

3.192 P. A. St. John, "Fluorometric Methods for Traces of Elements," in Trace Analysis, Chemical Analysis, Vol. 46, J. D. Winefordner, ed. (John Wiley and Sons, New York, 1976) pp. 213-277.

3.193 M. A. Konstantinova-Shlezinger, ed., Fluorometric Analysis (Daniel Davey and Co., New York, 1965).

3.194 H. H. Willard, L. L. Merritt, Jr., and J. A. Dean, Instrumental Methods of Analysis, 4th Ed. (D. Van Nostrand Co., New York, 1965), pp. 370-390

3.195 D. C. Manning and L. Capacho-Delgado, "Dissociation and Ionization Effects in Atomic Absorption Spectrochemical Analysis," Anal. Chim. Acta, 36, 312 (1966).

3.196 D. R. Jenkins, "An Analysis of the Optimum Conditions for the Detection of Metals in Flames by Atomic Fluorescence," Spectrochim. Acta, 23B, 167 (1967).

3.197 M. F. Bryant, K. O'Keefe, and H. V. Malmstadt, "Front-Face Laser Fluorescence Technique with Micro-Absorption Cells," Anal. Chem., 47, 2324 (1975).

3.198 Reference 3.70, pp. 41-42.

3.199 J. A. Perry, M. F. Bryant, and H. V. Malmstadt, "Microprocessor-Controlled, Scanning Dye Laser for Spectrometric Analytical Systems," Anal. Chem., 49, 1702 (1977).

3.200 Perkin-Elmer Corporation, Model AS-1 automatic sampling accessory for the model HGA-2100 Graphite Furnace.

3.201 K. Shimoda and T. Shimizu, "Nonlinear Spectroscopy of Molecules," Progress in Quantum Electrnics, Vol. 2, Part 2 (Pergamon Press, New York, 1972).

3.202 R. G. Brewer, "Nonlinear Spectroscopy," Science, 178, 247 (1972).

3.203 V. I. Bredikhin, M. D. Galanin, and V. N. Genkin, "Two-Photon Absorption and Spectroscopy," Sov. Phys. USp., 16, 299 (1973).

3.204 I. M. Beterov and R. I. Sokolovskii, "Nonlinear Effects in the Emission and Absorption Spectra of Gases in Resonant Optical Fields," Sov. Phys. Usp., 16, 339 (1973).

3.205 V. S. Letokhov, "Nonlinear High Resolution Laser Spectroscopy," Science, 190, 344 (1974).

3.206 W. M. McClain, "Two-Photon Molecular Spectroscopy," Accounts of Chemical Research, 7, 129 (1974).

3.207 K. Shimoda, ed. High-Resolution Laser Spectroscopy (Springer-Verlag, New York, 1976).

3.208 V. S. Letokhov and V. P. Chebotayev, Nonlinear Laser Spectroscopy (Springer-Verlag, New York, 1977).

3.209 V. S. Letokhov, "Nonlinear High Resolution Laser Spectroscopy," Opt. and Laser Tech., 10, 15 (1978).

3.210 K. Heilig, "Bibliography on Experimental Optical Isotope Shifts, 1918 Through October 1976," Spectrochim. Acta, 32B, 1 (1977).

3.211 P. Toschek, "General Survey of Laser Saturation Spectroscopy," Presented at the International Colloquium on "Doppler-Free Methods of Spectroscopy on Excited Levels of Simple Molecular Systems," Aussois, France, May 1973.

3.212 M. S. Sorem and A. L. Schawlow, "Saturation Spectroscopy in Molecular Iodine by Intermodulated Fluorescence," Opt. Comm., 5, 148 (1972).

3.213 C. Wieman and T. W. Hänsch, "Doppler-Free Laser Polarization Spectroscopy," Phys. Rev. Lett., 36, 1170 (1976).

3.214 T. W. Hänsch, M. D. Levenson, and A. L. Schawlow, "Complete Hyperfine Structure of a Molecular Iodine Line," Phys. Rev. Lett., 26, 946 (1971).

3.215 T. W. Hänsch, I. S. Shahin, and A. L. Schawlow, "High-Resolution Saturation Spectroscopy of the Sodium D Lines with a Pulsed Tunable Dye Laser," Phys. Rev. Lett., 27, 707 (1971).

3.216 K. Shimoda, "Limits of Sensitivity of Laser Spectrometers," Appl. Phys., 1, 77 (1973).

3.217 K. Pescht, H. Gerhardt, and E. Matthias, "Isotope Shift and HFS of D_1 Lines in Na-22 and 23 Measured by Saturation Spectroscopy," Z. Physik, A281, 199 (1977).

3.218 H. Walther, "Atomic and Molecular Spectroscopy with Lasers," in Laser Spectroscopy of Atoms and Molecules, Topics in Applied Physics, Vol. 2, H. Walther, ed. (Springer-Verlag, New York, 1976), pp. 1-124.

3.219 M. D. Leverson and N. Bloembergen, "Observation of Two-Photon Absorption Without Doppler Broadening on the 3S-5S Transition in Sodium Vapor," Phys. Rev. Lett., 32, 645 (1974).

3.220 J. E. Bjorkholm and P. F. Liao, "Resonant Enhancement of Two-Photon Absorption in Sodium Vapor," Phys. Rev. Lett., 33, 128 (1974).

3.221 T. W. Hänsch, K. C. Harvey, G. Meisel, and A. L. Schawlow, "Two-Photon Spectroscopy of Na 3s-4d Without Doppler Broadening Using a cw Dye Laser," Opt. Comm., 11, 50 (1974).

3.222 T. W. Hänsch, S. A. Lee, R. Wallenstein, and C. Wieman, "Doppler-Free Two-Photon Spectroscopy of Hydrogen 1S-2S," Phys. Rev. Lett., 34, 307 (1975).

3.223 B. A. Bushaw and T. J. Whitaker, "Two Photon Spectroscopy of Ground State Xenon," BNWL-SA-5916 (1976).

3.224 G. C. Bjorklund, C. P. Ausschnitt, R. R. Freeman, and R. H. Storz, "Detection of Atomic Hydrogen and Deuterium by Resonant Three-Photon Ionization," Appl. Phys. Lett., 33, 54 (1978).

3.225 G. S. Hurst, M. H. Nayfeh, and J. P. Young, "A Demonstration of One-Atom Detection," Appl. Phys. Lett., 30, 229 (1977).

3.226 G. S. Hurst, M. H. Nayfeh, And J. P. Young, "One-Atom Detection Using Resonance Ionization Spectroscopy," Phys. Rev. A, 15, 2283 (1977).

3.227 S. D. Kramer, C. E. Lamis, Jr., J. P. Young, and G. S. Hurst, "One-Atom Detection in Individual Ionization Tracks," Opt. Lett., 3, 16 (1978).

3.228 H. Gerhardt, R. Wenz, and E. Matthias, "Isotope Shifts of the 557 nm Transition in Even Krypton Isotopes," Phys. Lett., 61A, 377 (1977).

3.229 C. Brechignac, "Measurements of Isotope Shift in Visible Lines of KrI by Saturated-Absorption Techniques," J. Phys. B: Atom. Molec. Phys., 10, 2105 (1977).

3.230 D. E. Roberts and E. N. Fortson, "Rubidium Isotope Shifts and Hyperfine Structure by Two-Photon Spectroscopy with a Multi-Mode Laser," Opt. Comm., 14, 332 (1975).

UNLIMITED RELEASE
DISTRIBUTION:

Mr. T. B. Hindman, Jr., Director
Fuel Cycle Program Office
Savannah River Operations Office
P. O. Box A
Aiken, South Carolina 29801

Dr. E. J. Lukosius (3)
E. I. du Pont de Nemours & Company
Savannah River Laboratory
Aiken, South Carolina

Dr. R. S. Swingle, II
E. I. du Pont de Nemours & Company
Savannah River Laboratory
Aiken, South Carolina 29801

Dr. M. C. Thompson
E. I. du Pont de Nemours & Company
Savannah River Laboratory
Aiken South Carolina 29801

Dr. G. A. Huff
Analytical Services Department
Allied-General Nuclear Services
P. O. Box 847
Barnwell, South Carolina 29812

Technical Information Center (126)
P. O. Box 62
Oak Ridge, Tennessee

1750 J. E. Stiegler
1760 J. Jacobs
4000 A. Narath
4200 G. Yonas
4210 J. B. Gerardo (2)
4211 E. J. McGuire
4212 R. A. Gerber
4214 E. D. Jones
4216 A. W. Johnson
4216 J. C. Cummings
4216 P. Esherick
4216 K. L. Goin
4216 P. J. Hargis, Jr.
4216 R. A. Hill
4216 J. P. Hohimer (50)
4216 G. A. Laguna
4216 G. H. Miller
4216 A. J. Mulac

4230 M. Cowan, Jr.
4240 G. Yonas, Actg.
4300 R. L. Peurifoy, Jr.
4400 A. W. Snyder
4500 [illegible] H. Beckner
4700 J. H. Scott
8266 E. A. Aas (2)
3141 T. L. Werner (5)
3151 W. L. Garner (3)
[illegible] (UNLIMITED RELEASE)
3171-1 R. F. Campbell (25)